Characterisation of phenotypes of inflammation, fibrosis and remodelling in chronic rheumatic heart disease using multiparametric cardiovascular magnetic resonance and autophagy markers

OLUKAYODE OLASUNKANMI AREMU

ARMOLU002

SUBMITTED TO THE UNIVERSITY OF CAPE TOWN

DOCTOR OF PHILOSOPHY

Department of Medicine

Faculty of Health Sciences

University of Cape Town

Date of submission **August, 03 2022**

Supervisors: **Prof. Ntobeko Ntusi, Prof. Sebastian Skatulla**

Department of Medicine, Faculty of Health Sciences, University of Cape Town

Declaration of originality

I, **Olukayode Olasunkanmi Aremu (ARMOLU002)**, declare that this thesis is my own unaided work. It is being submitted for the degree of Doctor of Philosophy in Faculty of Health Sciences, University of Cape Town, Cape Town. The contents of this thesis have not been submitted for any other degree or examination in this university, or any other university.

Signed by candidate

Signed _____ Date 03 August, 2022

Declaration of ethical approval

I, **Olukayode Olasunkanmi Aremu (ARMOLU002)**, hereby confirm that the research in this thesis has the approval of the Ethical Committee of the University of Cape Town, South Africa. The ethical clearance number is HREC REF number: 554/2017.

Signed by candidate

Signed _____ Date 03 August, 2022

Acknowledgements

My heartfelt acknowledgement goes to the Almighty God, the embodiment of wisdom, my joy and strength, my glory, and the lifter up of my head, for the successful accomplishment of this program.

I gratefully thank my mentors, Prof. Ntobeko A. B. Ntusi and Prof. Sebastian Skatulla for their professional, academic, and financial support during this project. I am grateful for your unrelenting assistance, exceptional mentorship, and supervision.

My exclusive appreciation goes to my family, Abiola Esther Aremu, Gracious Irebami Aremu and Heritage Iyanuoluwa Aremu, and all other family members. You really supported me in prayers, advice and understanding throughout the period of the programme.

I also acknowledge the support from friends, colleagues, and research collaborators; Mrs. Petronella Samuels, Mr. Stephen Jermy, Dr. Evelyn Lumngwena, Mr. Daniel Mutithu, and other Cape Universities Body Imaging Centre and Cape Heart Institute staff and students.

I want to thank and acknowledge the intellectual contributions and diverse support from Prof. Richard Naidoo, Prof. Dhiren Govender, Mrs. Subash Govender, Dr. Riyaadh Roberts, Mr. Jurgen Geitner and other Anatomical Pathology staff who assisted in the cellular aspect of the study.

Express thanks to the University of Cape Town, South African Medical Research Council, Lily and Ernst Haussmann Trust, and National Research Foundation (Grant Nos. 104839 and 105858) for funding this project.

Dedication

I dedicate this study firstly to the Lord Almighty, the giver of life, wisdom, and strength, “For in Him, I live, I move and have my being… (Acts. 17:28a)”. To my lovely and pulchritudinous wife, Abiola Esther Aremu, for your support and endurance through all the severities in search of success in life. May you be blessed beyond measure in all ramifications in Jesus’ name.

I also dedicate this work to the body of knowledge, especially research that aims to eradicate cardiovascular diseases, one of which is rheumatic heart disease.

To the giants in cardiovascular research, Prof. Ntobeko Ntusi, Prof. Karen Sliwa and other important people. God bless you in all you do.

This page would not be complete without mentioning the immense contribution of the body of Christ, The Redeemed Christian Church of God, Latter House, Cape Town. This is where I find my comfort and solace in epochs of insomnia, depression, and disappointments. Special thanks to Pastor R.O Adelusi and other true ministers of the gospel for the seasonal and therapeutic messages and ministrations. May you continue to wax stronger in grace and anointing in Jesus’ name.

Declaration of plagiarism

I, **Olukayode Olasunkanmi Aremu (ARMOLU002)**, hereby declare that this thesis is my original work and, neither the whole work has been, is being, or is submitted for another degree in this or any other university.

Signed _____ Date _____

Table of contents

List of tables

List of figures

List of abbreviations

AHA/ACC	American Heart Association/American College of Cardiology
AF	Atrial fibrillation
AR	Aortic regurgitation
ARF	Acute rheumatic fever
AS	Aortic stenosis
Atg-WIP11	Autophagy related gene
AU	African Union
AV	Aortic valve
AVA	Aortic valve area
BAX	Bcl-2 Associated X-protein
Bcl	B-cell leukaemia/lymphoma 2
BSA	Bovine serum albumin
CMR	Cardiovascular magnetic resonance
CT	Computed tomography
CVD	Cardiovascular disease
DAB	Diaminobenzidine
DSVRT	Deceleration time of sweep volume
DSVRT50	50% diastolic sweep volume recovery time
DTPA	Diethylenetriamine pentaacetic acid
ECG	Electrocardiogram/electrocardiography
ECV	Extracellular volume fraction
eGFR	Estimated glomerular filtration rate
ER	Endoplasmic reticulum

FA	Flip angle
FLS	Fibroblast-like synoviocytes
g	grams
GAS	Group A streptococcus
GSH	Groote Schuur Hospital
H_2O_2	Hydrogen peroxide
HASTE	Half-Fourier Acquisition Single-shot Turbo spin Echo imaging
HICs	High-income countries
HPF	High per field
HREC	Human Research Ethics Committee
HRP	Horse radish protein
Hz	Hertz
IE	Infective endocarditis
IFNA	Interferon-alpha
IHC	Immunohistochemistry
LA	Left atrium/atrial
LC3	Light chain 3
LGE	Late gadolinium enhancement
LMICs	Low- and middle-income countries
LV	Left ventricle/ventricular
LVEDD	Left ventricular end diastolic diameter
LVEDV	Left ventricular end diastolic volume
LVEF	Left ventricular ejection fraction
LVESV	Left ventricular end systolic volume
LVMi	Left ventricular myocardial mass index

LVOT	Left ventricular outflow tract
MAVD	Mixed aortic valve disease
MMAVD	Mixed mitral and aortic valve disease
MVD	Mitral valve disease
MMVD	Mixed mitral valve disease
MOLLI	Modified Look-Locker Inversion recovery
MVR	Mitral valve replacement
mL	Milli litres
mM	Millimole
MRI	Magnetic Resonance Imaging
ms	milliseconds
MR	Mitral regurgitation
MS	Mitral stenosis
MV	Mitral valve
MVA	Mitral valve area
nfKB	Nuclear Factor kappa-light-chain-enhancer of activated B cells
NCDs	Non-communicable diseases
NYHA	New York Heart Association
PARF	Peptides associated with ARF
PE	Phosphatidylethanolamine
PISA	Proximal isovelocity surface area
PBS	Phosphate buffer saline
PSIR	Phase-sensitive inversion recovery
PSRA	Peak volume sweep rates in atrial systole

PSRE	peak volume sweep rates in early diastole
PV	Pulmonary valve
Px	Pixel
RA	Rheumatoid arthritis
RHD	Rheumatic heart disease
RV	Right ventricle/ventricular
SA	Short axis
SD	Standard deviation
SLE	Systemic lupus erythemathosus
SSFP	Steady state free precession
TEDTA	Tris - Ethylenediamine tetraacetic acid
T1	T1 relaxation time
T2	T2 relaxation time
TE	Echo time
TNF	Tumor necrosis factor
TOE	Transoesophageal echocardiography
TR	Tricuspid regurgitation
TR	Repetition time
TTE	Transthoracic echocardiography
TV	Tricuspid valve
ULK1	Unc-51 like autophagy activating kinase
Vps34	Vacuolar protein sorting 34
WHF	World Heart Federation
WHO	World Heart Organisation

Thesis outline

The main results of this doctoral research project have been condensed into an article structure and presented as a thesis.

Chapter One gives background evidence with a quick overview of a few key subjects. The aim and objectives of the study, the hypotheses, and any prospective outcomes are also emphasised.

Chapter Two describes some relevant literature review that explains the pathophysiology, pathogenesis, epidemiology, diagnosis, complications, as well as management strategies for rheumatic heart disease (RHD). We concluded this chapter with a literature review on the role of CMR and autophagy biomarkers in autoimmune related diseases, with a focus on RHD. Part of this review has been published in *International Journal of Cardiology*, an ISI accredited journal.

Chapter Three illustrates the research plan and methodologies used in the study. I emphasised the ethical considerations, sampling techniques, sample recruitment approach used, and the data acquisition and results analysis.

Chapter Four reports on the assessment of myocardial fibrosis in chronic RHD patients using multiparametric CMR. This manuscript is under review for submission to *Circulation Cardiovascular Imaging* for publication.

Chapter Five reports on myocardial strain in chronic RHD patients and its relationship with native T1 and extracellular volume (ECV).

Chapter Six describes the prevalence of valve lesions in RHD and its relationship with CMR tissue characteristics. This manuscript has been submitted to *Frontiers in Cardiovascular Medicine* for publication.

Chapter Seven reports on the role of Beclin 1, LC3, and p62/Sequestosome 1, BAX, Bcl-2 and caspase-3 in patients with RHD.

Chapter Eight highlights major limitations and makes recommendations for future studies.

Chapter Nine provides overall conclusions and implications of the research results.

List of published chapters

Chapter Two: Aremu OO, Samuels P, Jermy S, Lumngwena EN, Mutithu D, Cupido BJ, Skatulla S, Ntusi NAB. Cardiovascular imaging modalities in the diagnosis and management of rheumatic heart disease. Int J Cardiol. 2021 Feb 15; 325:176-185. doi: 10.1016/j.ijcard.2020.09.049. Epub 2020 Sep 25. PMID: 32980432.

Abstract

Background: Rheumatic heart disease (RHD), concomitant to valvular damage, heart failure, arrhythmias and pulmonary hypertension is the major source of cardiovascular morbidity and mortality in the young, predominantly in low- and middle-income countries (LMICs). We investigated the association of valve lesions in RHD with cardiovascular magnetic resonance (CMR) tissue characteristics and autophagy markers, in this study.

Methods: Forty-seven (47) patients (42 ± 12.8 years), with advanced RHD, awaiting valve replacement, confirmed on echocardiography, and matched with 30 healthy controls (39 ± 12.1 years), were scanned using a 3T Siemens Magnetom Skyra. CMR parameters were derived from the following acquisitions: cine imaging of the short and long axes, T1 mapping (MOLLI, 5(3)3, estimation of ECV and late gadolinium enhancement (LGE) imaging. For the cellular study, we analysed the immunoexpression of Beclin, LC3, p62, BAX, Bcl-2 and caspase-3 in patients confirmed with RHD and valvular heart disease.

Results: Mitral valve was commonly involved, with mitral regurgitation (MR) and mitral stenosis (MS) observed in 76% and 67% of RHD patients, respectively, followed by aortic regurgitation (AR) and aortic stenosis (AS) in 49% and 45%, respectively. According to disease severity, a severe form of MS, MR, and AR (44%, 72%, and 48%) was more common except for AS which had more of the mild form (44%). Valve lesions seen were divided into isolated (comprising of MS, MR and AS), and mixed (comprising of mixed mitral valve disease (MMVD), mixed aortic valve disease (MAVD) and mixed mitral and aortic valve disease (MMAVD) lesions). Out of the isolated valve lesions, isolated MR was most common (10.6%), compared with AS and MS (4.2% and 2.1%). MMAVD was most predominant (51%) compared with MMVD and MAVD (28% and 4.2%) respectively. Compared to controls, we

observed a significantly reduced left ventricular EF (45 ± 12.5% vs. 57 ± 5.2%, p< 0.001) and elevated LV mass index (60 ± 30.7 g/m^2 vs. 32 ± 8.38 g/m^2, p<0.001), increased LVEDV (113 ± 34.8 ml vs. 74 ± 13.4 ml, p< 0.001) and elevated LA diameter (42 ± 12.3 mm vs. 22 ± 3.1 mm, p<0.001). Elevated RV end-systolic and stroke volume indices were observed. RVEF was significantly reduced in patients and, below normal range compared to controls (41 ± 15.9% versus 54 ± 7.5%, p<0.001). Native T1 was significantly elevated (1280 ± 55.9 ms vs. 1213 ± 33.3 ms, <0.001) with a corresponding elevated ECV (33% vs. 28%, <0.0001). The total mass of myocardial enhancement with LGE imaging was significantly different from control (26 g vs. 15 g, <0.001). T2 values were similar between RHD patients and controls (39 ± 2.9 ms vs. 39 ± 2.4 ms, p = 0.75).

Myocardial radial strain, and diastolic strain rates were significantly reduced in RHD patients (25.4 ± 9.8 vs. 30.8 ± 10.5, p=0.027 and -1.7 ± 0.8 vs. -2.2 ± 0.9, p=0.008 respectively) compared to control, whereas systolic radial strain rate was similar compared to control (1.6 ± 0.9 s^{-1} vs. 1.7 ± 0.9 s^{-1}, p=0.592). Myocardial circumferential strain, systolic and diastolic strain rates were significantly lower in RHD patients (-17.7 ± 4.7% vs. -21.1 ± 2.7%, p=0.001; -0.9 ± 0.3 s^{-1} vs. -1.1 ± 0.2 s^{-1}, p=0.003; and 0.9 ± 0.3 s^{-1} vs. 1.5 ± 0.4 s^{-1}, p=0.001 respectively), compared to controls. Moreover, we observed a significantly reduced longitudinal strain, systolic and diastolic strain rates in RHD patients (-15.1 ± 6.5% vs. -20.2 ± 2.9%, p=0.001; -0.8 ± 0.4 s^{-1} vs. -1.0 ± 0.2 s^{-1}, p=0.018 respectively) compared to control.

Linear regression analysis shows a significant moderate correlation between native T1, and global circumferential and longitudinal strains (r=0.29*, CI= [0.08, 0.5], p=0.01; and, r=0.32**, CI= [0.12, 0.50], p<0.001 respectively]. We observed a moderate association

between native T1 and circumferential and longitudinal systolic strain rates [(r=0.29**, CI= [0.09, 0.48], p<0.01; and, r=0.26*, CI= [0.09, 0.41], p<0.03 respectively].

A significantly moderate association between ECV and, global circumferential strain and circumferential systolic rates [(r=0.28*, CI= [0.11, -0.48], p=0.02; and, r=0.29*, CI= [0.12, 0.48], p=0.01 respectively] was also observed. There was a significant moderate correlation between ECV and radial longitudinal diastolic strain rates [(r=0.27**, CI= [0.09, 0.44], p=0.02; and, r=-0.27*, CI= [-0.41, -0.15], p=0.02 respectively] whereas a strong correlation was observed between ECV and circumferential diastolic strain rates [(r=-0.44**, CI= [-0.56, -0.31], p<0.001)].

Stromal and macrophage intensity and proportion were similar in RHD and degenerative AS groups compared to control, as they all show a strong intensity and proportion. However, RHD shows a reduced number of positively- stained macrophages compared to degenerative AS and compared control, respectively. The ongoing inflammatory process shown by haematoxylin and eosin (H&E) stain, by the presence of inflammatory cells was also observed in the strong stromal and macrophage expression of Beclin in both RHD and degenerative AS tissue samples. CD68 staining shows a high expression of macrophages in the RHD and degenerative AS groups compared to control. There was a moderate staining of BAX, BCL-2 and caspase-3 observed in the RHD and degenerative AS cases compared to control.

Conclusion: We used a multiparametric CMR to study the phenotypes of myocardial inflammation, fibrosis in patients with chronic RHD. We observed evidence of myocardial fibrosis on LGE imaging in all patients, with no distinct pattern of enhancement and therefore cannot report a specific phenotype of LGE in RHD. Furthermore, we found statistically significant differences in LV functional parameters between patients and controls. LVEF was reduced in patients and as expected, the valves most affected were the mitral and aortic valves.

Strain was abnormal in RHD. Furthermore, native T1 was elevated in patients which correlates well with the finding of LGE in all patients. In conclusion, isolated and mixed patterns of valve disease are commonly seen in RHD. Most of RHD patients have severe form of MS, MR, and AS. High frequency of MMAVD with elevated native T1 was observed, indicating a phenotypic myocardial fibrosis. Using CMR tissue characteristic parameters, valvular lesions could be stratified in RHD and therefore, CMR can adequately complement echocardiography in valvular disease diagnosis. We used IHC to investigate autophagy in rheumatic and degenerative AS valves in this study. The results of this study probably suggest an ongoing inflammation in the pathogenesis of RHD and degenerative AS due to the presence a moderate to strong staining of the markers (Beclin 1, LC3, p62, BAX, Bcl-2 and caspase-3) investigated. However, further research is required to ascertain the influence of autophagy in the degree of progression of the disease, and to generate a good statistical power. This might require a prospective comparison of excised valves from a range of between "slow" and "rapid" progressors of rheumatic heart disease.

Keywords: Cardiovascular magnetic resonance, myocardial fibrosis, acute rheumatic fever, valve lesions, autophagy, rheumatic heart disease, immunohistochemistry.

Chapter 1
Introduction and study rationale

1. The burden of rheumatic heart disease in Africa

South Africa has the utmost worldwide predominance of rheumatic heart disease (RHD) and reported incident rates of 13.4/100,000 due to significant underdiagnoses or a lack of classical acute rheumatic fever (ARF) manifestations in the universal population.[1,2,3] Over a 14-year period, the annual incidence of new cases of RHD in Soweto was reported to be 24 cases per 100,000 people.[4] RHD has historically been prevalent in Sub-Saharan African (SSA) countries; Latin America and the Pacific Asian regions are no exceptions.[5] RHD is a poverty and overcrowding disease.[6] Longo-Benza *et al*. found a prevalence of 22.2 per 1,000 children living in semi-urban areas, compared to 4 per 1000 children attending city schools [7], demonstrating the significant impact of socioeconomic status on RHD epidemiology. Despite a documented decrease in the global incidence of RHD in industrialised countries, the disease remains endemic in South America, Asia, Australasia, and with a high predominance in SSA.[8,9]

RHD is a longstanding manifestation of ARF that describes the late adverse effect of one or more severe recurrent episodes of ARF on the heart.[10] ARF is caused by group A streptococcal infection (GAS), and it greatly impacts the joints, central nervous system and the heart.[11] RHD remains the most prominent non-communicable cardiovascular disease (CVD) in low- and middle-income countries (LMICs).[1,12] RHD has a global impact of 15.6-19.6 million affected individuals and over 233, 000 deaths per year.[13–15] Malnutrition, inadequate housing, a lack of access to care, overcrowding, delayed diagnosis, noncompliance with treatment, genetic

susceptibility, and a limited use of secondary prophylaxis all contribute to the persistence of ARF and RHD in LMICs.[12,16]

To reduce the number of fatalities from non-communicable diseases (NCDs) by 25% by 2025, the World Heart Federation (WHF), World Health Organization (WHO), and African Union (AU) have officially resolved to eradicate RHD.[17]

Among other diagnostic techniques, cardiovascular magnetic resonance (CMR) is a potent method for the regular evaluation of CVD. Due to its high spatial and temporal resolution and ability to characterise tissues, CMR is a perfect modality for investigating disease mechanisms, stratifying phenotypes and identifying biomarkers that predict outcome in RHD.[18]

Activation of inflammatory processes by a dysregulated immune system is a central mechanism in the development of autoimmune diseases, including psoriasis, systemic lupus erythematosus (SLE), rheumatoid arthritis, and/or rheumatic heart disease (RHD).[19]

Autophagy describes a catabolic process which involves bulk degradation of cellular proteins and delivery of these contents for lysosomal degradation via double-membrane organelles called autophagosomes.[20] Three types of autophagy that exists are macroautophagy (hereafter autophagy), microautophagy, and chaperone-mediated autophagy.[21] The major molecular players involved in autophagy signalling include ULK1 protein kinases, Atg-WIP11 and Vps34-Beclin 1 class PI3-kinase complexes, and the Atg12 and LC3 conjugation systems.[22] Briefly, autophagy is initiated with the Atg4-mediated conversion of pro- LC3 to LC3-I, followed by the conjugation of LC3-I with phosphatidylethanolamine (PE) to generate LC3-II, which is later recruited into the autophagosomal membrane to aid in membrane elongation. Despite the fact that numerous molecular markers have been studied, the conversion of LC3-I to LC3-II via PE conjugation remains the workhorse for autophagosome formation.[23,24]

Autophagy can be selective, due to presence of autophagy receptors which are able to recognise ligand-bound cargo.[25–28] Sequestosome (SQSTSM1), also known as p62 is one of the best studied autophagy receptors and, is involved in autophagy-dependent destruction of many different cargo including ubiquinated protein aggregates and bacteria.[29–31] Beclin 1 (BECN1) plays a central role in autophagy in coordinately regulating membrane trafficking involved in several physiological and pathological processes.[32]

Although putative pathways of autophagy in RHD are unknown, several lines of evidence indicate a crucial role of autophagy in autoimmune including SLE, RA, Crohn's disease, and vitiligo.[33–35] Therefore, autophagy may have probable pathogenic involvement in RHD.

1 Study rationale

RHD is very common in South Africa, and this remains a major public health challenge. There are significant gaps in our knowledge about the pathophysiologic events in the progression of RHD. Scientific information on use of CMR for diagnosis and characterisation of RHD is limited. Given the epidemiology of RHD locally, it is opportune to use a combination of CMR and histopathology/autophagy biomarkers to provide answers for these existing knowledge gaps. We have access to affected patients and the infrastructure locally to conduct such studies. Our findings add to the body of knowledge on RHD development.

1.1 Aim and objectives

Using CMR and autophagy markers, we aim to characterise the clinical profile and correlates of inflammation and fibrosis in individuals with RHD.

Objectives

To fulfill the aims of the present study, the following objectives as shown below were pursued:

A) We aimed to characterise the imaging phenotypes and tissue characteristics of RHD using multiparametric CMR

a. Primary objectives

i. Determine demographics, clinical characteristics and CMR findings in patients with RHD.

ii. Histological analysis of the valve tissue biopsies obtained from RHD patients during valve replacement surgery.

b. Secondary objectives

i. Evaluate ongoing myocardial inflammation in patients with RHD using T1 and T2 mapping.

ii. Evaluate evidence of fibrosis using myocardial late gadolinium enhancement (LGE), native T1 mapping and ECV.

iii. Evaluate evidence of myocardial deformation (strain and strain rate) using myocardial feature tracking.

iv. Quantify hemodynamic parameters in diseased valves using CMR.

B) Using selected autophagy biomarkers, we aimed to characterise the phenotypes of inflammatory diseases in RHD.

i. Detect presence and expression of Beclin-1, LC3 and p62, BAX, Bcl2 and caspase-3 in valves excised from RHD patients matched with controls.

2 Introduction

RHD, a longstanding manifestation of ARF, describes a late damage caused by one or more recurrent episodes of ARF on the heart.[10] ARF is initiated by group A β-streptococcal (GAS) infection, primarily affecting the joints, skin, central nervous system and the heart.[11] RHD is the major source of acquired CVD in low- and LMICs;[1,36] and contributes to an overall global burden of 15.6-19.6 million affected lives and over 233,000 deaths annually (Figure 2.1).[13,14,37]

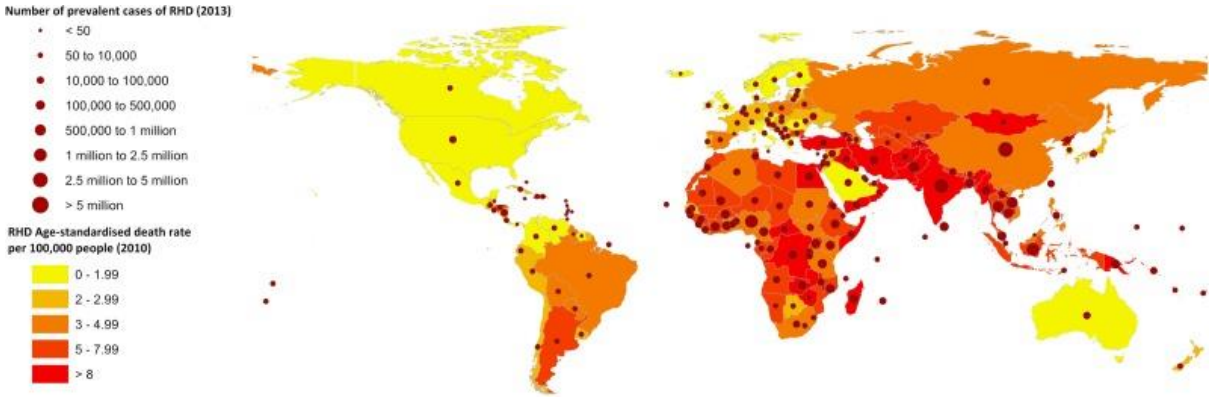

Figure 2.1 Global prevalence and mortality rates of RHD (Adapted from [1])

Malnutrition, inadequate housing, a lack of access to care, overcrowding, delayed diagnosis, noncompliance with treatment, genetic susceptibility, and a limited use of secondary prophylaxis all contribute to the persistence of ARF and RHD in LMICs (Figure 2.2).[12,16]

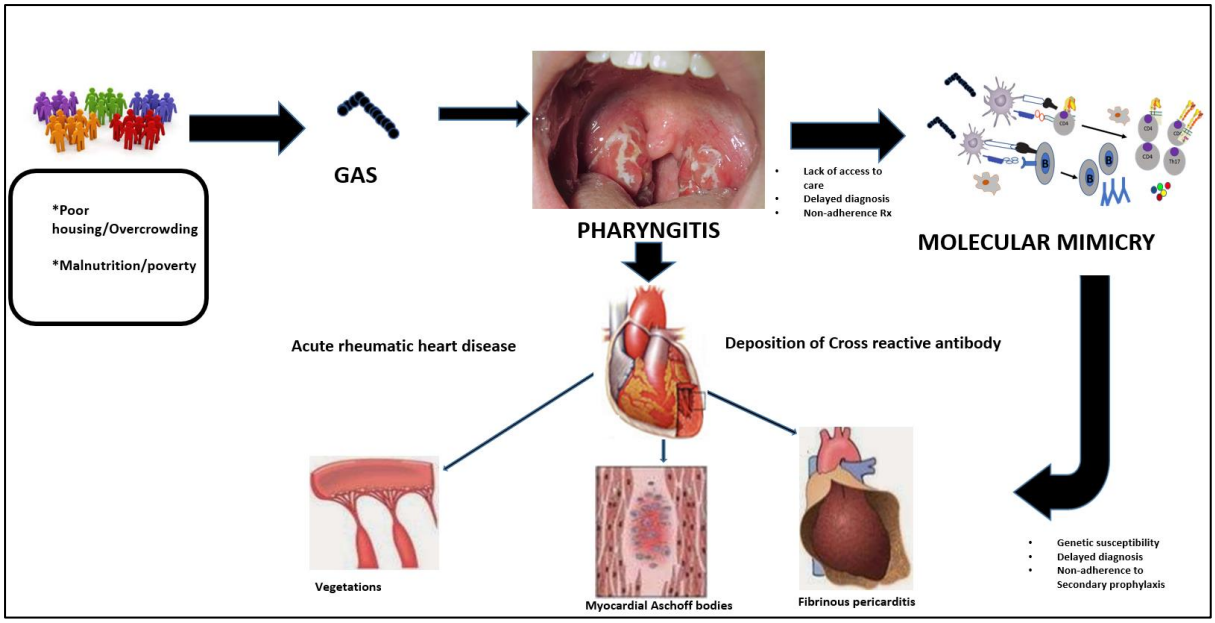

Figure 2.2 Pathophysiology of RHD.
Environmental factors such as overcrowding, poor housing, poverty and malnutrition predispose people to GAS infection, resulting into pharyngitis. Recurrent pharyngitis leads to ARF, due to molecular mimicry. Untreated ARF results into RHD where the pericardium, myocardium and endocardium are adversely affected thereby leading to heart failure, arrhythmia, pulmonary hypertension, and premature mortality.

Cardiovascular imaging is important for diagnosing RHD, assessing cardiac functions and structure, severity and haemodynamic adaptations, disease mechanism(s), and ventricular remodeling, all of which impact on prognosis.[38,39] Echocardiography is the first imaging tool of choice used in the assessment of the vast majority of patients with RHD worldwide. The major imaging modalities including echocardiography, CMR and computed tomography (CT) are variably employed in assessing RHD.[40] The use of scintigraphic techniques, including ^{18}F-fluorodeoxyglucose positron emission tomography fused with the conventional single photon emission computed tomography, has changed over time,[41] and is currently not recommended for routine diagnostic assessment of ARF and RHD.[42]

GAS is the agent responsible for starting ARF in a vulnerable host, although the precise processes by which GAS contributes to the pathophysiology of ARF and RHD are unknown.[43–

[46] Molecular mimicry is critical in the initiation of tissue insult in ARF and carditis.[47,48] Following GAS pharyngeal infection, the innate immune system is triggered, resulting in GAS antigen presentation to T cells and, production of immunoglobulin M and G antibodies, and activation of CD4+ T cells.[47,49] This immune reaction causes a cross-reactive response mediated by molecular mimicry, leading in the clinical features of ARF, including carditis (due to antibody binding and T cells infiltration), transitory arthritis (due to the formation of immune complexes), chorea (due to the binding of antibodies to the basal ganglia), and skin manifestations (due to a delayed hypersensitivity reaction).[50]

Carditis affects approximately about 42-60% of ARF patients.[51] The α-helical coiled structure of streptococcal M protein and N-acetyl-beta-D-glucosamine (carbohydrate antigen of GAS) share epitopes with cardiac myosin, and antibodies against these antigens cross-react with human tissue.[48,52] Heart M protein T-cells have been extracted from both the myocardium and valves of RHD patients.[53] Recent research has revealed the pathological findings of subendothelial and perivascular connective tissues in ARF, emphasising the importance of collagen in the aetiology of ARF.[54]

Peptides associated with ARF (PARF) bind to the cyanogen binding fragment 3 (CB3) region of collagen type IV resulting to an antibody response to the collagen and inflammation.[52] Among 74 GAS strains associated with ARF, only one GAS isolate contained the PARF motif, suggesting that additional and complementary mechanisms may be involved in the pathogenesis of ARF.[55] Additionally, antibodies against N-acetyl glucosamine are also involved in the pathogenesis of ARF and RHD via cross-reaction against valvular glycoprotein.[56] These findings suggest that ARF/RHD is caused by a complex interaction of streptococcal antigens, cross-reactive antibodies, and multi-pronged immune targets.[17]

2.1 Epidemiology of GAS, ARF/RHD

The most common infection caused by GAS is pharyngitis, followed by impetigo, and it affects children aged 5-15 years of age, primarily in LMICs.[13,57] ARF/RHD prevalence of >10 cases per 1,000 population was reported in an Eastern and Central African study in 2017, with an estimated mortality rate of 266,200 to 303,300.[58] The prevalence of RHD was 0.3 cases per 1,000, which was significantly lower than the 3.4 cases per 1,000 children reported in 1980 in Sudan.[59] Furthermore, studies in Ethiopia revealed 14 cases per 1,000 school children with RHD involving heart valve abnormalities, such as mild aortic, mitral, or tricuspid regurgitation.[60–64]

In 1981, South Africa reported a prevalence of 33.2% overall with a significant disparity between rates for blacks (45%) and whites (23.2%).[65] In another study conducted in a black community in Bloemfontein, 42% of participants were infected with GAS.[66] In South African observational studies, the majority of antenatal mortality was linked to RHD, with heart failure being the most common presentation in pregnancy.[2,67,68] A recent systematic review of the incidence, prevalence, and outcomes of RHD in South Africa over the last 20 years found a prevalence of 20.2 cases of asymptomatic RHD per 1,000 schoolchildren.[1,69]

2.2 Risk factors for RHD

The risk factors for ARF and RHD include sex, age, and environmental factors.[45] ARF generally affects children between 5-15 years of age, sometimes affecting even children younger than 5 years.[70,71] ARF progresses to RHD, presenting in individuals between 20-30 years of age, although its burden in children and adolescents remains substantial.[70] While ARF incidence is similar in both males and females, the risk factors for RHD is more common in

females possibly due to intrinsic/hormonal factors, GAS exposure during child rearing, physiological complications during pregnancy and, limited access to health services.[72–74]

Streptococcus pyogenes spread is aided by environmental factors such as malnutrition and household congestion.[10]

2.3 Complications of RHD

RHD is followed by overwhelming consequences such as cardiac failure, pregnancy-related complications, stroke, atrial fibrillation (AF), infective endocarditis (IE), and premature mortality.[1,70,75,76] Although 11 million people in LMICs were impacted by stroke;[77] there were only around 345,000 to 862,500 RHD-related stroke annually,[78] compared to the 3-7.5 percent of strokes reported in settings with poor resources.[13]

2.4 Phenotypes of RHD

Inflammation

The reviewed Jones criteria classified carditis as a typical pancarditis which involves the pericardium, epicardium, myocardium and endocardium.[79] Carditis can range from mild subclinical involvement to severe carditis, and often leads to congestive heart failure and untimely death. Endocarditis causes valvulopathy and valvulitis, and commonly initiating mitral regurgitation (MR) and to a lesser degree, aortic regurgitation (AR).[10] Only in 2% of patients have isolated aortic valve disease, and right-sided valvulitis is seen only as a conjunction with left-sided valvulitis.[80] In patients with mild or moderate MR, auscultation reveals a characteristic pansystolic murmur, however in severe cases, additional diastolic murmurs (from mitral stenosis (MS), AR, and the Carey-Coombs murmur) and cardiomegaly are observed..[10] In endocarditis, echocardiography provides significant anatomic, functional,

haemodynamic and presence of vegetation, number of leaflets, and pathological information regarding valve thickness.[81]

Fibrosis

RHD classically affects the valves and myocardium. There is an association between RHD and myocardial interstitial fibrosis in the chronic stage of RHD, using T1 mapping. Snail1 is a new biomarker found to positively relate with atrial fibrosis in individuals with AF and RHD and, is implicated in the initiation and maintenance of the disease condition.[82] Compared to non-rheumatic mitral valve tissue, patients with rheumatic mitral valves exhibit increased collagen (I and III) deposition levels.[45] RHD and myxomatous valves have been reported to have decreased collagen VI expression, increased vitronectin expression, and identical lumican expression.[83]

Atrial and ventricular remodelling

In patients with chronic MR, left atrial (LA) enlargement has good prognostic implications.[84,85] LA dilatation may be linked with chronic mitral valve disease (MVD), LV systolic and diastolic dysfunction.[86] Massive/giant LA and right atrial (RA) were reported in a 68 years old woman who presented with chronic rheumatic MS and severe tricuspid regurgitation (TR). The RA enlargement was suggested to be as a result of severe pulmonary hypertension due to MS and severe TR.[87] Increased and prolonged afterload as a result of AS causes hypertrophic remodelling of the LV.[88] Mitral valve replacement (MVR) improves the NYHA functional class and LVEF, reduces LV end-diastolic diameter (LVEDD), and LA size after total chordal preservation.[89]

2.5 Imaging modalities for assessment of RHD

Echocardiography and cardiac catheterisation have traditionally been the main diagnostic modalities employed in the assessment of RHD.[90] They provide clinically important information, which is useful for planning definitive management. However, these techniques might not be adequate for assessing intricate anatomic changes of the cardiac chambers and associated vessels.[91] Due to their limitations, there is a growing interest in using CMR to assess RHD.

Echocardiography

Echocardiography is a reliable and essential diagnostic tool in the evaluation of RHD.[17] Echocardiography is extremely useful in diagnosing valvular disorders, the most common of which is mitral regurgitation. (Figure 2.3). Two-dimensional echocardiography shows thickened, elongated tendinae chordae that cause prolapse of the anterior mitral valve leaflet. Echocardiography is particularly crucial for determining LV size and function, as well as severity of regurgitant lesions and haemodynamic significance of valve lesions.[92]

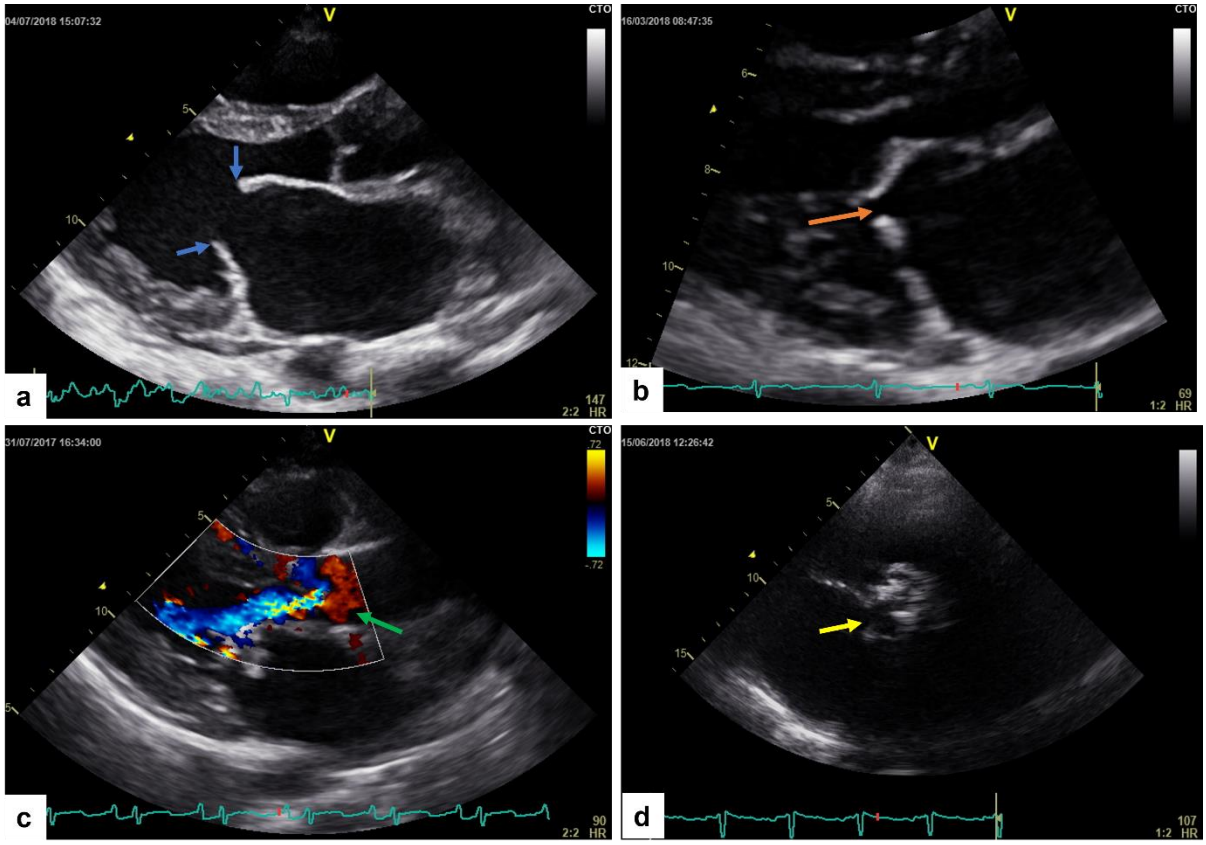

Figure 2.3 Echocardiographic images of a RHD patient with multiple valvular lesions
(a) blue arrows show a regurgitant mitral valve with thickened mitral valve leaflets (b) orange arrow shows stenosed mitral with a diameter of <1.0 cm. Colour Doppler echocardiographic image revealing (c) green arrow shows aortic regurgitation with Doppler beam revealing the severity of regurgitation across the valve (d) yellow arrow shows aortic stenosis (Note the narrowed and incomplete opening of the valve).

Transthoracic echocardiography (TTE) and transoesophageal echocardiography (TOE) are the main modalities for assessing MR, with the aim of defining the cause of MR (ischaemic or non-ischaemic), mechanism (using the Carpentier classification), extent of calcification and the localisation of lesion (using either the Carpentier or Duran nomenclature for scallops).[93] TOE offers better imaging quality and significant information such as assessment of the vena contracta (VC), distal jet area and ratio, and flow convergence analysis which calculates the proximal isovelocity surface area (PISA) by using colour flow Doppler to measure the effective regurgitant orifice area (EROA).[94] Severe MR is indicated as a distal jet area >40% of LA area.[95] The method has been shown to be highly sensitive and specific[96] but is limited by

underestimation of the severity of eccentric jets.[97] However, vena contracta jet is measured at the regurgitant orifice in the LA in the parasternal long-axis view, in order to avoid overestimation. Regardless of aetiology or jet eccentricity, measurement of this portion by TOE accurately predicts MR severity when compared to angiography. VC width of ≥ 0.7 cm indicates severe MR.[98] Three dimensional (3D) echocardiography may improve the specificity and sensitivity of RHD detection in mild valvular involvement and facilitate improved surgical preparation for patients with advanced disease.[99]

Valvular thickening occurs in about 56-100% of patients with rheumatic carditis.[100] The thickening is mostly located at the free edge of the valve leaflets, where the chordae fuse with the leaflet tips, although nodularity is also seen along the length of the leaflet. The 2012 World Health Organization (WHO) classification criteria for abnormally thickened valves include chordal thickening and an objective measurement of the MV without harmonic imaging.[101]

CMR techniques

CMR is unique in its ability to characterise myocardial tissues. LGE-CMR imaging is helpful in the non-invasive workup for the assessment of a new onset of myocardial dysfunction. LGE-CMR reveals various patterns of fibrosis including focal, diffuse, patchy, and intramural (see image below).[102] However, due to the inherent limitation of LGE imaging in adequately quantifying myocardial fibrosis, there is a need to quantify the scarred or fibrotic portion of the myocardium.[103,104] T1 and T2 mapping allow direct quantification of T1 time, T2 time, and ECV of the myocardial tissue, by providing tissue-specific T1 and T2 time values, and allowing comparison of quantified myocardial parameters with normal referenced values obtained from the scanner.[105]

Native T1 mapping

T1 relaxation time is a biological magnetic resonance parameter which indicates how fast nuclei recover towards thermodynamic equilibrium along the B_0 direction.[106] T1 values depends on the rate of energy dissipation from an excited proton to its environment. The rate of energy transfer varies according to the molecular environment, including molecular size, viscosity, temperature, shape and magnetic field strength.[107] Native T1 depends on the magnetic field strength, age and sex. Normal myocardial values have been reported to be 960 ± 30 ms and 1150 ± 60 ms at 1.5 T and 3 T, respectively.[108] Men and older participants show slightly higher native T1 values than women and younger participants.[109] Further, native T1 is low in pathologies including inflammation, oedema, myocardial fibrosis, infiltrative diseases including amyloidosis and hemosiderosis. T1 values are low in iron overload, fatty deposition (e.g. Fabry's disease) and fatty metaplasia of the myocardium.[110–116]

T2 mapping

T2 relaxation time is a measure of spin-spin interaction that takes place. Free water contains molecules which are small and wide apart, resulting into slower T2 relaxation time but longer T1 relaxation times. Conversely, water molecules bound to large molecules are slowed down and interact, leading to faster T2 relaxation and shorter T2 relaxation times. Therefore, in diseased state such as an inflammatory process, when water content increases, T2 value also increases. T2 relaxation time decays due to loss of coherence in spin moments, interactions between neighbouring protons and inhomogeneity in the applied magnetic field. The combined effects of T2 relaxation and magnetic field non-uniformity is known as T2*.

Extracellular volume fraction

The myocardium comprises of the cellular and extracellular or interstitial components.[117] The cellular components include the muscle fibres, which are interconnected by structures such as intercalated discs, and contain nuclei, sarcolemma, sarcoplasmic reticulum, as well as the contents of vascular elements.[118] ECV is a surrogate marker of myocardial tissue remodelling and allows more sensitive identification and quantification of diffuse myocardial fibrosis and oedema.[117,119] Contrast-enhanced T1 mapping is mostly used for estimating the ECV in combination with native T1. Contrast-enhanced T1 values are more variable and are influenced by the dosage of contrast agent, time elapsed between contrast administration, T1 measurement and renal clearance.[103,120] In healthy participants, ECV values of 25.3 ± 3.5% and 26.0 ± 0.04% have been reported on 1.5T and 3T respectively.[121] Elevated ECV values have been demonstrated in RA,[122] systemic sclerosis[123] and degenerative valve stenosis.[124]

2.6 Cardiovascular magnetic resonance imaging of mitral and aortic valve lesions

CMR is a robust imaging modality, free of ionising radiation, with high spatial and temporal resolution, performed via excitation of hydrogen protons within a static magnetic field. The magnetic field aligns the nuclear magnetisation spins of the hydrogen protons, which are then excited by RF pulses. After the RF pulses are switched off, the protons dissipate energy as they precess back to their equilibrium magnetization. This dissipated energy is detected by the receiver coils. Fourier transformation is then used to convert frequencies into images.[125] CMR usually involves electrocardiographic (ECG) vector gating and breath-hold acquisitions to circumvent artefacts. Balanced steady-state free precession (SSFP) sequences are applied in the short-axis plane and in 2-, 3-, and 4-chamber planes to allow morphologic assessment of valvular insufficiencies.

LGE CMR offers the capability to directly discriminate fibrotic or infarcted tissue from normal myocardium and indicates the severity and extent of myocardial injury.[125] Similar to cine CMR, tagging may be acquired to assess cardiac motion and deformation; and provides more direct and accurate quantification of the regional motion and strain. Velocity-encoded phase contrast CMR provides haemodynamic data on pressure gradients and regurgitant volumes across the valves.

AHA/ACC guidelines have recommended the use of CMR for the assessment of MR severity when TTE is technically limited. Studies have reported the importance of CMR in confirming MV morphology and pathology despite scarce data.[126–128] Kon *et al* demonstrated the use of a combination of velocity-encoded and cine SSFP sequences in quantifying MR.[129] CMR is accurate for quantification of MR severity, when compared with 2D echocardiography and has no systematic overestimation.[130,131] Although CMR balanced SSFP sequences provide information about anatomy of the MV, gradient echo cine pulse sequences are more useful for localisation and sizing of regurgitant jets.[132] There is reported inconsistency in semi-quantitative assessments of MR jets by visualisation and/or depth of penetration of MR into the LA on CMR.[133,134] Therefore, assessment of severity in MR may be done by either calculating the regurgitant volume (using the difference between RV and LV volumes, or calculated as the difference between LV stroke volume (SV) and aortic outflow SV.[134] Regurgitant fraction is calculated as the ratio of regurgitant volume to the LV stroke volume, and a regurgitant fraction>48% indicates severe MR.[135]

Although CMR has been reported to diagnose (Figure 2.4) and perform planimetry of the mitral orifice and pressure half-time assessment, it may miscalculate MS severity due to overestimation of the mitral valve area.[136] Newer CMR sequences that incorporate mitral annular tracking devices are resolving this problem.[137] CMR measurements of peak volume

sweep rates in early diastole (PSRE) and atrial systole (PSRA), PSRE/PSRA ratio, deceleration time of sweep volume (DTSV), and 50% diastolic sweep volume recovery time (DSVRT50) showed a good correlation when compared to TTE diastolic measurements.[138] Feature-tracking CMR not only provided motion and strain quantification using SSFP imaging,[139] but also showed excellent intra- and inter-observer variability.[140]

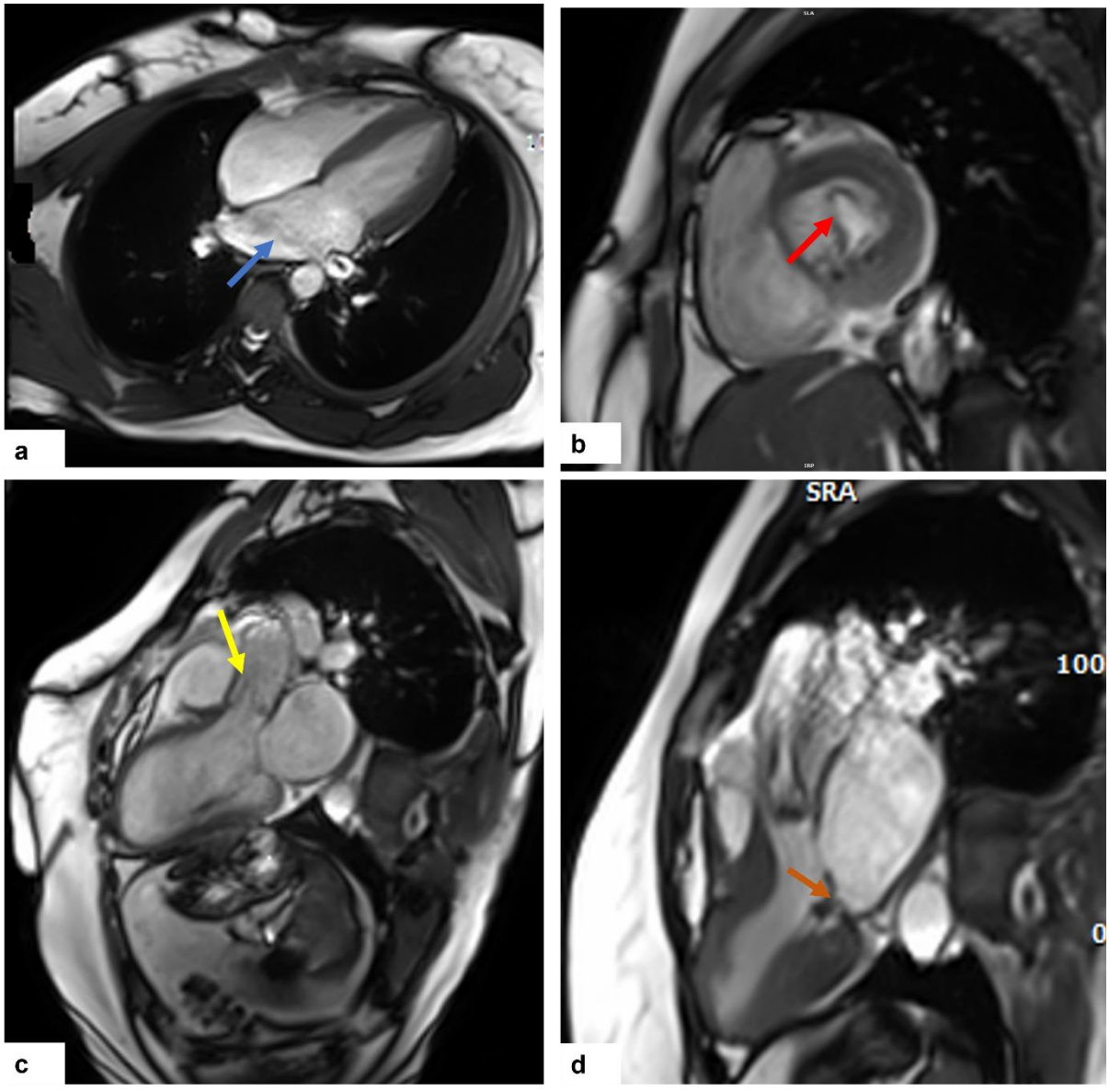

Figure 2.4 CMR images of a RHD patient with multiple valvular lesions

Cine MRI in 4 chamber view (a) blue arrow shows mitral valve incompetence with a backward blood flow into the LV (b) red arrow shows mitral stenosis with a fish-mouth appearance and thickened anterior and posterior mitral valve leaflets. SSFP in 3-chamber view (c) yellow arrow

shows aortic regurgitation with a flow acceleration jet across the valve (d) brown arrow shows aortic stenosis, and the thickened valve leaflets with incomplete opening of the valve.

CMR may be used to assess the consequences of AR on LV volumes using standard cine sequences. Phase contrast CMR or velocity encoded CMR is commonly used to assess haemodynamics of AR, including regurgitant volumes and fraction, as well as to visualise the regurgitant jet. Phase contrast CMR can directly quantify regurgitant volumes and quantify response to volume overload, as opposed echocardiography which secondarily estimates severity using indices such as vena contracta or proximal isovelocity surface area. CMR is useful for risk stratification of patients with asymptomatic moderate or severe AR, proposing the ability of CMR to quantify AR and LV volumes.[141,142] CMR is validated as a superior method in the assessment of LV mass, but echocardiography is preferred due to its lower cost, easy availability and better tolerabilty.[143] Quantitative CMR is potentially useful in supplementing echocardiography for management decisions and assessment of medical therapies in patients with AR.[144]

CMR is commonly used in tracking asymptomatic patients with severe AS, assessing reduced LVEF before referral for surgery.[145] Similar to echocardiography, CMR provides reliable information regarding flow and velocity across stenotic or regurgitant valve although maximum peak velocity could be underestimated due to its temporal resolution and possible misregistration in the precise moment of cardiac cycle. Using balanced SSFP sequences, CMR planimetry can measure the anatomical AVA based on direct visualisation of the valve orifice.[145] Contrastingly, LGE CMR plays a key role in predicting patients' eligibility for transcatheter AV replacement.[146]

2.7 Management of ARF/RHD

The best way to manage ARF/RHD is with anti-inflammatory medications that reduce pharyngitis and carditis, get rid of GAS, and stop relapses of ARF.[17] In order to treat acute inflammation, aspirin and steroids are frequently advised, however they have drawbacks.[147] For individuals who experience heart failure symptoms and/or have severe ventricular enlargement, severe mitral regurgitation, or severe aortic regurgitation, conventional heart failure therapy and surgical intervention are advised.[148] Invasive treatment of RHD during pregnancy may be necessary due to the related higher cardiac output seen during pregnancy, especially for patients with stenotic valve abnormalities. In order to decrease ARF recurrences, oral or intramuscular penicillin is used for pharyngeal GAS infection eradication. [148,149]

2.8 Conclusion

Echocardiography is first-line imaging modality for diagnosing rheumatic valvular heart disease due to its ease of use and widespread availability. CMR is regarded as second-line modality and plays a complementary role when echocardiography results are suboptimal.

3 Methods

A detailed description of the materials and methods used for each study is included in the following chapters. A brief overview of the thesis methodology is described in this chapter.

3.1 Materials and methods

The materials used in the study are listed below. Methods are explained sequentially with a detailed description of the technical aspects in the appendices.

Materials

3 T Siemens Magnetom Skyra scanner (Erlangen, Germany), radiofrequency coils (18 channel body array coils with integrated spine coils), electrocardiogram (ECG) leads; pair of NordicNeuroLab (NNL) headphones (slim design fitting 32 channel head coil), squeeze/panic ball, gadolinium (Magnevist, Bayer (Pty), South Africa). Consumables include syringes (10 and 20 mL), 10 mL sodium chloride, 22-gauge jelco needle, and extension tube and alcohol swabs.

Anti-LC3B (rabbit polyclonal, clone DU4C) and p62/SQSTM1 (mouse monoclonal, clone D5L7G) antibodies were purchased from Cell Signalling Technology (Danvers, Massachusetts), Beclin 1(BECN1), (mouse monoclonal, clone G-11), BAX (mouse monoclonal, clone 2D2), Bcl2 (mouse monoclonal, clone C2), and caspae-3 (mouse monoclonal, clone E-8) antibodies were obtained from Santa Cruz (Dallas, Texas), whereas liquid DAB + substrate chromogen system, Envision horse raddish protein (HRP) system labelled polymer anti-mouse and, Envision HRP system labelled polymer anti-rabbit were obtained from Dako (California, USA).

3.2 Study design

This is a cross-sectional study with comparative analysis of participants confirmed with RHD. The study was approved by the University of Cape Town Human Research Ethics Committee (HREC) of the Faculty of Health Sciences (HREC Reference number: 554/2017) and is in compliance with the Helsinki declaration.[150] Data collection only commenced after approval from the HREC was obtained. Informed consent was obtained from individual participants included in the project. Enrolled participants in this study were patients diagnosed with RHD on echocardiography and referred for valve replacement surgery by the cardiologists at Groote Schuur Hospital. Individuals of ages 18-65 were enrolled in the study. Seventy-seven (77) participants comprising of forty-seven (47) RHD patients, and thirty (30) healthy controls without a history of cardiovascular disease (CVD) were recruited. We obtained clinical information regarding each participant's family history, demographics (specifically, age, sex, and ethnicity) from their medical folder. Recruitment for the study began in August 2017 and, data were obtained until August 2019.

The frequency of RHD utilising echocardiography in Cape Town areas was 20/1000, as was previously described.[151] We predicted that the difference in T1 values is normally distributed with a standard deviation of 29 based on the pilot data produced at GSH. To be able to reject the null hypothesis that the difference is zero with a probability (power) of 0.99, we would need to analyse 47 people if the genuine difference in tissue features between RHD patients and controls is 0.5. The likelihood of a type I error in this test of the null hypothesis was 0.01. The study population grew to 50 RHD patients based on our patient numbers and availability of the MRI scanner, making the tentative sample size for this project 47 RHD patients.

3.3 Research data collection and measurements

For CMR, eligible participants were scanned with a 3T MRI Siemens Magnetom Skyra scanner with an 18-channel phased array body coil and integrated spine coils (Siemens, Erlangen, Germany). The scanning was conducted at the Cape Universities Body Imaging Centre (CUBIC). In myocardial imaging, LV and RV mass and volumes, the presence of oedema/inflammation (T2 imaging/T2 mapping), myocardial deformation (circumferential and longitudinal strains, and strain rates), fibrosis (focal LGE, global extracellular volume assessment with pre- and post-contrast T1 mapping) and haemodynamic parameter quantification (phase contrast) were investigated.

Participant preparation

Eligible participants were positioned on the MRI table. Radiofrequency coils were placed on the chest. Computer commands were operated by the technician, after which images were obtained. The images were post-processed with CVI42® software (Circle Cardiovascular Imaging, Calgary, Alberta, Canada); and data obtained were used to assess the following parameters:

- LV and RV volumes
- Tissue characterisation (oedema and myocardial fibrosis)
- Haemodynamic parameters
- Myocardial deformation (strain and strain rate).

Left and right ventricular volumetric assessment

Localiser, transverse, and coronal HASTE images were obtained to determine patient's position in the scanner and to get an overview of the anatomical structures when assessing patient's extra-cardiac abnormalities. Pilot images were acquired in a 2-chamber, 4-chamber, and short axis (SA) to position the heart in the isocentre of the scanner. Balanced SSFP cine images were acquired in the long-axis (2-chamber, 4-chamber) of the left and right ventricles, followed by complete short-axis stack to assess cardiac size, volume, and function.

Tissue characterisation

For tissue characterisation, images were acquired using T2 short Tau inversion recovery (STIR), and a combination of T1 and T2 Myomaps® for the assessment of oedema and myocardial inflammation/fibrosis respectively. Results for ventricular volumes, EF and LV myocardial mass were derived from short axis slices after manually tracing the epi- and endocardial borders, excluding papillary muscles from the myocardium. ECV was estimated in keeping with previously standardised report.[152] Pre-contrast and post-contrast myocardial and blood T1 values were measured, and ECV and lambda estimation was based on multipoint regression, integrating all available pre-contrast and post-contrast points, to increase the strength of the estimates by increasing the number of underlying data points.[122] ECV was calculated as: (1 – haematocrit). For ECV estimation, we calculated post-contrast T1 value using the post- contrast T1 map acquired at 20 min.

Myocardial deformation (strain and strain rate)

CMR cine images were acquired in short axis stacks at the base, middle and apex of the heart to evaluate myocardial deformation using feature tracking analysis. Myocardial deformation was assessed by calculating circumferential, radial, and longitudinal strain, and strain rates from cine images.

Late gadolinium enhancement imaging

The basic principle of LGE is altered gadolinium kinetics in the tissue with an increase in the extracellular space. Gadolinium is a paramagnetic ion which is toxic in its unbound state. Consequently, gadolinium contrast agents consist of a large molecule which comprises a gadolinium ion and a carrier agent that enhances adequate binding and movement of gadolinium.[153]

Contrast injection

Gadolinium-DTPA (Magnevist, Bayer, South Africa) was injected intravenously at a standard dose of 0.2 mmol/kg to patients with sustained renal function (eGFR>30 ml/min). Early gadolinium imaging was acquired in short axis stack using a phase contrast inversion recovery (PSIR) for the assessment of the presence of intracardiac thrombus. Qualitative analysis such as the presence and extent of LGE was done by two readers with >5 years of CMR experience and blinded to echocardiography reports. To evaluate focal myocardial fibrosis, LGE imaging was carried out 6-15 minutes after gadolinium administration, and images were acquired using a short axis stack, 2 chamber, 4 chamber, and LVOT images.

3.4 Immunohistochemistry

Sample collection

Heart valve tissues were excised from patients undergoing cardiothoracic surgery at the GSH, Cape Town. Suitable patients were approached for consent before surgery, as per patient information list and consent form submitted to the University of Cape Town HREC (see Appendix A). Tissue samples were immediately transferred into 10% formalin solution once excised by the surgeons to enable proper fixation of the valves.

For this preliminary study, 2 patients, each with confirmed RHD and degenerative AS, matched with 2 cadaveric controls were enrolled from August of 2017 to May of 2019. In addition, cadaveric valve samples, matched for age, sex were obtained from participant, and used for the control group. Cadaveric participants were excluded if they showed evidence of previous cardiac surgery or had a history of CVD; LV hypertrophy (>15 mm measured 2 cm below the valve); heart weight outside the normal range (i.e. men: 212 – 373 g, women: 164 – 317 g); coronary artery (CA) atherosclerosis occluding >50% luminal surface area in right CA, left mainstem CA, left anterior descending CA, or circumflex artery; macroscopic previous myocardial infarction with area of fibrosis; subjective thickening, calcification or fusion of valve cusps or chordae tendineae; current or previous pericarditis (adhesions); and, had history or observation of sepsis infection at autopsy.

Processing of valve tissues

Valve tissue samples were processed overnight in an automated Leica tissue processing machine, Leica TP 1020 (Leica microsystems, Nussloch Germany). This procedure entailed the tissues passing through solutions of graded alcohols, xylene and wax to fix properly. The following morning the tissues were embedded in paraffin wax to complete the tissue

processing. This process took approximately 22 hours (See table 3.1). After successful processing of tissues, they were embedded using the Leica EG1140H embedder (Leica microsystems, Nussloch Germany) and Leica EG1140C chiller plate (Leica microsystems, Nussloch Germany) was used to cool and harden the waxed tissue blocks.

Table 3.1 Tissue Processing Schedule (Leica Tissue Processor)

Reagent	Time
10% Formalin	Optional delayed start
70% Ethanol	2 hours
96% Ethanol	2 hours
96% Ethanol	2 hours
100% Ethanol	2 hours
100% Ethanol	2 hours
100% Ethanol	2 hours
100% Ethanol	2 hours
Xylene	2 hours
Xylene	2 hours
Paraffin wax (55-56°C)	2 hours
Paraffin wax (55-56°C)	2 hours

Number of tissue samples

For this preliminary study, two (2) tissue blocks were randomly chosen each for the RHD and degenerative AS cases and compared with 2 cadaveric negative controls. Due to valvular tissue being collagenous and some calcified owing to disease we were restricted to this number. The tissues chosen had to withstand the harsh process of antigen retrieval which is part of the immunohistochemical process.

Immunohistochemistry method

Three-micron (3µm) paraffin wax embedded tissue sections were cut, picked up onto Histobond slides (Marienfeld-Germany) and heat-fixed on a hotplate for 10 - 15 minutes. Sections were de-waxed through xylene, cleared in ethanol and rehydrated in water.

Endogenous peroxidase activity was blocked by treating the slides with a 3% hydrogen peroxide (H_2O_2) solution for 10 minutes. Slides were properly washed in water. Antigen retrieval was performed by pressure-cooking slides in 10 mM Tris base, 1 mM EDTA (TEDTA) solution, pH9 or 0.01 M citric acid solution, pH 6 (refer to table 3.2) for 1 minute 30 seconds at full pressure. This was followed by washing in tap water. Thereafter, slides were rinsed with phosphate buffered saline solution (PBS pH 7.6), (Oxoid, Hampshire, England). Non-specific binding was blocked by treating slides with a 1% Bovine serum albumin solution (BSA), (Roche Diagnostics, Indianapolis, USA). Serum was then removed and tissue sections were incubated with primary antibody for the designated durations and dilutions at room temperature (see table 3.2). The slides were then washed well with PBS. This was followed by incubation with either the polyclonal DAKO envision labelled polymer or monoclonal variant (DAKO- USA) for 30 minutes at room temperature (see Table 3.2 and 3.3). Sections were washed well with PBS buffer. Positivity was developed by applying the chromogenic substrate 3.3 –diaminobenzidine (DAB), (DAKO- USA) for 5-10 minutes. Slides were washed in running tap water and counterstained with Mayer's haematoxylin for approximately 3 minutes (Appendix B). Sections were blued in ammoniated water. Finally, the slides were dehydrated through alcohols, cleared with xylene, and mounted with Entellan, (MERK- Germany).

Controls

To optimize each immunohistochemistry (IHC) run, a combination of a diagnostic tissue was used with a negative reagent control in which the primary antibody was swapped out for PBS. (see Table 3.2).

Table 3.2 Primary antibody information

Primary antibody	Clonality	Supplier	Antigen retrieval	Dilution	Incubation time	Diagnostic control
Beclin 1(BECN1)	G-11 Monoclonal	Santa Cruz	TEDTA	1:50	Overnight	Skeletal muscle
SQSTM1/p62	D5L7G Monoclonal	Cell Signalling	Citric acid	1:800	1 hour	Colon cancer
LC3A/B	D3U4C Polyclonal	Cell Signalling	Citric acid	1:100	Overnight	Lung cancer
BAX	2D2 Monoclonal	Santa Cruz	TEDTA	1:100	1 hour	Spleen
Bcl2	C2 Monoclonal	Santa Cruz	TEDTA	1:50	1 hour	Normal Colon
Caspase-3	E-8 Monoclonal	Santa Cruz	TEDTA	1:200	1 hour	Duodenum

Table 3.3 Secondary antibody information

Kits	Supplier
Envision HRP system labelled polymer anti-mouse	Dako – CA, USA
Envision HRP system labelled polymer anti-rabbit	Dako - CA, USA
Liquid DAB + substrate chromogen system	Dako - CA, USA

Preparation of reagents

In 1000 ml of distilled water, haematoxylin, aluminium potassium sulphate, and sodium iodate were dissolved. Thereafter, both chloral hydrate and citric acid were added and dissolved. This solution was then boiled for 10 minutes, cooled, and finally filtered (see details in Appendix B).

Tissue immunohistological analysis

Staining was assessed by two experienced pathologists who were unaware of the patients' medical and clinicopathological history. Detection of stroma and macrophages was performed by assessing the intensity, proportion and number of stroma and macrophages. Stromal and macrophage intensity was graded as 0,1,2,3 equivalent to, no staining, mild, moderate and strong respectively, whereas stromal and macrophage proportion was graded as 0, 1, 2, 3, 4, 5, as the percentage of the cells that are stained (i.e., 0 =No staining, 1= 1%, 2 = 2-10%, 3 = 10-32%, 4 = 33-66% and 5 = >66%). Number of macrophages were counted in 10 high per fields (HPF). The photographs were taken using the Olympus VS 120 slide microscope colour camera (Tokyo, Japan) at 20 x-magnification of objective lens of Olympus slide microscope with a total magnification of 200 x.

3.5 Statistical analysis

Normality of data was tested using the Shapiro-Wilk test. Normally distributed data are presented as mean ± standard deviation (SD) or, where highly skewed, as median (interquartile range); discrete data are presented as numbers (percentages). The chi-square test or Fisher's exact test was utilised to compare discrete data, as appropriate. Mann-Whitney U test was used to compare not normally distributed data. Bivariate correlations were assessed using the Pearson "R" and Spearman "R_S" coefficients, as appropriate. Linear regression analysis of determinants of myocardial inflammation, fibrosis and deformational characteristics was performed. All statistical tests were two-tailed, with p-values of less than 0.05 considered

statistically significant. All analysis was performed using SPSS version 26 (IBM, Armonk, New York, USA).

Chapter 4
Results

Multiparametric assessment of myocardial fibrosis in chronic rheumatic heart disease patients using cardiovascular magnetic resonance

4 Introduction

ARF and RHD, a delayed sequela of an immunological response to Group A β-haemolytic streptococcal (GAS) pharyngitis, is one of the leading CVD in SSA[1,13]. ARF patients frequently present with valvulitis at first episode,[154] subsequently resulting in established valvular disease in chronic RHD.[51] Sixty percent of ARF patients progress to chronic RHD after the first episode of ARF.[13]

LGE, a sensitive and reproducible technique in CMR remains the workhorse technique for myocardial characterisation and, evaluation of focal myocardial fibrosis.[155] Since LGE is based on extracellular space difference in different areas of the myocardium, making it difficult to sufficiently identify diffuse myocardial fibrosis, it is only useful in localised disease (such as seen in myocardial infarction).[153] Native T_1 and ECV have evolved to be useful biomarkers for evaluating diffuse fibrosis.[107] Myocardial ECV denotes the percentage of tissue volume equivalent to the extracellular space, this increases in the presence of diffuse fibrosis and inflammation.[156] ECV is effective in visualising and quantifying both focal and diffuse myocardial fibrosis of ischaemic or non-ischaemic aetiology.[157,158] There are limited data of tissue characterisation in RHD patients. [155,159] Therefore, we aimed to investigate the presence of myocardial fibrosis using CMR, T1 mapping and ECV in chronic RHD.

4.1 Methods

Patient

Forty-seven (47) patients, confirmed with RHD were enrolled between August 2017 and August 2019, at the Cardiac Clinic of the Groote Schuur Hospital, Cape Town. Patients with pericardial disease, coronary heart disease, concomitant congenital heart disease, cardiomyopathy, hypertension, hyperthyroidism, any other valvular abnormality not of RHD aetiology and, any contraindication for CMR (severe renal dysfunction, estimated glomerular filtration rate (eGFR) <30 mL/min, electronic or metallic implant, pregnant, claustrophobic, and unable to lay still during the examination) and suboptimal imaging data were excluded from the study.

The Human Research Ethics Committee of the University of Cape Town's Faculty of Health Sciences reviewed and granted ethical clearance (HREC REF: 554/2017), with a written informed consent obtained for all the enrolled participants. Data collection only commenced after approval from the UCT HREC was obtained. The study protocol obeyed the ethical guidelines of the 2013 Declaration of Helsinki.

CMR protocol

For CMR, eligible participants were scanned with a 3T MRI Siemens Magnetom Skyra scanner with an 18-channel phased array body coil and integrated spine coils (Siemens, Erlangen, Germany). LV volumes and masses were obtained during expiratory breath-hold for approximately 12 seconds and were prospectively ECG gated. LV volumes and mass were acquired using a standard CMR protocols (3T MRI Siemens Magnetom Skyra scanner, Siemens, Erlangen, Germany). Balanced steady-state-free-precession imaging (repetition time = 43.08 ms, echo time = 1.61 ms, flip angle = 40 deg, matrix size = 149 x 208, bandwidth = 962Hz/Px, slice = 8 mm thickness, 25 phases). SSFP imaging was acquired over 9 heartbeats per slice. SSFP cines were performed to obtain the long axis cines and a contiguous short axis

stack for assessment of LV volumes, mass, and EF. LGE imaging was performed 6-15 minutes after gadolinium administration, and acquired using a short axis stack, 2 chamber, 4 chamber, and LVOT images to assess focal myocardial fibrosis. A standard dose of 0.2 mmol/kg of gadolinium-DTPA (Magnevist, Bayer, South Africa) was administered intravenously in patients with preserved renal function (eGFR>30 ml/min). Early gadolinium imaging was acquired in short stacks using a PSIR for the assessment of the presence of thrombus.

CMR image analysis

To analyse the LV volumes, including the LVEDV, LVESV, LVEF and LVM, the endocardial and epicardial contours of the LV were manually drawn from a stack of short-axis slices, excluding the papillary muscles on CVI42® software (Circle Cardiovascular Imaging, Calgary, Alberta). These parameters, except for LVEF, were indexed to the body surface area.

Tissue characterisation

The presence and extent of LGE was done by two readers with >5 years of CMR experience and blinded to the diagnosis of participants. The assessment of cardiac function and chamber sizes were performed in standard views in the long-axis (horizontal and vertical) and short-axis planes. To visually quantify LGE, we performed a manual planimetry of all highly enhanced pixels on the short axis stacks of LGE images. For comparison, a semi-automated gray-scale threshold technique was performed using 2 SDs above the mean signal intensity of the normal nulled myocardium and 2 SDs above noise (i.e., mean signal intensity of a region located outside the body). LGE quantity was expressed in grams and as a percentage of the total LV myocardial mass: $\left(\left(\frac{\mathrm{MLGE}}{\mathrm{MM}}\right) X\ 100\right)$, with LGE mass ($M_{LGE}$), and myocardial mass ($M_M$) in

grams.[160] We recorded variables such as presence or absence of LGE, distribution patterns of LGE in different areas of the myocardium, and valvular enhancement. We defined myocardial fibrosis as a region of LGE with higher signal enhancement than the signal intensity of non-enhanced portion of the myocardium. EF for the LV was assessed with the following formula:

$$Ejection\ fraction\ (EF) = \frac{EDV - ESV}{EDV}$$

EDV, end diastolic volume, ESV, end systolic volume.

For the T1 and T2 mapping, CVI42® software was used to process the images. Each ECV measurement was obtained by subtracting pre- and post-contrast maps with haematocrit correction, which is usually obtained approximately 15 minutes after the administration of contrast. The standard formula used is as follows:

$$ECV = (1 - heamatocrit) * \{1/\text{T1 post contrast (myo)} - 1/\text{T1 pre} - \text{contrast (myo)}\} / \{1/\text{T1 post contrast (blood)} - 1/\text{T1 pre} - \text{contrast (blood)}\}$$

Statistical data analysis

Normality of data were tested using the Shapiro-Wilk normality test. Normally distributed data are presented as mean ± standard deviation (SD) or, where highly skewed, as median (interquartile range); non-parametric data are presented as numbers (percentages). The Chi-square test or the Mann-Whitney U test were utilised for non-parametric data. Unpaired samples between groups were assessed by the unpaired 2-tailed Student t test. Correlation was assessed using the Pearson's 'R' coefficient, as appropriate. All statistical tests were two-tailed,

with p-values of less than 0.05 considered statistically significant. All analysis were performed using SPSS version 25 (IBM, Armonk, New York, USA).

4.2 Results

Forty-seven patients (62% female), matched with 30 healthy participants were included in the study. The mean age of the study population was 42 ± 12.8 years vs. 39 ± 12.3 years for RHD and healthy participants, respectively. As expected, RHD patients were matched in height, weight, BMI and BSA compared to controls (Table 4.1). Over half (55%) of patients with RHD reported symptoms of effort intolerance (NYHA Class II, 32%; NYHA Class III 23%). AF, secondary to RHD, was noted in 27.3% of patients. Hypertension (32%) and smoking (15%) were the most commonly encountered co-morbidities in the RHD group. There were no reported symptoms or co-morbidities in the control group. RHD patients showed an increased indexed LVEDV, LVESV, LVSV and LV mass compared to controls (all $p<0.001$). LVEF was significantly lower in RHD (45 ± 12.5%) compared to controls (57 ± 5.2%), $p <0.001$). LV myocardial mass index (LVMi) was significantly increased in RHD compared with controls (60 ± 30.7 g/m^2 vs. 32 ± 8.38 g/m^2, $p<0.001$). There was significant LA dilatation in RHD patients compared to controls (42 ± 12.3 mm versus 22 ± 3.13 mm, p=001). Increased indexed RVEDV, RVESV, RVSV were observed in RHD compared to controls. RVEF was significantly lower in RHD compared to controls (41 ± 15.9% versus 54 ± 7.5%, p=0.001) (Table 4.2).

LGE was evident in all 47 (100%) patients with confirmed RHD, with linear (26%), patchy (36%) and diffuse (38%) patterns of enhancement. Mitral valve enhancement was evident in 29 (62%) patients, while aortic valve enhancement was seen in 2 (4%) of these patients.

Other notable findings included pericardial effusion in 3 (7%), and myocardial crypts in 1 (2%) of RHD patients (Table 4.3).

Native T1 times were elevated in RHD (1280 ± 55.9 ms versus 1213 ± 33.3 ms, p=0.004) (Figure 4.1). ECV was elevated in RHD (36 ± 0.05% versus 28 ± 0.01%, p<0.001) (Figure 4.1, 4.2, 4.3 and 4.4).

Table 4.1 Demographics of RHD patients and controls

Parameters	Patients (n=47)	Controls (n=30)	P-values (p<0.05)
Age, years	42 ± 12.8	39 ± 12.3	0.28
Sex (Female), n (%) (Male)	29(62) 18(38)	16(53) 14(47)	0.49 0.49
Heart rate, bpm	82 ± 28.0	73 ± 15.9	0.07
Height, m	1.6 ± 0.1	1.7 ± 0.1	0.53
Weight, kg	77 ± 21.8	77 ± 19.4	0.96
BMI, kg/m^2	28 ± 7.3	28 ± 5.7	0.68
BSA, m^2	1.9 ± 0.3	1.9 ± 0.3	0.84
NYHA, n (%)			
NYHA I NYHA II NYHA III NYHA IV	21 (44.7) 15(31.9) 11 (23.4) 0(0)	- - - -	- - - -
Comorbidities			
Hypertension, n (%)	15 (32)	-	-
Dyslipidaemia, n (%)	1 (0.02)	-	-
Obesity, n (%)	1 (0.02)	-	-
HIV, n (%)	2 (0.04)	-	-

Smoking, n (%)	7 (15)	-	-
Hyperthyroidism, n (%)	1 (0.02)	-	-
Anaemia	1 (0.02)	-	-
Diabetes	2 (0.04)	-	-
Gout	1(0.02)	-	-

Continuous data are mean ± SD unless otherwise indicated. Characteristics are presented as 95% confidence interval (CI). bpm beats per minute; m, meter; kg, kilograms; BMI, body mass index; BSA, body surface area.

Table 4.2 CMR characteristics of the RHD patients and controls

Parameters	Patients (n=47)	Controls (n=30)	P-values (p<0.05)
LVEDV*i*, ml/m^2	113 ± 34.8	74 ± 13.4	0.001
LVESV*i*, ml/m^2	55 ± 18.8	32 ± 8.4	0.001
LVSV*i*, ml/m^2	46 ± 18.7	42 ± 7.5	0.001
LVEF, %	45 ± 12.5	57 ± 5.2	0.001
LVM*i*, g/m^2	60 ± 30.7	32 ± 8.4	0.001
LA diameter, mm	42 ± 12.3	22 ± 3.1	0.001
RVEDV*i*, ml/m^2	77 ± 24.8	74 ± 13.5	0.31
RVESV*i*, ml/m^2	47 ± 21.7	34 ± 9.6	0.01
RVSV*i*, ml/m^2	33 ± 14.2	39 ± 7.3	0.04
RVEF, %	41 ± 15.9	54 ± 7.5	0.001

Continuous data are mean ± SD, unless otherwise indicated. Values are indexed to body surface area. LVEDVi, left ventricular end-diastolic volume index; LVESVi, left ventricular end-systolic volume index; LVSVi, left ventricular systolic volume index; LVEF, left ventricular ejection fraction; LVMi, left ventricular mass index; LA, Left atrium; RVEDVi, right ventricular end-diastolic volume index; RVESVi, right ventricular end-systolic volume index; RVSVi, right ventricular systolic volume index; RVEF, right ventricular ejection fraction; RA, right atrium.

Table 4.3 Late gadolinium enhancement, tissue characterisation and other findings in RHD patients and controls

Parameters	Patients (n=47)	Controls (n=30)	P-value (p<0.05)
Presence of LGE n (%)	47 (100)	6 (27)	0.001

Valvular enhancement n (%)	32 (68)	-	-
Myocardial T1 SI ratio, %	0.9 ± 0.5	0.9 ± 0.1	0.98
Myocardial T2 STIR SI ratio, %	1.3 ± 0.3	1.5 ± 0.2	0.02
Pericardial effusion, n (%)	46 (98)	-	-
Pleural effusion, n (%)	3 (7)	-	-
Crypts, n (%)	1 (2)	-	-

Continuous data are mean ± SD unless otherwise indicated. LGE, late gadolinium enhancement; SI, signal intensity. Values are presented as mean ± standard deviation (SD).

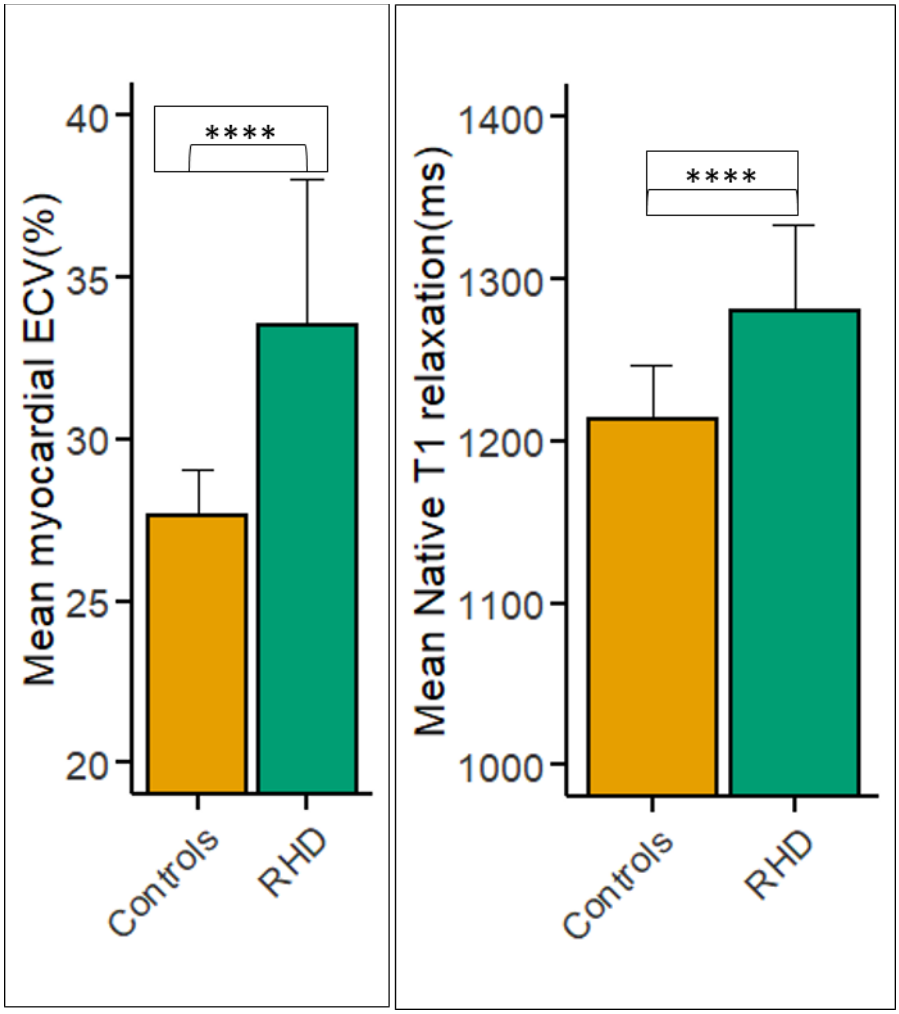

Figure 4.1. Tissue characteristics of RHD patients and controls
Graphs showing elevated ECV and native T1 values in RHD patients compared with controls. *p<0.05.

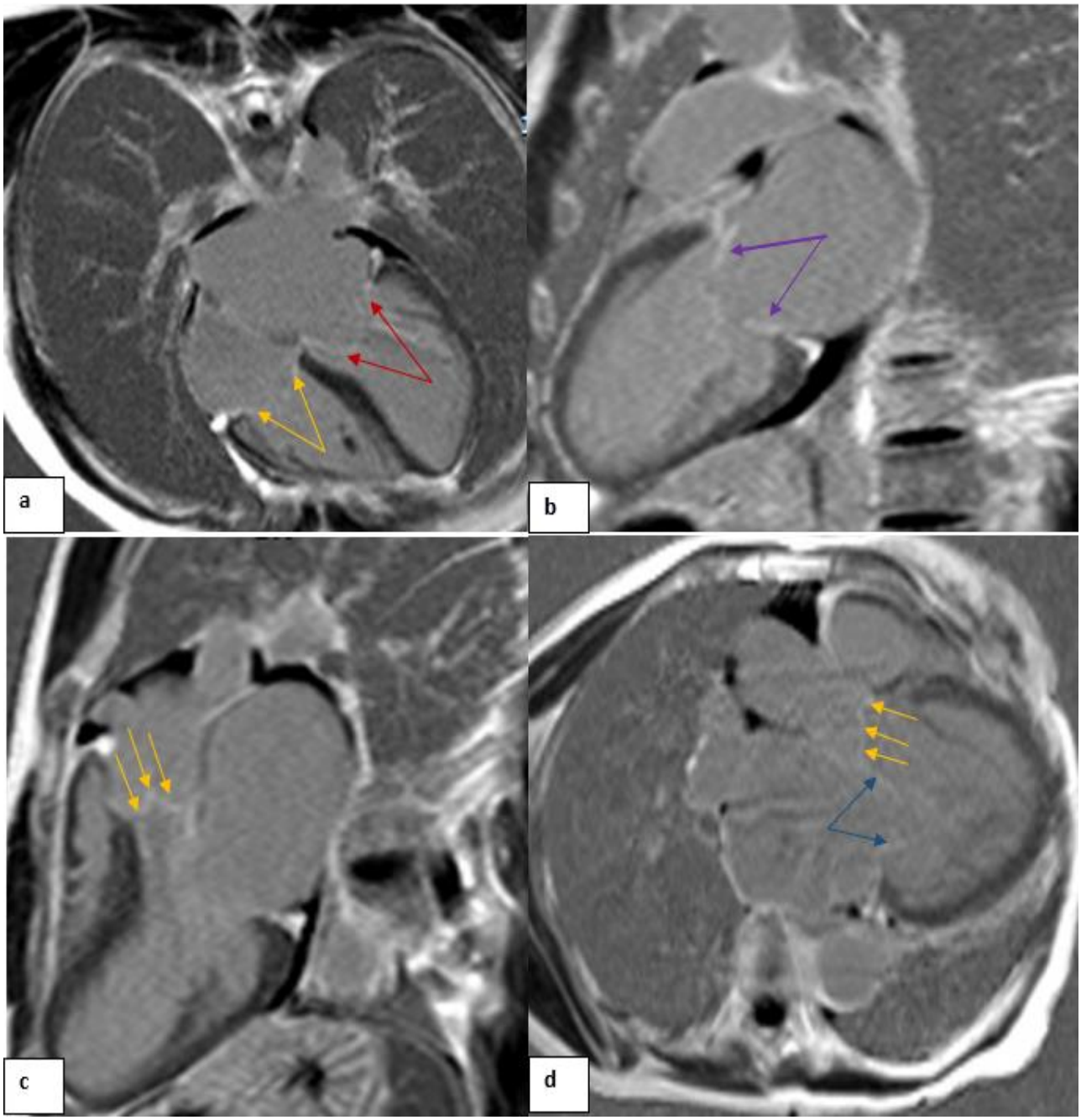

Figure 4.2. Subtle valvular enhancement in RHD
a) 4-CH showing mitral and tricuspid valve enhancement indicated by red and orange arrows respectively. b) 2-CH showing mitral valve enhancement indicated by purple arrows. c) 3-CH showing aortic valve enhancement indicated by orange arrows. d) 3-CH showing aortic and mitral valve enhancement indicated by orange and blue arrows respectively.

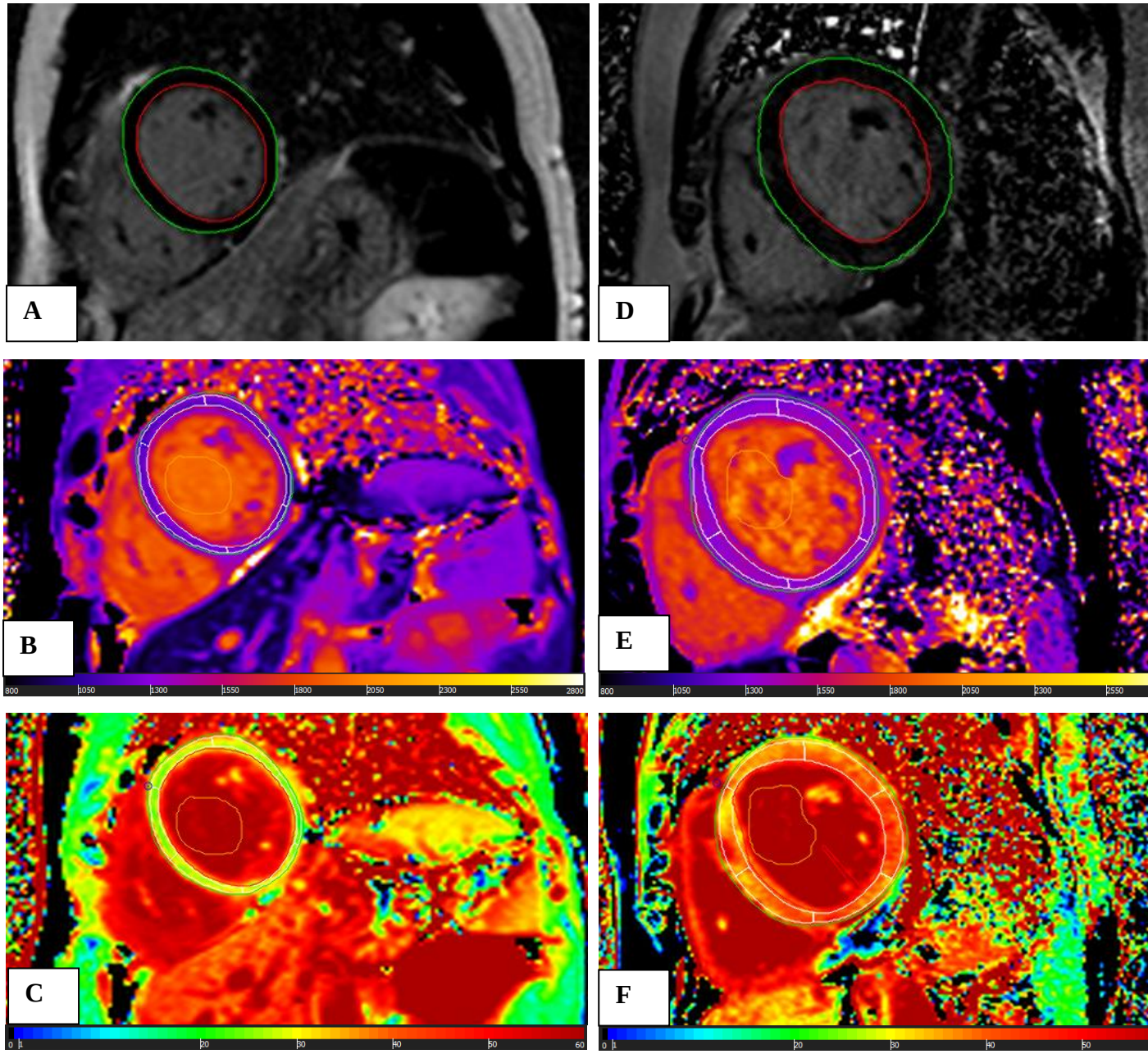

Figure 4.3. **Multi-parametric tissue characterisation at mid-slice in rheumatic heart disease compared to controls.**
On ECV-maps, red areas represent ECV greater than 30%. T1-mapping was done using a modified Look-Locker Inversion Recovery (MOLLI) pulse sequence on 3T Siemens Magnetom Skyra scanner (Siemens, Erlangen, Germany). Multi-parametric tissue characterization at mid-slice in rheumatic heart disease (EF = 52, EDD = 61 mm, T1 = 1348 ms, ECV = 42%) and healthy control (EF = 51, EDD = 48 mm, T1 = 1183 ms, ECV = 28%) reveals an LGE image with no evidence of focal LGE but diffusely increased native T1 values and high ECV values.

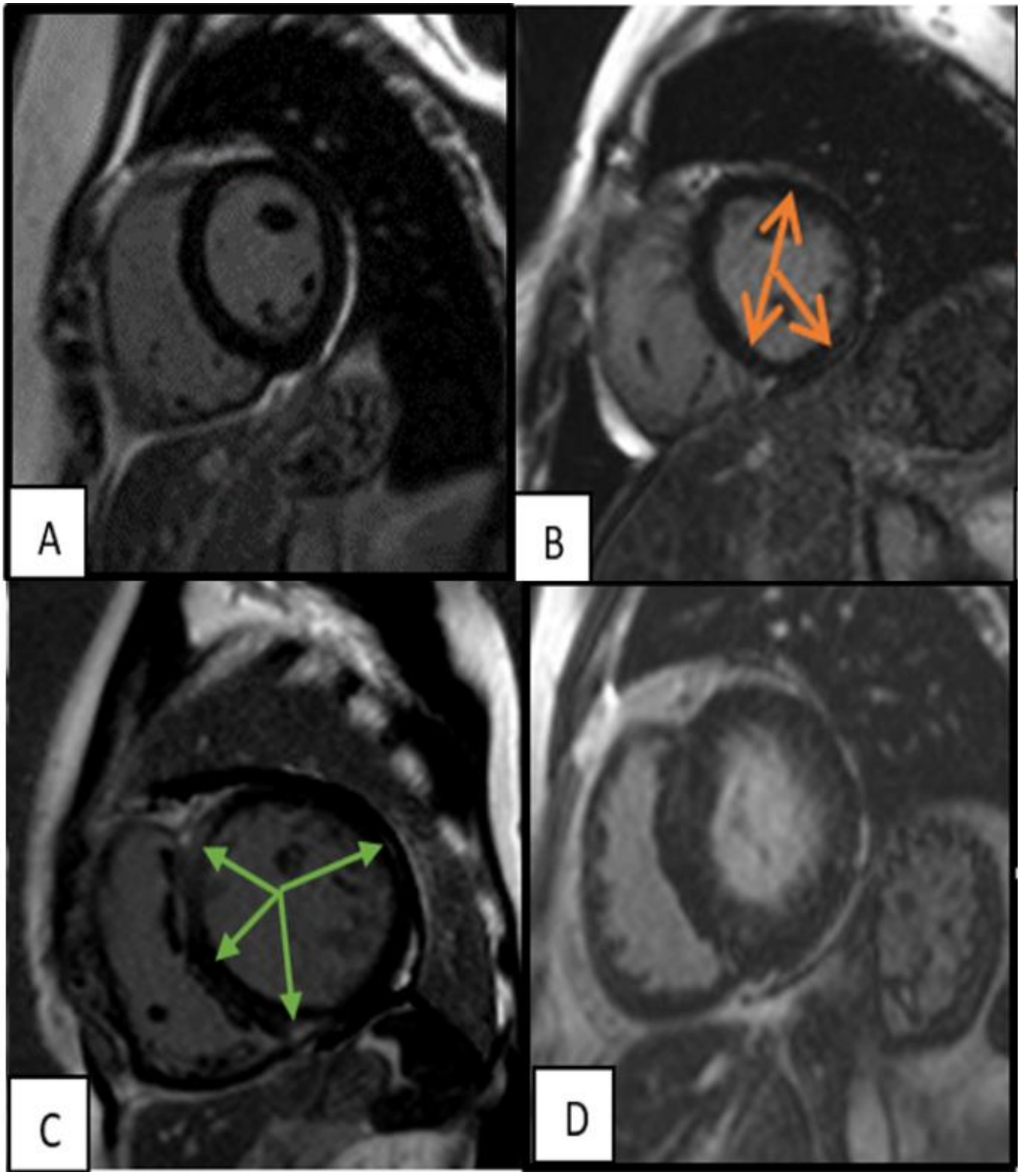

Figure 4.4. Patterns of LGE in RHD
A) Healthy control with no LGE. B) Patchy mid-wall enhancement in all segments of the LV myocardium - orange arrows. C) Linear mid-wall enhancement in all segments green arrows. D) Diffuse enhancement involving the entire myocardium

4.3 Discussion

CMR is the gold-standard imaging modality for the investigation of various CVD of different aetiologies,[161–165] and allows full characterisation of morphological, functional, metabolic, tissue and haemodynamic outcomes of cardiovascular pathologies.[18] In this study, we assessed myocardial fibrosis using a multiparametric CMR protocol to assess the structural and functional cardiac changes in patients with chronic RHD. Forty-seven patients known with RHD, with a predominance of females (64%) and NYHA functional classification ranging between I to III were investigated, and compared to 30 age- and sex matched, healthy volunteers. CMR detected myocardial fibrosis in all patients (majority of patients had moderate to severe mitral valve regurgitation, followed by mitral stenosis, aortic stenosis, and aortic regurgitation). The key findings in our study include abnormal biventricular systolic function, biatrial enlargement, and high incidence of fibrosis throughout myocardium in those with RHD, and elevated native T1 values and ECV. Myocardial fibrosis is demonstrably frequent in RHD patients with advanced disease and may be one of the mechanisms through which clinical complications, including arrhythmias and heart failure, may be mediated.

RHD is the main pathological cause of valvular heart disease in children and young adults in LMICs.[148,166] MR is the most prevalent valve lesion in RHD, followed by MS, AR and AS.[81] Chronic RHD is characterised by subclinical inflammation and diffuse myocardial fibrosis.[167] Several inflammatory mediators that attract proinflammatory cytokines and other soluble mediators, are involved in the initiation and maintenance of the inflammatory process in RHD, characterised by local inflammation and tissue injury with subsequent cellular matrix disorganisation, which ultimately results in LV remodelling as well as valve tissue changes, leading to regurgitant and stenotic lesions.[83,168]

LGE imaging uses the principle of relative difference in volume of distribution of intravenously administered gadolinium (and subsequent variation of longitudinal relaxation (T1) times) between normal and abnormal myocardium.[18] LGE is a sensitive, specific and reproducible measure of focal myocardial fibrosis and predicts prognosis in patients with ischaemic and non-ischemic cardiac disease.[169–171] In this study, LGE was evident in all RHD patients; observed patterns of enhancement were: linear (26%), patchy (36%) and diffuse (38%); LGE was observed in 20% of controls (p=0.001). Contrastingly, Meel and colleagues reported LGE in 18% of RHD patients, who did not have the same extent of disease severity as in our study.[172] LGE has also been reported in the atrial walls of 3 patients chronic RHD.[173] In our study, LGE was observed in the atrial walls of 73% of RHD patients: LGE in LA and RA (50%), LGE in LA only (23%), and LGE in RA only (2%). We also observed RV free wall enhancement in 1 patient. In addition, we observed valve enhancement mitral valve 62%, aortic valve 4% and tricuspid valve 2% (Table 4.3). RHD predominantly affects the mitral valve, while the involvement of aortic valve was observed in 20-30% of cases (usually in combination with mitral valve involvement, and the tricuspid valve may be less commonly affected.[1,14] Multivalvular involvement and evidence of fibrosis in valves, atria and LV likely reflect a combination of both haemodynamic and inflammatory changes in RHD patients.[18,101]

T1 mapping is effective for identifying diffuse myocardial fibrosis and other changes which may be difficult to quantify with LGE.[103] T1 mapping relies on a pixel-wise illustration of absolute T1 relaxation times in the myocardium, allowing direct T1 quantification. In this study, mean native T1 values were elevated in RHD patients. A diagnosis of diffuse fibrosis based on elevated native T1 values is further corroborated by the prevalent LGE findings in our patient cohort. We also found significantly increased ECV values in RHD.

Taken together, we used a multiparametric CMR approach to assess myocardial, atrial and valve phenotypes in RHD. Evidence of myocardial fibrosis on LGE imaging in all patients was observed. Similarly, enhancement of the mitral and aortic valves was common, as was atrial enhancement. Further, we observed significant differences in LV functional parameters, with reduction in systolic function and increased LV dimensions in those with RHD. Native T1 and ECV values were elevated in RHD patients, further support for prevalent myocardial fibrosis in this cohort.

Our study has some limitations. These include a small sample size, inclusion of only RHD patients with advanced disease, and referral bias as these cases were recruited from a tertiary/quaternary academic centre. Notwithstanding these limitations, significant differences were observed between RHD and demographically matched controls.

In conclusion, we studied echocardiographically diagnosed RHD patients recruited just before valve replacement surgery and demonstrated abnormal valve function – moderate to severe mitral valve regurgitation, followed by mitral stenosis, aortic stenosis, and aortic regurgitation – and impaired LV systolic function. In addition, frequent myocardial fibrosis was detected on LGE, native T1 and ECV imaging. We postulate that fibrosis may be a central mechanism through which RHD complications like heart failure and arrhythmia are mediated. There is a paucity of literature on CMR in RHD to compare from, with most of the available studies and case reports limited by small sample sizes. CMR may be a valuable tool for diagnosis, assessment of severity and tracking of disease progress in RHD.

4.4 Acknowledgements

We appreciate the patients who voluntarily took part in this research. In addition, we thank staff at the Cape Universities Body Imaging Centre, including Mrs Patricia Maishi and

Marianne Jafta. Prof. Ntusi gratefully acknowledges support from the South African Medical Research Council, National Research Foundation and the Lily and Ernst Haussmann Trust. This research has been supported by the National Research Foundation by grants to Professors Skatulla and Ntusi (Grant Nos. 104839 and 105858).

4.5 Conflict of interests

None

Chapter 5
Results

Myocardial strain in chronic rheumatic heart disease patients and its association with native T1 and ECV

5 Introduction

RHD, an autoimmune disease characterised by myocardial inflammation and fibrosis, can result in severe clinical complications, including arrhythmias, heart failure, pulmonary hypertension, thromboembolism, and sudden cardiac death.[174] Myocardial strain imaging has been shown detect early contractile abnormality in various CVD such as RHD,[175] and provides a noninvasive and reproducible technique to evaluate cardiac mechanics.[176] Myocardial strain quantifies the degree of distortion of a myocardial area from its initial length to its maximum length, in the longitudinal, circumferential and radial directions.[177]

Longitudinal strain describes the longitudinal shortening from the base to the apex. Radial strain represents the LV thickening and thinning motion during the cardiac cycle. Circumferential strain is derived from LV myocardial fibre shortening across the circular perimeter in short axis view[178,179] CMR employs various techniques for assessing strain and strain rate, with feature tracking being widely used due to its reliance on acquired cine images, without the need for additional sequences [180–184] Previous research have demonstrated good agreement between strain parameters derived from tissue tagging and feature tracking.[185]

CMR-derived native T1, ECV and strain are noninvasive biomarkers of myocardial fibrosis.[186,187] The usefulness of T1 mapping indices have been reported to sufficiently identify subclinical myocardial involvement in systemic sclerosis and systemic lupus erythematosus; with these indices suggesting subclinical inflammation, myocardial infiltration and/or

interstitial fibrosis in patients with no history of previous cardiac diseases.[188,189] Focal fibrosis on LGE was reported in 46% of rheumatoid arthritis patients, with strong correlation observed when myocardial native T1 and ECV were correlated with myocardial strain, compared with control subjects.[122] Incidence of myocardial fibrosis of 18% due to increased collagen degradation has been reported in RHD,[190] however, the authors did not perform T1 mapping and ECV. In the present study, we sought to investigate the relationship of CMR-derived myocardial strain in patients with chronic RHD and their association with native T1 and ECV.

5.1 Methods

Patient population and study design

Between August 2017 and August 2019, forty-seven (47) eligible patients were enrolled from the Cardiac Clinic of the Groote Schuur Hospital and scanned at the Cape Universities Body Imaging Centre (CUBIC), in Cape Town, South Africa. Patients between the ages of 18 and 65 with a diagnosis of echocardiographically confirmed RHD referred for valve replacement surgery were included. Exclusion criteria were a diagnosis of coronary artery disease, concomitant congenital heart disease, non-rheumatic valvular heart disease, hypertension, cardiomyopathy, pregnancy, any contraindication to CMR (severe renal dysfunction – estimated glomerular filtration rate (eGFR) < 30 ml/min, metallic implants, claustrophobia, and inability to lay still during the examination) and suboptimal imaging data.

The Human Research Ethics Committee of the University of Cape Town Faculty of Health Sciences reviewed and granted ethical clearance (HREC REF: 554/2017), with informed consent obtained from all the enrolled participants. The study protocol also agrees with the

ethical guidelines of the 2013 Declaration of Helsinki as reflected in a prior approval by the institution's human research committee.

CMR imaging protocol

Eligible participants were scanned with a 3T MRI Siemens Magnetom Skyra scanner (Siemens Health Systems, Erlangen, Germany) with an 18-channel phased array body coil. Left ventricular (LV) volumes and masses were obtained during expiratory breath-hold for approximately 12 seconds and were prospectively electrocardiographic (ECG) gated. LV volumes and mass were acquired using a standard CMR protocols). SSFP imaging (acquired over nine heartbeats per slice) was conducted to obtain the long-axis cines and a contiguous short axis stack cines for assessment of LV volumes, mass, and EF. The imaging parameters were as follows: repetition time/echo time, 43.08/1.61 ms, flip angle = 40^{o}, field of view = 350 – 410 mm, matrix size = 149 x 208 pixels, Bandwidth = 962Hz/Px, slice thickness = 8 mm, 25 phases.

LGE imaging, including a short axis stack, 2 chamber, 4 chamber, and LVOT images was performed 6-15 minutes after intravenous injection of gadolinium contrast agent (Gadolinium-DTPA, Magnevist, Bayer, South Africa) at 0.2 mmol/kg and 2 ml/s, followed by a 20 ml saline flush, using PSIR. The imaging parameters were as follows: TR/TE =750/1.96ms, flip angle = 20°, matrix =140 x 256, slice thickness = 8mm.

CMR imaging analysis

Three observers (OA, PS and SJ) visually assessed individual scans. Conflicting opinions were resolved by the fourth observer (NABN) (with over 10 years of CMR experience and blinded to the diagnosis of participants) before we reached a consensus. Two (2) images with poor

quality were excluded from further analysis. The CMR images were analysed on CVI42® software (Circle Cardiovascular Imaging, Calgary, Alberta, Canada) at CUBIC. To calculate the LV and right ventricular (RV) end diastolic volume (EDV), end systolic volume (ESV), stroke volume (SV), EF and LV mass, LV endocardial and epicardial borders were manually contoured from a stack of short-axis slices, excluding the papillary muscles. Then, biventricular end diastolic volume, end systolic volume, stroke volume and EF, and LV mass were indexed to the body surface area.

Tissue characterisation

The presence and extent of LGE were observed on a workstation using CVI42® software, ensuring minimal error and bias. To visually quantify LGE, we performed a manual planimetry of all highly enhanced pixels on the short axis stacks of LGE images. For comparison, a semi-automated gray-scale threshold technique was performed using 2SDs above the mean signal intensity of the normal nulled myocardium and 2 SDs above noise (i.e., mean signal intensity of a region located outside the body). LGE quantity was expressed in grams and as a percentage of the total LV myocardial mass: $\left(\left(\frac{\mathrm{MLGE}}{\mathrm{MM}}\right) X\ 100\right)$, with LGE mass ($M_{LGE}$), and myocardial mass ($M_M$) in grams.[160] We recorded variables such as presence or absence of LGE, distribution patterns of LGE in different areas of the myocardium, valvular and atrial enhancement. We defined myocardial fibrosis as a region of LGE with higher signal enhancement than the signal intensity of non-enhanced myocardium.

We calculated LVEF using the following formula:

$$Ejection\ fraction\ (EF) = \frac{EDV - ESV}{EDV}$$

ESV, end systolic volume EDV, end diastolic volume.

We used CVI42® software to postprocess and, analyse the images for the T1 and T2 mapping. Each ECV measurement was obtained by subtracting pre- and post-contrast maps with haematocrit correction, obtained approximately 15 minutes after the administration of contrast. The standard formula used is as follows:

$$ECV = (1 - haematocrit) * \{1/\text{T1 post contrast (myo)} - 1/\text{T1 pre} - \text{contrast (myo)}\} / \{1/\text{T1 post contrast (blood)} - 1/\text{T1 pre} - \text{contrast (blood)}\}$$

Myocardial strain analysis

Feature tracking-CMR (FT-CMR) analysis was performed using CVI42® software (Tissue Tracking, Circle Cardiovascular Imaging, Calgary, Alberta, Canada). Epicardial and endocardial borders of all slices were manually traced during the LV end diastolic phase from SSFP cine images; and the drawn contour was subsequently projected and automatically propagated on the consecutive frames throughout the cardiac cycle. These contours were reviewed in every phase and manually corrected to optimise endocardial tracking. We excluded the papillary muscles and endocardial trabeculae, re-tracked and the algorithm reapplied in cases of unsatisfactory visual assessment. Short-axis SSFP cine images were used to derive the global strain in the longitudinal (LS), radial (RS), and circumferential (CS strain) directions. Segmental global systolic RS and CS were also calculated automatically (Figure 5.1).

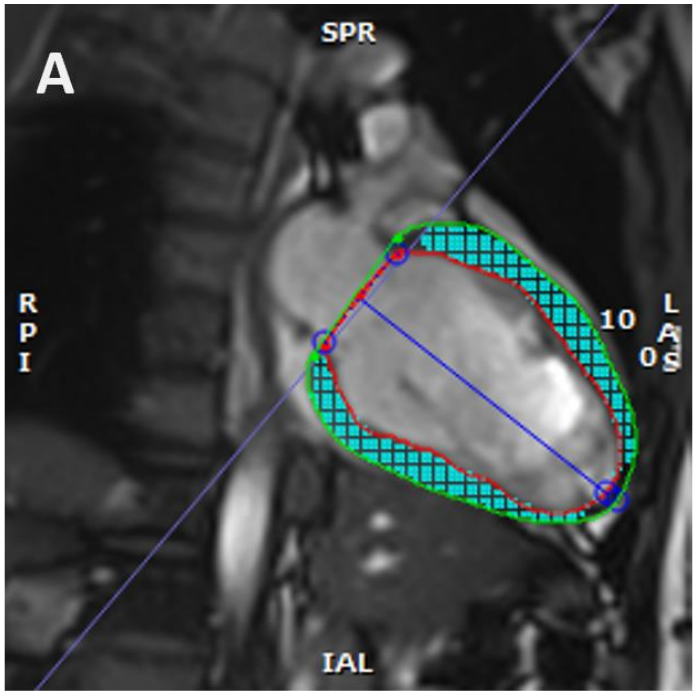
A
SPR
R
P
I
10
0
L
A
S
IAL

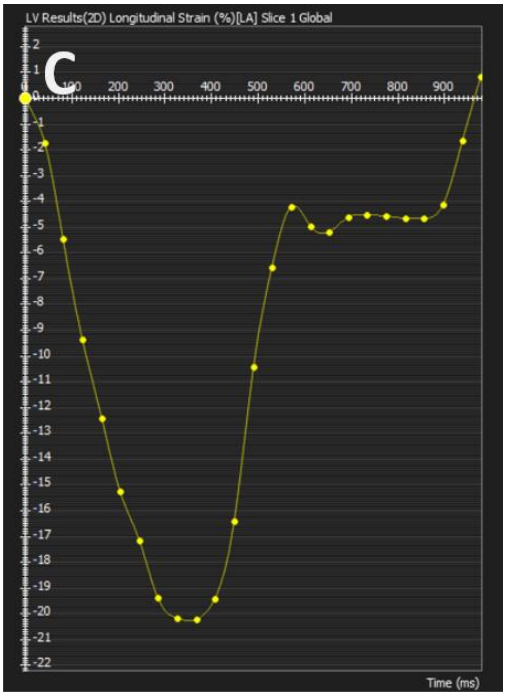
LV Results(2D) Longitudinal Strain (%)[LA] Slice 1 Global
C
Time (ms)

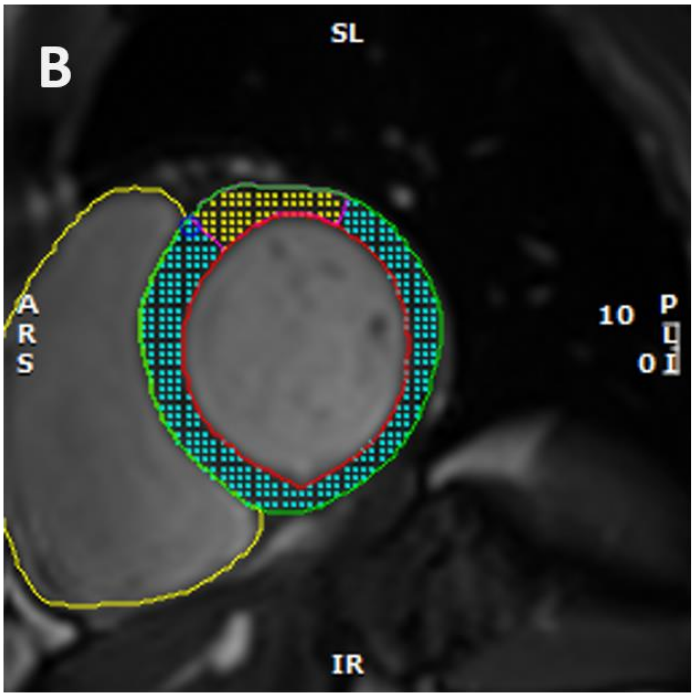
B
SL
A
R
S
10
0
P
I
IR

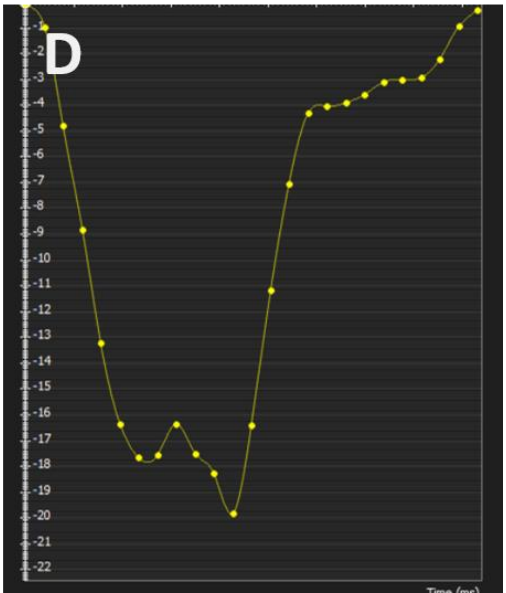
D
Time (ms)

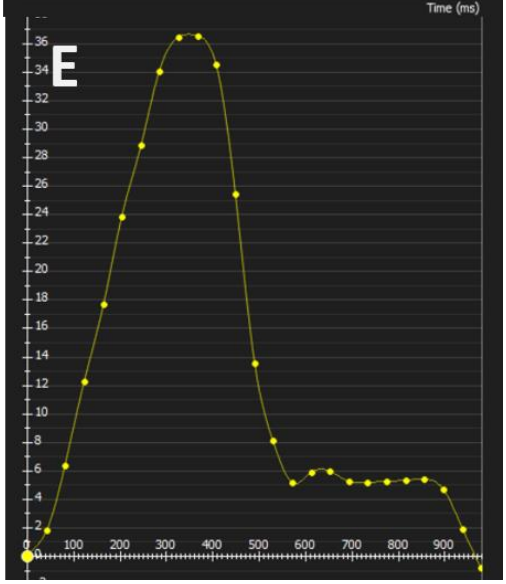
E

Figure 5.1. Example of coloured strain analysis with a feature tracking software (Circle CVI42®). From 4-CH long-axis, SSFP cine image (a) longitudinal strain curve is derived (b) and short-axis SSFP image (c) is used for calculating circumferential (d) and radial strain curves (e)

Statistical data analysis

All analysis were performed using SPSS version 25 (IBM, Armonk, New York, USA). Normality of data were tested using the Shapiro-Wilk normality test. Normally distributed data were presented as mean ± standard deviation (SD), categorical variables as median (interquartile range); and non-parametric data as numbers (percentages). The Mann-Whitney U test were utilised for non-parametric data. Unpaired samples between groups were assessed by the unpaired 2-tailed Student t test. Correlation was assessed using the Pearson's 'R' coefficient, as appropriate. All statistical tests were two-tailed, with p-values of less than 0.05 considered statistically significant.

5.2 Results

Out of forty-seven patients included in the study, there were 29 (62%) females and 18 (38%) males. The mean age of the study population was 42 ± 12.8 versus 39 ± 12.3 years for RHD patients and healthy controls, respectively. Due to adequate matching, there were no significant differences in height, weight, BMI and BSA in RHD patients compared to controls.

We observed a significantly lower LVEF in patients compared to controls (45 ± 12.5% versus 57 ± 5.2%, $p < 0.001$). LA diameter significantly increased in patients compared with controls (42 ± 12.3 mm versus 22 ± 3.1 mm, $p<0.001$).

Native T1 mapping values were significantly elevated in RHD (1280 ± 55.9 ms versus 1213 ± 33.3 ms, p<0.001). ECV values were significantly elevated in RHD (33 ± 4.4% vs. 28 ± 0.01%, p<0.001). T2 values were similar in RHD patients compared to controls (39 ± 2.9 ms vs. 39 ± 2.4 ms, p = 0.75) (Table 5.2).

Global radial strain, and diastolic radial strain rates were significantly reduced in RHD (25.4 ± 9.8% vs. 30.8 ± 10.5%, p=0.027 and -1.7 ± 0.8 s^{-1} vs. -2.2 ± 0.9 s^{-1}, p=0.008) respectively, compared to controls, whereas systolic radial strain rate was similar to control (1.6 ± 0.9 s^{-1} vs. 1.7 ± 0.9 s^{-1}, p=0.592) (Table 5.3). Global circumferential strain, systolic and diastolic circumferential strain rates were significantly lower in RHD patients (-17.7 ± 4.7% vs. -21.1 ± 2.7%, p=0.001; -0.9 ± 0.3 s^{-1} vs. -1.1 ± 0.2 s^{-1}, p=0.003; and 0.9 ± 0.3 s^{-1} vs. 1.5 ± 0.4 s^{-1}, p=0.001), respectively (Table 5.3), compared to controls. We observed a significantly reduced global longitudinal strain, systolic and diastolic longitudinal strain rates in RHD patients (-15.1 ± 6.5% vs. -20.2 ± 2.9%, p=0.001; -0.8 ± 0.4 s^{-1} vs. -1.0 ± 0.2 s^{-1}, p=0.018), respectively compared to controls (Table 5.3).

Linear regression analysis showed a significant moderate correlation between native T1, and global circumferential and longitudinal strains (r=0.29*, CI= [0.08, 0.5], p=0.01; and r=0.32**, CI= [0.12, 0.50], p<0.001 respectively] (Figure 5.1). There was a moderate correlation between native T1 and circumferential and longitudinal systolic strain rates [(r=0.29**, CI= [0.09, 0.48], p<0.01; and r=0.26*, CI= [0.09, 0.41], p<0.03 respectively] (Figure 5.2).

There was significant moderate correlation between ECV and, global circumferential strain and circumferential systolic rates [(r=0.28*, CI= [0.11, -0.48], p=0.02; and r=0.29*, CI= [0.12, 0.48], p=0.01 respectively] (Figure 5.3). There was a significantly moderate correlation between ECV and radial longitudinal diastolic strain rates [(r=0.27**, CI= [0.09, 0.44], p=0.02;

and, r=-0.27*, CI= [-0.41, -0.15], p=0.02 respectively] whereas a strong correlation was noticed between ECV and circumferential diastolic strain rates [(r=-0.44**, CI= [-0.56, -0.31], p<0.001)] (Figure 5.4).

Table 5.1 Demographic, clinical features, and CMR characteristics of RHD patients and controls

Parameters	Patients (n=47)	Controls (n=30)	P-values (p<0.05)
Age, years	42 ± 12.8	39 ± 12.3	0.28
Sex (Female), n (%) (Male)	29(62) 18(38)	16(53) 14(47)	0.49 0.49
Heart rate, bpm	82 ± 28.0	73 ± 15.9	0.07
Height, m	1.6 ± 0.1	1.7 ± 0.1	0.52
Weight, kg	77 ± 21.7	77 ± 19.4	0.98
BMI, kg/m2	28 ± 7.3	28 ± 5.7	0.16
BSA, m2	1.9 ± 0.3	1.9 ± 0.3	0.82
NYHA, n (%) NYHA I NYHA II NYHA III NYHA IV	 21 (45) 11 (23) 15 (32) 0(0)	 - - - -	 - - - -
AF, n (%)	12(27.3)	-	-
LVESVi, ml/m2	55 ± 19.3	32 ± 8.4	0.001
LVSVi, ml/m2	46 ± 18.7	42 ± 7.5	<0.001
LVEF, %	44 ± 13.3	57 ± 5.2	<0.001
LA diameter, mm	41 ± 11.8	22 ± 3.1	<0.001
RVEDVi, ml/m2	77 ± 24.8	74 ± 13.5	0.45
RVESVi, ml/m2	47 ± 21.6	34 ± 9.6	0.01
RVSVi, ml/m2	33 ± 14.2	39 ± 7.3	0.02
RVEF, %	41 ± 15.9	54 ± 7.5	<0.001

Continuous data are mean ± SD, unless otherwise indicated. bpm beats per minute; m, meter; kg, kilograms; BMI, body mass index; BSA, body surface area. Values are indexed to body surface area. LVEDVi, left ventricular end-diastolic volume index; LVESVi, left ventricular end-systolic volume index; LVSVi, left ventricular systolic volume index; LVEF, left

ventricular ejection fraction; LA, Left atrium; RVEDVi, right ventricular end-diastolic volume index; RVESVi, right ventricular end-systolic volume index; RVSVi, right ventricular systolic volume index; RVEF, right ventricular ejection fraction; RA, right atrium.

Table 5.2 Tissue characteristics

Parameter	Patients (n=47)	Controls (n=30)	P-values (p<0.05)
Native T1 mapping, ms	1280 ± 55.9	1213 ± 33.3	0.004
ECV, %	33 ± 4.4	28 ± 0.01	0.001
T2 mapping	39 ± 2.9	39 ± 2.4	0.75

Continuous data are mean ± SD unless otherwise indicated. ECV, Extracellular volume fraction. Continuous data are mean ± SD unless otherwise indicated.

Table 5.3. Myocardial deformational characteristics

Parameter	Patients (n=47)	Controls (n=30)	P-values (p<0.05)
Global radial strain, %	25.4 ± 9.8	30.8 ± 10.5	0.027
Global circumferential strain, %	-17.7 ± 4.7	-21.1 ± 2.7	0.001
Global longitudinal strain, %	-15.1 ± 6.5	-20.2 ± 2.9	0.001
Radial systolic strain rate, s^{-1}	1.6 ± 0.9	1.7 ± 0.9	0.592
Circumferential systolic strain rate, s^{-1}	-0.9 ± 0.3	-1.1 ± 0.2	0.003
Longitudinal systolic strain rate, s^{-1}	-0.8 ± 0.4	-1.0 ± 0.2	0.018
Radial diastolic strain rate, s^{-1}	-1.7 ± 0.8	-2.2 ± 0.9	0.008
Circumferential diastolic strain rate, s^{-1}	0.9 ± 0.3	1.5 ± 0.4	0.001
Longitudinal diastolic strain rate, s^{-1}	0.7 ± 0.6	1.3 ± 0.3	0.001

*Continuous data are mean ± SD unless otherwise indicated.

Association between myocardial native T1, ECV, and strain

We ran a linear regression analysis to assess the association between native T1 and ECV versus strain. The association of global strain with native T1 (Figure 5.1), systolic strain rates with native T1 (Figure 5.2), global strain and systolic strain rates with ECV (Figure 5.3), and diastolic strain rates with ECV (Figure 5.4) were presented.

Association between native T1, ECV and strain parameters

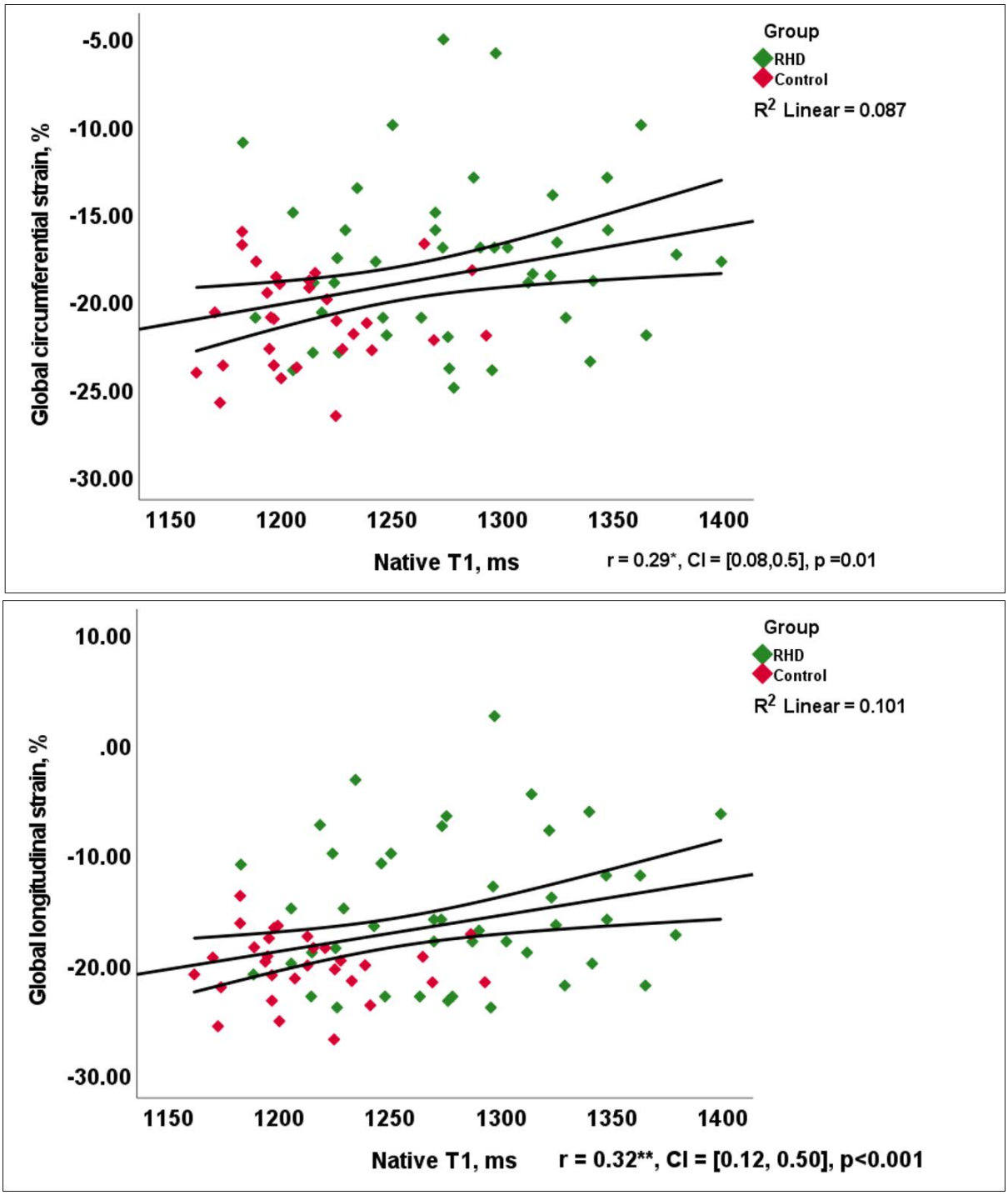

Figure 5.2. Association of global strain with native T1. Continuous data are mean ± SD,

unless otherwise indicated. Values are presented as mean ± SD. ** Correlation is significant at the 0.01 level (2-tailed) * Correlation is significant at the 0.05 level (2-tailed).

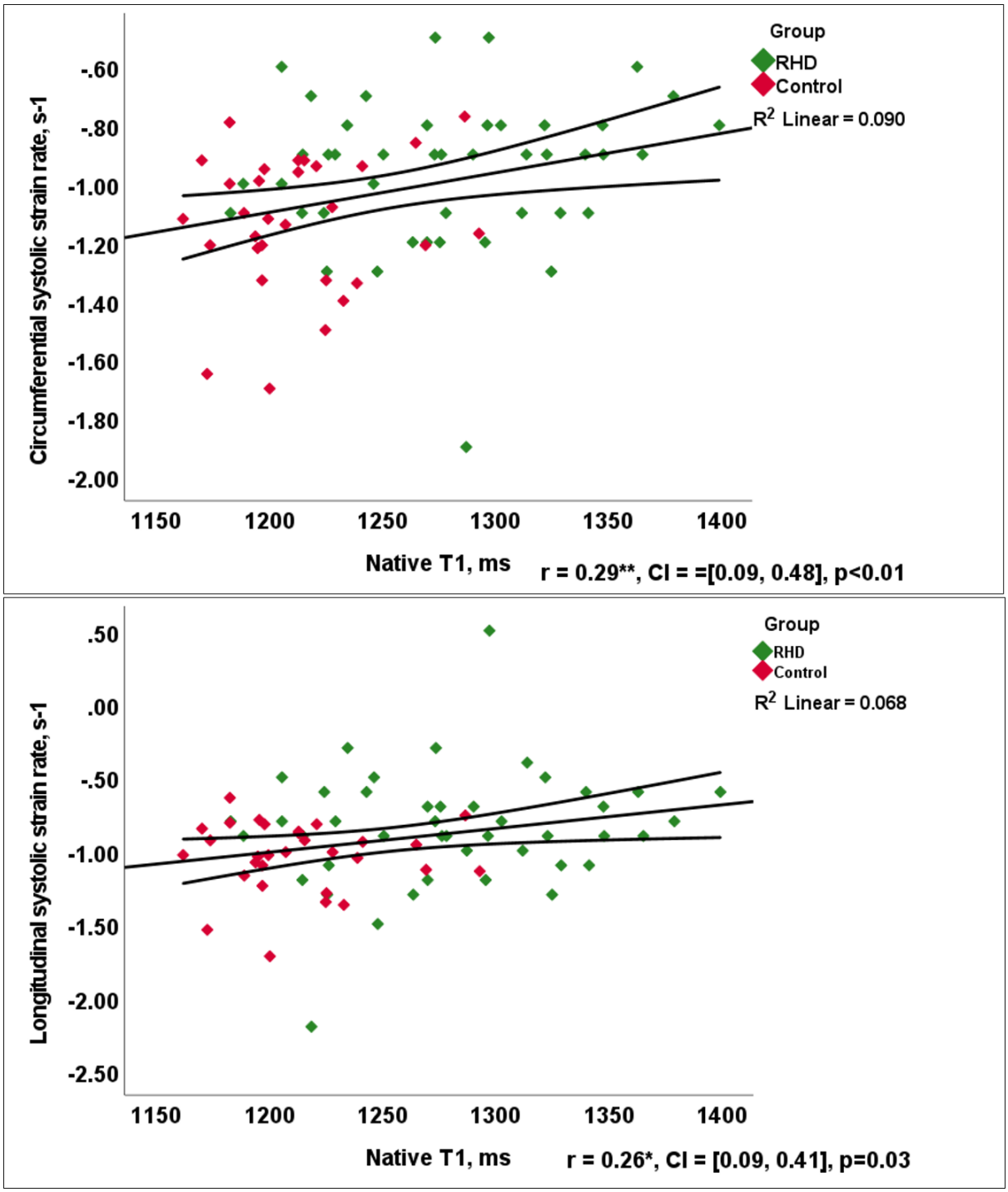

Figure 5.3. Association of systolic strain rates with native T1. Continuous data are mean ± SD, unless otherwise indicated. Values are presented as mean ± SD. ** Correlation is significant at the 0.01 level (2-tailed) * Correlation is significant at the 0.05 level (2-tailed).

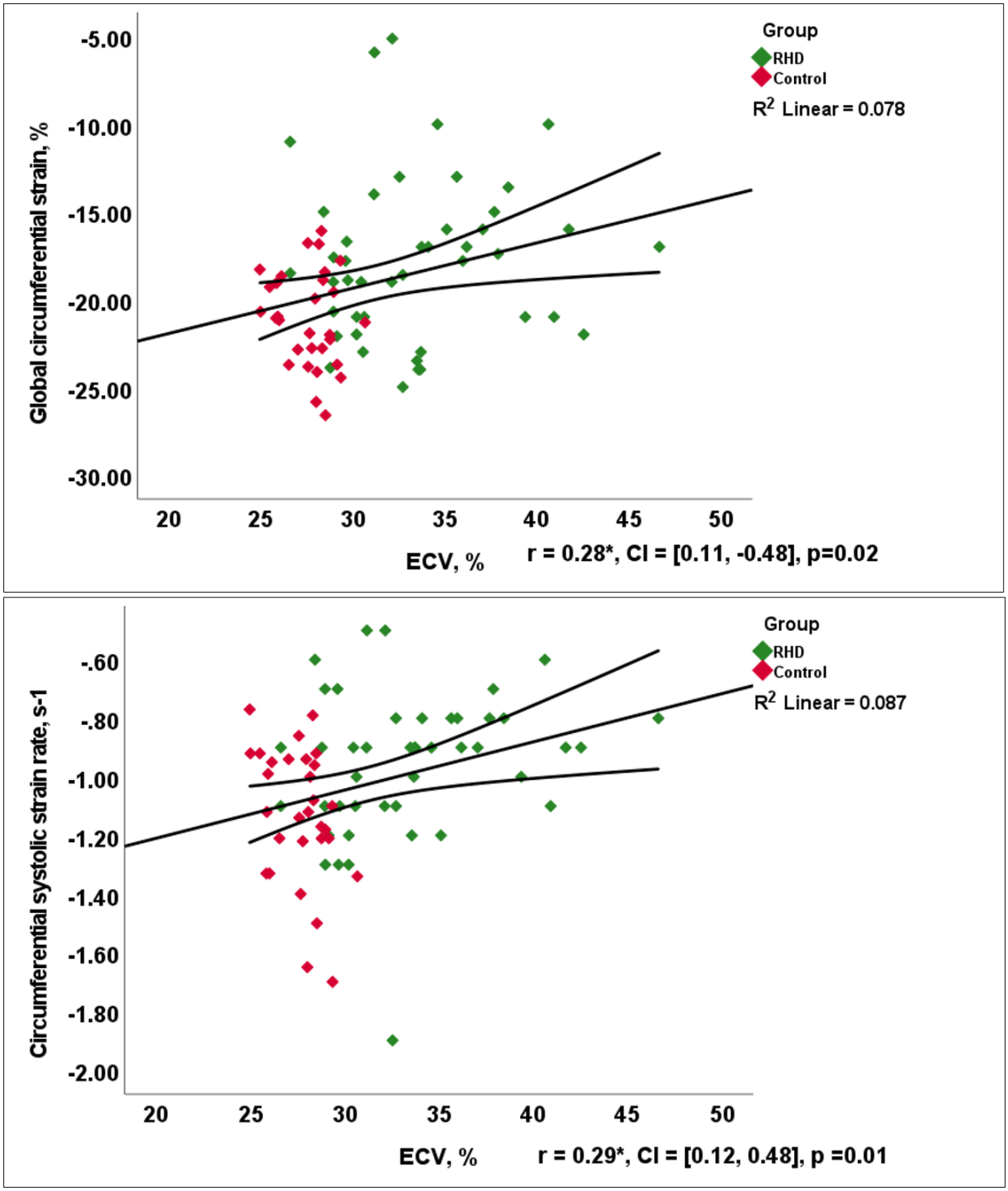

Figure 5.4. Association of global strain and systolic strain rate with ECV. Continuous data are mean ± SD, unless otherwise indicated. Values are presented as mean ± SD. ** Correlation is significant at the 0.01 level (2-tailed) * Correlation is significant at the 0.05 level (2-tailed).

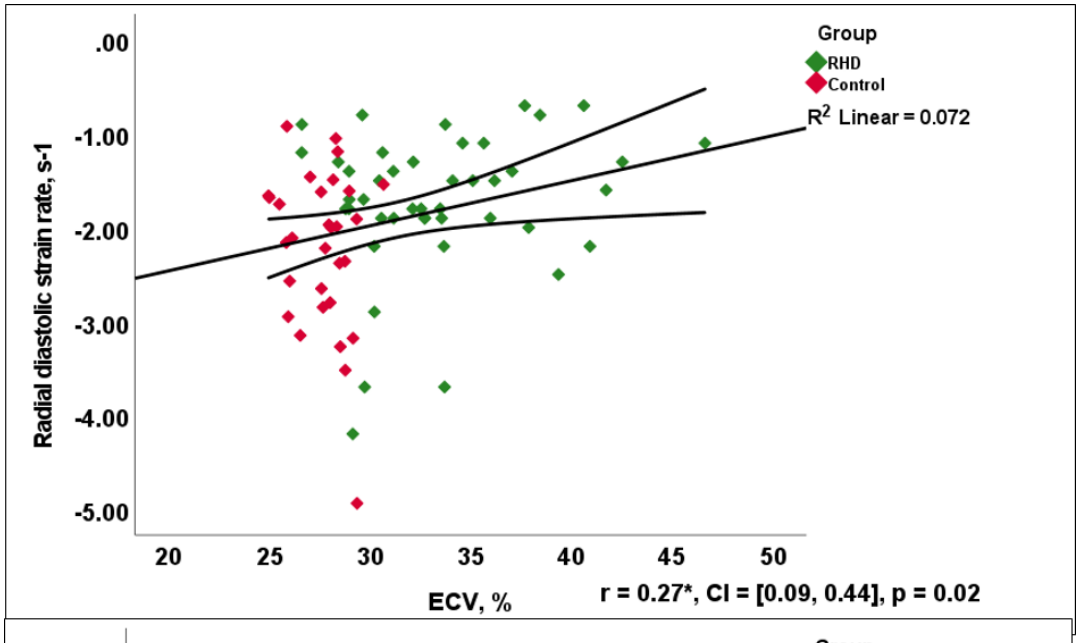
Group
RHD
Control
R^2 Linear = 0.072
Radial diastolic strain rate, s-1
.00
-1.00
-2.00
-3.00
-4.00
-5.00
20
25
30
35
40
45
50
ECV, %
r = 0.27*, CI = [0.09, 0.44], p = 0.02

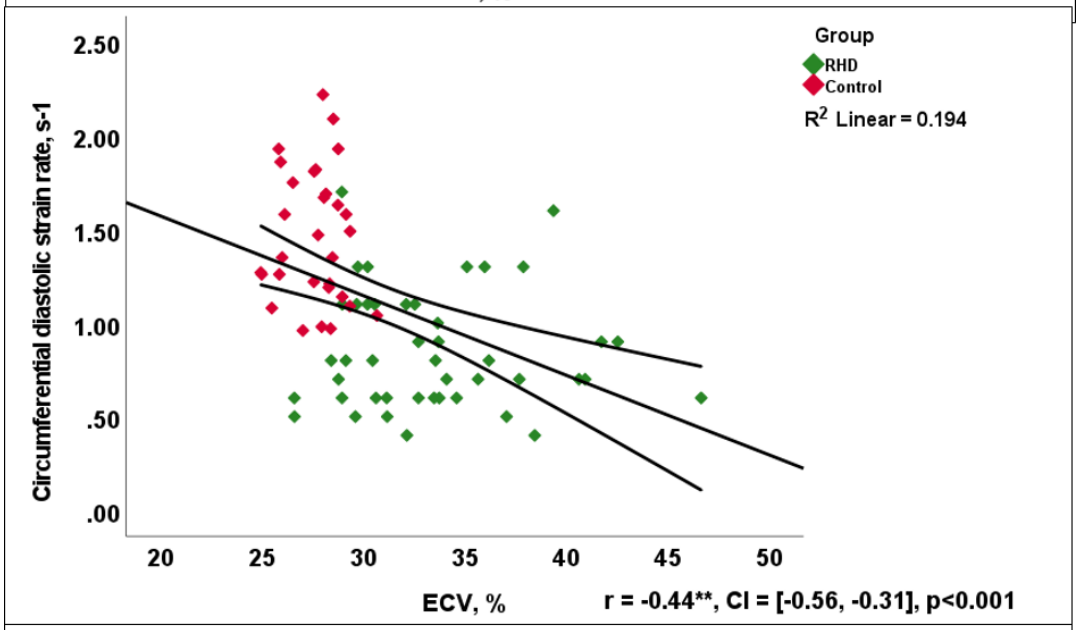
Group
RHD
Control
R^2 Linear = 0.194
Circumferential diastolic strain rate, s-1
2.50
2.00
1.50
1.00
.50
.00
20
25
30
35
40
45
50
ECV, %
r = -0.44**, CI = [-0.56, -0.31], p<0.001

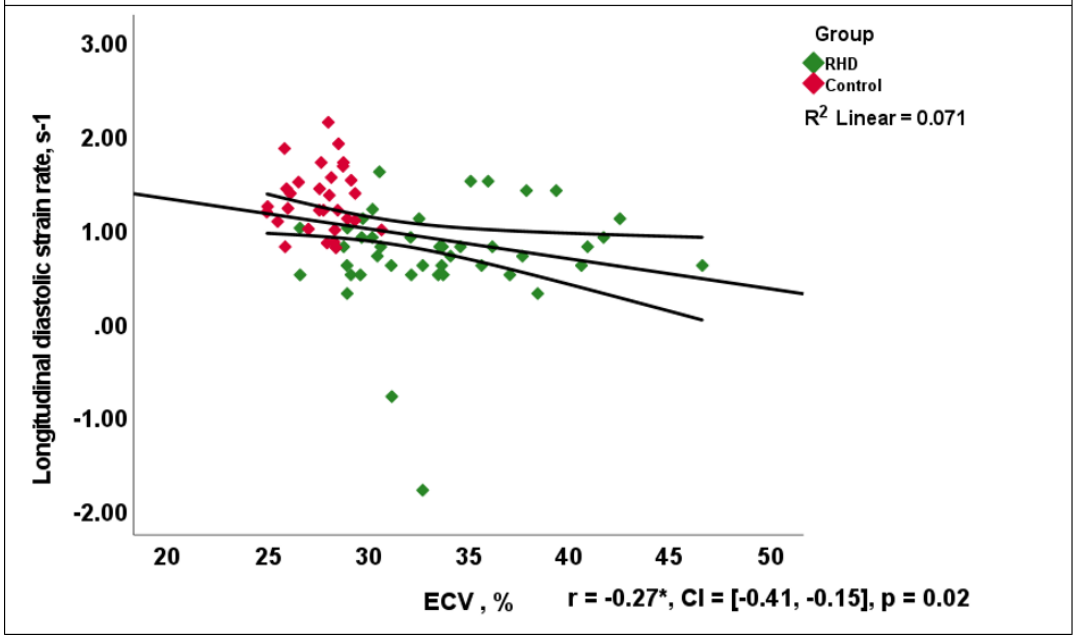
Group
RHD
Control
R^2 Linear = 0.071
Longitudinal diastolic strain rate, s-1
3.00
2.00
1.00
.00
-1.00
-2.00
20
25
30
35
40
45
50
ECV , %
r = -0.27*, CI = [-0.41, -0.15], p = 0.02

Figure 5.5. Association of diastolic strain rates with ECV. Continuous data are mean ± SD, unless otherwise indicated. Values are presented as mean ± SD. ** Correlation is significant at the 0.01 level (2-tailed) * Correlation is significant at the 0.05 level (2-tailed).

5.3 Discussion

Myocardial strain imaging allows for evaluation of different spatial components of contractile functions in radial strain (RS), circumferential strain (CS), longitudinal strain (LS) directions regionally and globally. Alteration in myocardial strain provides additional prognostic values over maintained or reduced EF in a multitude of clinical scenarios, ranging from asymptomatic adults with a previous history of cardiovascular pathology, to valvular heart disease.[191–194] In this study, we observed a reduced myocardial strain parameters including radial, circumferential, and longitudinal values for global strain, systolic strain rates and, diastolic strain rates in our patient cohort. We also report that native T1 and ECV moderately correlated with diastolic circumferential strain rate and diastolic longitudinal strain rate, respectively, indicative of expansion of the extracellular matrix and volume, which in turn has an adverse effect on LV contractility.

Despite significant pathophysiological differences, LA and LV strain indices showed no significant difference in MR of RHD aetiology, on speckle tracking echocardiography.[195] However, RHD patients with asymptomatic MR in mitral valve prolapse show a spectrum of myocardial fibrosis with reduced myocardial strain using native T1 and ECV.[196] Approximately 20% of patients with severe degenerative aortic stenosis who survived after 1 year of aortic replacement had abnormal LV global longitudinal strain, despite improved postoperative LVEF and regressed LV mass.[197] Reduced global radial strains, longitudinal, and circumferential were associated with increased native T1 and ECV, and remained

predictors of outcome risks in multivariate models.[198] In our study, we demonstrate decreased myocardial strain with moderate association with native T1 and ECV.

Prolonged afterload as a result of aortic stenosis causes hypertrophic remodeling of the LV.[199] Combinations of RHD valve lesions could affect pathophysiologic factors such as cardiac output, LV performance, LA and LV sizes, LV end-systolic and end-diastolic volumes; and EF, resulting in myocardial dysfunction and heart failure.[200] In this study, we observed a moderate increase in LV functional parameters (such as LVEDVi and LVESVi), indicative of LV remodeling to mitral and aortic valvular dysfunction.

Measurement of native T1 and ECV by CMR allow quantification of diffuse myocardial fibrosis, which adversely affect myocardial strain. Native T1 and ECV are sensitive indicators of myocardial inflammation and other CVD such as sarcoid, amyloid, fatty infiltration and/or diffuse or replacement fibrosis.[112,122,188,189,201] Elevated native T1 and ECV indicate both myocardial fibrosis and inflammation, respectively.[111,120,201,202] Elevated myocardial native T1 predicted clinical outcome in valve diseases such as mitral regurgitation and aortic stenosis.[203,204] In this study, we observed an elevated native T1 and ECV, indicative of diffuse myocardial fibrosis.

We have demonstrated abnormal tissue characteristics in chronic RHD patients and the relationship with strain parameters. We postulate that these data would support the ongoing controversial regarding the routine utilisation of myocardial strain imaging to clinically inform practitioners about RHD patients.

5.4 Limitations

In this study, we concentrated on the parametric CMR tissue characteristics in RHD. Although myocardial native T1 and ECV values are elevated because of other infiltrative CV diseases such as cardiac amyloidosis[205,206], we did not observe myocardial infiltration and, patients with an eGFR<30 were excluded due to the risk of nephrogenic systemic fibrosis to avoid selection bias. The sample size in this study was small and therefore we could not draw necessary conclusions regarding the extent of myocardial deformation strain pattern observed in RHD patients. Lastly, CMR tagging method which is known as the main technique for evaluating myocardial deformation was not used since it is time-consuming and requires dedicated image acquisition.[181]

Conclusion

Our results establish the ability of CMR to assess myocardial deformation by strain imaging, native T1 and ECV in chronic patients RHD with lower LV systolic function and elevated indices of myocardial fibrosis and ongoing inflammation, and correlate with impaired systolic and diastolic strain indices. In future, CMR including strain imaging may be a potential useful imaging biomarker in chronic RHD patients to assess the degree of myocardial deformation.

5.5 Perspectives

- Abnormal functional, tissue characteristic and myocardial strain parameters are common in RHD. Strain abnormalities correlated moderately with T1 and ECV.

- The need for larger prospective studies evaluating CMR imaging markers and their ability to predict clinical events and outcomes.

- Future consideration of comparative studies of CMR parameters and other immunological and molecular biological mechanistic biomarkers.

5.6 Acknowledgements

We thank the patients who voluntarily took part in this research. In addition, we thank staff at the Cape Universities Body Imaging Centre, including Patricia Maishi and Marianne Jafta. Prof. Ntusi gratefully acknowledges support from the South African Medical Research Council, National Research Foundation and the Lily and Ernst Haussmann Trust. This research was supported by the National Research Foundation by grants to Professors Skatulla and Ntusi (Grant Nos. 104839 and 105858).

Chapter 6
Results

Functional and pathophysiological characterisation of valve lesion in RHD using CMR

6 Introduction

ARF and RHD are underdiagnosed, highly prevalent in Africa, and other LMICs where they affect young people.[207] RHD pathophysiology is related to a combination of immune, genetic and environmental factors.[208] Prevalence of RHD among children and adolescents is 5.7 per 1000.[6,209] Although the incidence of RHD is declining in HICs due to improved public health and prevention strategies like availability and use of penicillin, ARF and RHD occur frequently in LMICs.[210]

Echocardiography is the traditional modality for the diagnosis and prognostication in RHD.[211,212] CMR, amongst other imaging modalities, is recommended in diagnosing valvular involvement in RHD.[96,213] CMR supplements echocardiography for management decisions in various rheumatic lesions by evaluating anatomy, function, tissue characteristics, haemodynamics, regurgitant volumes and fractions.[214] Histopathological characterisation of mitral valve lesions shows moderate to marked fibrosis, elevated calcification, as well as intense endocardial inflammatory infiltrate, with predominance of mononuclear cells.[215]

Gomes and colleagues, reported isolated MS in 45% and MVD in 35% of RHD patients.[215] Shafi and colleagues reported MR in 65% and AR in 52% of RHD patients.[216] Recently, we reported a high burden of myocardial fibrosis in RHD patients, detailing valvular (LGE, and minimal ongoing inflammation.[217] Data on relationship of valve lesion with tissue characteristics are limited. Therefore, we aimed to investigate the functional and pathophysiological characterisation of valve lesions using multiparametric CMR.

6.1 Methods

Patient

Forty-seven (47) patients, confirmed with RHD were enrolled between August 2017 and August 2019, at the Cardiac Clinic of the Groote Schuur Hospital, Cape Town. Patients with concomitant congenital heart disease, hypertension, hyperthyroidism, coronary heart disease, cardiomyopathy, pericardial disease, any other valvular abnormality not of RHD aetiology and, any contraindication for CMR (severe renal dysfunction – estimated glomerular filtration rate (eGFR) <30 ml/min, metallic implant, pregnant, claustrophobic, and unable to lay still during the examination) and 2 suboptimal imaging data were excluded from the study.

The ethical clearance (HREC REF: 554/2017) for the study was obtained from the Human Research Ethics Committee of the University of Cape Town's Faculty of Health Sciences after a thorough review of the study proposal. Written informed consent was given to all the enrolled participants. Data collection only commenced after the UCT HREC approved and issued the ethical clearance. The study protocol obeys the ethical guidelines of the 2013 Declaration of Helsinki.

CMR protocol

Eligible participants were scanned with a 3T MRI Siemens Magnetom Skyra scanner with an 18-channel phased array body coil. We obtained the LV volumes and masses during expiratory breath-hold for approximately 12 seconds and, were prospectively ECG gated. LV volumes and mass were acquired using a standard CMR protocols (3T MRI Siemens Magnetom Skyra scanner, Siemens, Erlangen, Germany). Steady-state-free-precession imaging (repetition time = 43.08 ms, echo time = 1.61 ms, flip angle = 40 degrees, matrix size = 149 x 208, bandwidth = 962Hz/Px, slice = 8 mm thickness, 25 phases). SSFP imaging was acquired over 9 heartbeats

per slice. SSFP cines were performed to obtain the long axis cines and a contagious short axis stack for assessment of LV volumes, EF, and mass. LGE imaging was performed 6-15 minutes after gadolinium administration, and acquired using a short axis stack, 2 chamber, 4 chamber, and LVOT images to assess focal myocardial fibrosis. A standard dose of 0.2 mmol/kg of gadolinium-DTPA (Magnevist, Bayer, South Africa) was administered intravenously in patients with preserved renal function (eGFR>30 ml/min). Early gadolinium imaging was acquired in short stacks using a PSIR for the assessment of the presence of thrombus.

CMR image analysis

To analyse the LV volumes, including the LVEDV, LVESV, LVEF and LVM, the endocardial and epicardial contours of the left ventricle were manually contoured from a stack of short-axis slices, excluding the papillary muscles on CVI42® software (Circle Cardiovascular Imaging, Calgary, Alberta). We indexed these parameters, except for LVEF, to the body surface area.

Tissue characterisation

The presence and extent of LGE was done by two readers with >5 years of CMR experience and blinded to the diagnosis of participants. We performed the assessment of cardiac function and chamber sizes in standard views in the long-axis (horizontal and vertical) and short-axis planes. To visually quantify LGE, we performed a manual planimetry of all highly enhanced pixels on the short axis stacks of LGE images. For comparison, a semi-automated gray-scale threshold technique was performed using 2 SDs above the mean signal intensity of the normal nulled myocardium and 2 SDs above noise (i.e., mean signal intensity of a region located outside the body). LGE quantity was expressed in grams and as a percentage of the total LV

myocardial mass: $\left(\left(\frac{\text{MLGE}}{\text{MM}}\right) X\ 100\right)$, with LGE mass ($M_{LGE}$), and myocardial mass ($M_M$) in grams.[160] We recorded variables such as presence or absence of LGE, distribution patterns of LGE in different areas of the myocardium, and valvular enhancement. Myocardial fibrosis was defined as a region of LGE with signal enhancement greater than the signal intensity of non-enhanced myocardium. Ejection fraction for the LV was assessed with the following formula:

$$Ejection\ fraction\ (EF) = \frac{EDV - ESV}{EDV}$$

EDV, end diastolic volume, ESV, end systolic volume.

For the T1 and T2 mapping, CVI42® software was used to process the images. Each ECV measurement was obtained by subtracting pre- and post-contrast maps with haematocrit correction, which is usually obtained approximately 15 minutes after the administration of contrast. The standard formula used is as follows:

$$ECV = (1 - haematocrit) * \{1/\text{T1 post contrast (myo)} - 1/\text{T1 pre} - \text{contrast (myo)}\} / \{1/\text{T1 post contrast (blood)} - 1/\text{T1 pre} - \text{contrast (blood)}\}$$

Statistical data analysis

Normality of data were tested using the Shapiro-Wilk normality test. Normally distributed data are presented as mean ± standard deviation (SD) or, where highly skewed, as median (interquartile range); and non-parametric data as numbers (percentages). The Chi-square test or the Mann-Whitney U test were used for non-parametric data. Unpaired samples between groups were assessed by the unpaired 2-tailed Student t test. Correlation was assessed using the Pearson's 'R' coefficient, as appropriate. All statistical tests were two-tailed, with p-values

of less than 0.05 considered statistically significant. All analysis were performed using SPSS version 25 (IBM, Armonk, New York, USA).

6.2 Results

Forty-seven (47) RHD patients (42 ± 12.8 years) and 30 healthy controls (39 ± 12.1 years), were equally matched for age, gender, ethnicity, and other demographic parameters. These parameters were similar compared to control (Table 1).

We observed a significantly reduced EF (45 ± 12.5% vs. 57 ± 5.2%, p< 0.001) and elevated LV mass index (60 ± 30.7 mm/m^2 vs. 32 ± 8.38 mm/m^2, p = 0.001), LVEDV (113 ± 34.8 ml vs. 74 ± 13.4 ml, p< 0.001) and LA diameter (42 ± 12.3 mm vs. 22 ± 3.1 mm, p<0.001), compared to controls (Table 6.1).

Table 6.1. Demographics, clinical features and CMR characteristics of RHD patients and controls

Parameters	Patients (n=47)	Controls (n=30)	P–values (p<0.05)
Age, years	42 ± 12.8	39 ± 12.1	0.28
Sex (Female), n (%) (Male)	29(62) 18(38)	16(53) 14(47)	0.49 0.49
Ethnicity, n (%) Black Mixed	 19(40) 28(60)	 14(47) 16(53)	 0.59
Heart rate, bpm	82 ± 28.0	73 ± 15.9	0.07
Height, m	1.6 ± 0.1	1.7 ± 0.1	0.52
Weight, kg	77 ± 21.7	77 ± 19.4	0.98
BMI, kg/m^2	28 ± 7.3	28 ± 5.7	0.16
BSA, m^2	1.9 ± 0.3	1.9 ± 0.3	0.82

NYHA, n (%)			
NYHA I	21 (44.7)	-	-
NYHA II	15(31.9)	-	-
NYHA III	11 (23.4)	-	-
NYHA IV	0(0)	-	-
LVEDVi, ml/ m^2	113 ± 34.8	74 ± 13.4	<0.001
LVESV*i*, ml/m^2	55 ± 18.8	32 ± 8.4	0.001
LVSV*i*, ml/m^2	46 ± 18.7	42 ± 7.5	<0.001
LVEF, %	45 ± 12.5	57 ± 5.2	<0.001
LVMI, g/m^2	60 ± 30.7	32 ± 8.38	0.001
LA diameter, mm	42 ± 12.3	22 ± 3.1	<0.001
RVEDV*i*, ml/m^2	77 ± 24.8	74 ± 13.5	0.45
RVESV*i*, ml/m^2	47 ± 21.7	34 ± 9.6	0.002
RVSV*i*, ml/m^2	33 ± 14.2	39 ± 7.3	0.02
RVEF, %	41 ± 15.9	54 ± 7.5	<0.001

Continuous data are presented as (mean ± SD), and non-parametric data as numbers (percentages). *p<0.05

The MV was most commonly involved, with MR and MS observed in 76% and 67% of RHD patients, respectively, followed by AR and AS in 49% and 45%, respectively (Table 6.2). In order of disease severity, we observed a severe form of MR, MS, and AR (72%, 44%, and 48%, respectively). However, in the AS group, 44% mild aortic stenotic lesion was observed (Table 6.2).

Table 6.2. Distribution of valve lesions in RHD

Valvular involvement	Frequency (n =47)	Percentage (%)
Mitral stenosis	**34**	**67**
Mild	7	21

Moderate	12	35
Severe	15	44
Mitral regurgitation	**39**	**76**
Mild	6	15
Moderate	5	13
Severe	28	72
Aortic stenosis	**18**	**45**
Mild	8	44
Moderate	5	28
Severe	5	28
Aortic regurgitation	**25**	**49**
Mild	6	24
Moderate	7	28
Severe	12	48

Valve lesions observed were divided into isolated (comprising of MS, MR and AS), and mixed (comprising of mixed mitral valve disease (MMVD), mixed aortic valve disease (MAVD) and mixed mitral and aortic valve disease (MMAVD) lesions). Out of the isolated valve lesions, isolated MR was most common (10.6%), compared with AS and MS (4.2% and 2.1%, respectively). MMAVD was most predominant (51%) compared with MMVD and MAVD (28% and 4.2%) (Table 6.3).

Table 6.3 Type of Isolated and combination of valve lesion

Valve lesions	Frequency, (n=47)	Percentage (%)
Isolated lesion		

MS	1	2
MR	5	11
AS	2	4
Combination		
MMVD	13	28
MAVD	2	4
MMAVD	24	51

Valve lesion distribution in rheumatic heart disease. MS, mitral stenosis, MR, mitral regurgitation, MMVD, Mixed mitral valve disease, MAVD, Mixed aortic valve disease, MMAVD, Mixed mitral and aortic valve disease.

Native T1 was significantly elevated (1280 ± 55.9 ms vs. 1213 ± 33.3 ms, <0.001) with a corresponding elevated ECV (33% vs. 28%, <0.001). T2 values which is an indication of oedema, shows a similar pattern compared to controls, but still within normal ranges (39 ± 2.9 vs. 39 ± 2.4 ms, p = 0.75). The total volume of myocardial enhancement with LGE imaging was significantly different from control (26 g vs. 15 g, <0.001) (Table 6.4).

Table 6.4. CMR tissue characteristics in RHD patients and controls

Tissue characteristics	Patients (n=47)	Controls (n=30)	P-values (p<0.05)
LGE, total volume enhanced, g	26 ± 10.5	15 ± 6.0	<0.001
Native T1, ms	1280 ± 55.9	1213 ± 33.3	<0.001
T2 value, ms	39 ± 2.9	39 ± 2.4	0.75
ECV, %	33 ± 4.4	28 ± 1.4	<0.001

Continuous data are mean ± SD, unless otherwise indicated. ECV, extracellular volume; ms, milliseconds. Values are presented as mean ± SD. LGE, late gadolinium enhancement, T2 STIR, short Tau inversion recovery. *p<0.05

Results show the pictorial presentation isolated valve diseases (Figure 6.1), MMVD (Figure 6.2), MAVD (Figure 6.3), and MMAVD (Figure 6.4). Further, LVEF, LGE, Native T1 and

ECV were similar when compared among the mixed and isolated lesion. However, significantly elevated native T1 was observed in MMAVD compared to isolated lesion (p = 0.04) (Figure 6.5).

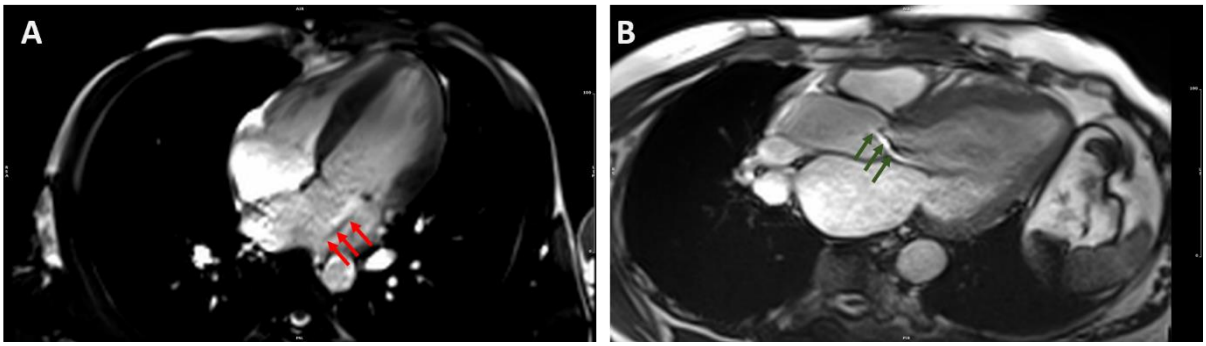

Figure 6.1 Isolated valve disease.
Panels illustrate isolated valve disease with (A) moderate MR depicted by the red arrows. (B) Isolated mild AS shown by the green arrows. MR, mitral regurgitation; AS, aortic stenosis.

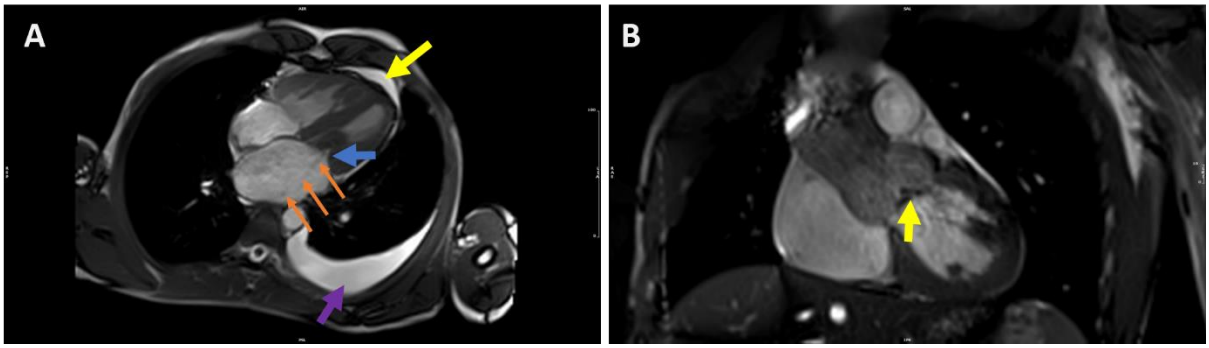

Figure 6.2. Mixed valve disease
Panels illustrate (A) MMVD, with moderate MR (orange arrows), moderate MS (blue arrow), pleural effusion (with purple arrow) and pericardial effusion (with a yellow arrow) (B) MAVD, with moderate AS, depicted by a yellow arrow. MMVD, mixed mitral valve disease; MAVD, mixed aortic valve disease MR, mitral regurgitation; MS, mitral stenosis.

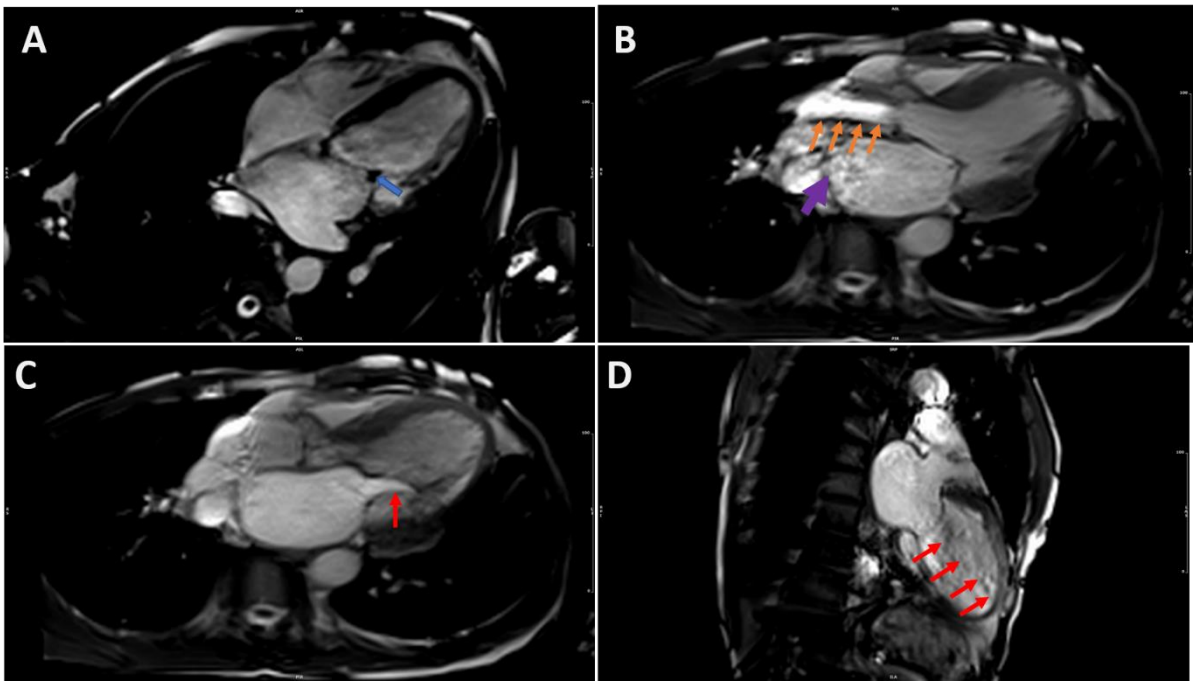

Figure 6.3. Mixed mitral and aortic valve disease
Panels illustrate (A) Thickened mitral valve (blue arrow) (B) Severe AS indicated by a stenotic jet across the aortic valve (orange arrows) and, severe MR (purple arrow) (C) MS depicted by a red arrow (D) Severe MR (red arrows). MS, mitral stenosis; MR mitral regurgitation.

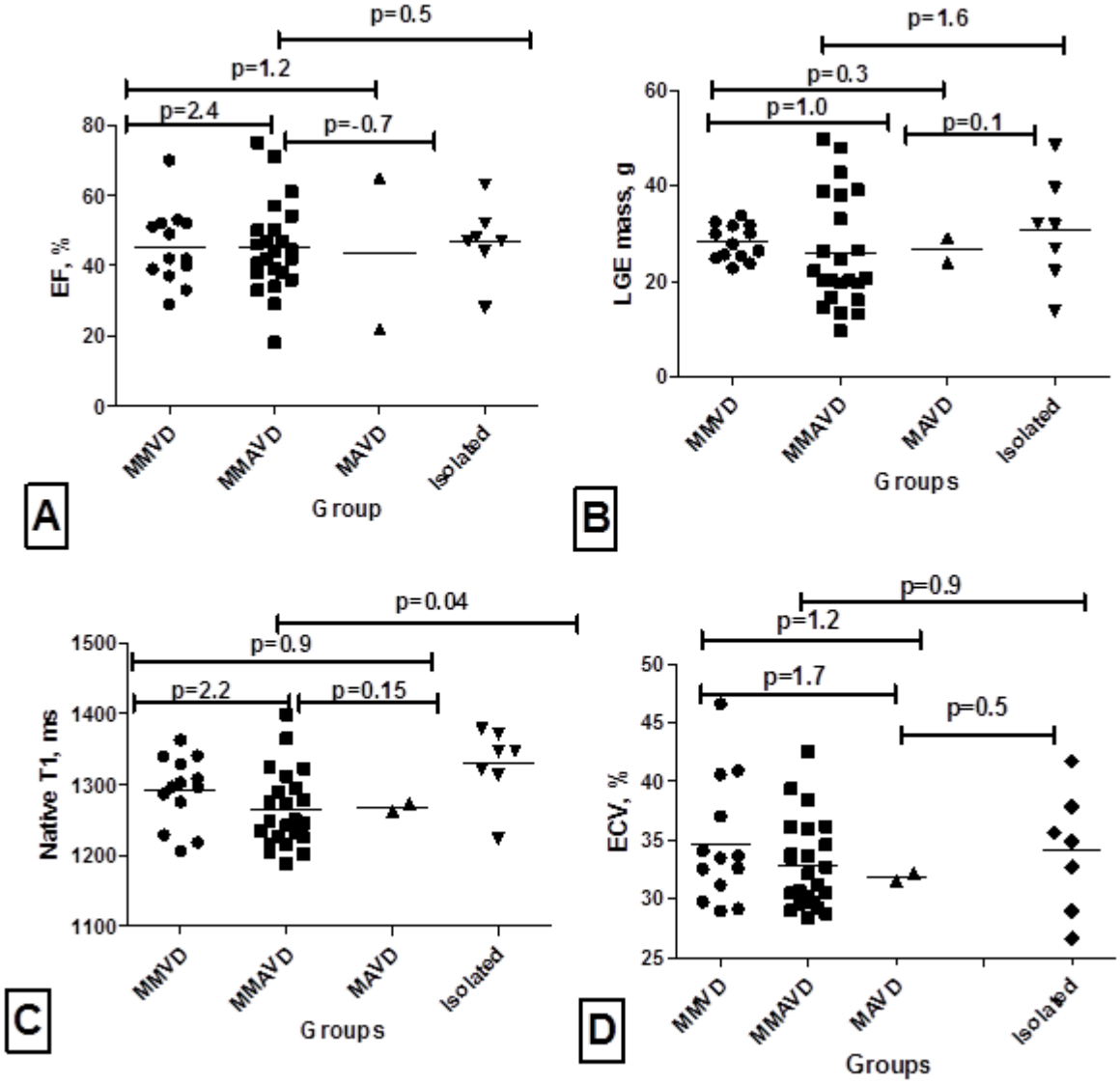

Figure 6.5. Distribution of functional and pathophysiological tissue characteristics in mixed valve lesion

Panels illustrate (A) LVEF. (B) LGE (C) Native T1 (D) ECV**.** LVEF, left ventricular ejection fraction; LGE, late gadolinium enhancement; EC, extracellular volume fraction; MMVD, mixed mitral valvular disease; MMAVD, mixed mitral and aortic valve disease; MAVD, mixed aortic valve disease. *p<0.05

6.3 Discussion

RHD accounts for most cases of aortic stenosis globally.[218] MR is the predominant lesion commonly seen in RHD.[45,88] Pathogenesis of RHD is a combination of a triggered immune response by GAS infection, resulting in a cascade of cellular and humoral processes, leading to the production of antibodies, generating self-reactive cluster of T-lymphocytes which interacts with valve components to cause valve leaflet degeneration.[219] In rheumatic valve pathology, all the valves may be involved, but the mitral valve is mostly affected, with MR at the initial stage and MS at the later stage and, this is often followed by the aortic valve involvement, resulting into aortic calcification.[215]

There are limited reports on the prevalence of valve lesions in RHD. A recent study reported 80% mixed mitral lesions in RHD. [220] In a different study, 28% prevalence of mixed MR, 20% MMAVD, 8% pure MS and 3% AR were reported.[221] A study from Nepal reported 46% isolated MV involvement, followed by 34% MMAVD, 9% isolated AV disease.[222] Another recent study found 87.2% pure MR, 85.1% pure MS and, 29.8% mixed (MR+MS+TR) and, 27.7% mixed (MR+MS+TR+AR) lesions.[223] Altogether, these results corroborate our findings, as we report 28% of MMVD, and 51% MMAVD, but 2% pure MS and 11% MR.

Mitral and aortic valve lesions may be due to abnormal immune effector, and functional abnormalities which result from alteration in the anatomic disruption of valve apparatus, matrix architecture and cellular components, thereby impairing direct blood circulation through the blood chambers.[83,199,224,225] Deficient circulating levels of the regulatory T-cell have been reported in RHD patients with multivalvular involvement.[226] The order of valvular lesion involvement in our study – mitral valve lesion, followed by aortic valve lesion, is similar to previous reports.[227] Geographical location-based variations in prevalence patterns, associated

with access to health care in sub-Saharan Africa have been reported.[228] Few studies have demonstrated the distribution of valve lesions with tissue characteristics. Elevated myocardial native T1 was reported in aortic stenosis and mitral regurgitation compared to controls.[203,229] Similarly, increased myocardial native T1 was seen in AS patients, compared with control participants (1,232 vs. 1,185 ms), and thus predicted adverse outcome in the cohort.[230] Increased ECV measured left ventricular decompensation in patients with severe aortic stenosis.[146] Strong correlation of ECV with interstitial fibrosis in patients with AR have been demonstrated.[231,232] Similarly, ECV index and LGE have shown a strong correlation with diffuse histological fibrosis on myocardial biopsies, and was increased in patients with aortic stenosis.[146,233] Elevated ECV, but not LGE or T1 has been reported in patients with mitral and aortic valve disease, and correlated well with aortic stenosis, and track well with cardiac decompensation.[232] In this study, we report the distribution of native T1, LGE, ECV and, EF in both isolated and mixed valve lesions in patients with chronic RHD. The distribution of native T1, ECV, LGE and EF were similar in both isolated and mixed valve diseases. However, native T1 was significantly higher in MMAVD compared with isolated valve disease.

6.4 Limitation

The main limitation of our study was the sample size of the patients. Being a single-centre study with such sample size, we recommend a larger cohort and multi-centre study to grasp a true representation of the valve lesions observed in RHD.

6.5 Conclusion

Isolated and mixed are commonly seen in RHD, being a disease of the valve and myocardium. Most of RHD patients have severe form of MS, MR, and AS. High frequency of MMAVD with elevated native T1 was observed, indicating a phenotypic myocardial fibrosis. CMR, using its functional and pathophysiological could be used to stratify the valvular lesions in RHD and can adequately complements echocardiography.

6.6 Acknowledgements

We are grateful to the patients who voluntarily participated in this research. In addition, we thank staff at the Cape Universities Body Imaging Centre, including Ms Patricia Maishi and Marianne Jafta. Prof. Ntusi gratefully acknowledges support from the South African Medical Research Council, National Research Foundation and the Lily and Ernst Haussmann Trust. This research was supported by the National Research Foundation by grants to Professors Skatulla and Ntusi (Grant Nos. 104839 and 105858).

Chapter 7
Results

Expression analysis of Beclin-1, LC3A&B, p62/Sequestosome, BAX, BCL-2 and Caspase-3 indicate that triggered autophagy is associated with a negative prognosis in chronic rheumatic heart disease

7 Introduction

Autophagy is a 'self-destruction' cell death process, which is highly regulated and used by cells to recycle cellular contents for survival. This process is characterised by bulk degradation of cellular proteins.[234] The 3 existing forms of autophagy are (1) chaperone-mediated autophagy (CMA), (2) microautophagy and (3) macroautophagy. Chaperone – mediated autophagy describes the lysosomal pathway of proteolysis responsible for the degradation of 30% of cytosolic proteins under conditions of prolonged nutrient deprivation.[235,236] Microautophagy is a constitutive process that involves a direct engulfment of cytoplasmic cargo by the lysosomes or vacuoles in yeast or plant. Macroautophagy (hereafter referred to as autophagy) is an evolutionary conserved lysosomal degradation pathway in eukaryotic organisms.[237] Autophagy maintains cell homeostasis and organelle quality control by regulating residual cargo removal, cellular metabolism, and renovation of cell differentiation and development.[238]

The major molecular players involved in autophagy signalling include unc-51-like kinase 1 (ULK1) protein kinases, autophagy related gene – phosphoinositide-interacting 1 (Atg-WIP11) and vacuole protein sorting – Beclin 1 (Vps34-Beclin 1) class phosphoinositol-3-phosphates-kinase (PI3-kinase) complexes, and the autophagy related gene 12 (Atg12) and protein 1 light chain 3 (LC3) conjugation systems.[239] Briefly, autophagy begins with the Atg4-mediated conversion of pro-LC3 to LC3-I. This followed by the conjugation of LC3-I with phospatidylethanolamine (PE) to generate LC3-II, which is later recruited into the autophagosomal membrane to aid in membrane elongation. Despite the fact that several molecular markers have been studied to date, demonstration of conversion of LC3-I to LC3-II

via PE conjugation remains the gold standard for validation of autophagosome formation.[240–243]

Autophagy is a selective process, due to the presence of autophagy receptors which are able to recognise ligand-bound cargo, thereby interacting with the autophagy machinery in a specific manner.[240,244,245] Sequestosome1 (SQSTSM1), also known as p62, is one of the best studied autophagy receptors involved in autophagy-dependent destruction of different cellular cargo including ubiquinated protein aggregates and bacteria. Autophagy plays a vital role in the immunological processes including pathogen detection and destruction, antigen presentation, lymphocyte development and effector function, and inflammatory regulation.[246] Dysregulation of autophagy exacerbates pro-inflammatory processes through the promotion of excessive cytokine production.[34] Substantial evidence has shown an interplay between autophagy and the NF-κB signalling pathway, which regulates the transcription of genes involved in cell proliferation, survival, differentiation, and development.[247,248] Regulation of T-cell receptor-mediator NF-κB activation is associated with p62/SQSTM1, which has been shown to modulate NLRP3-inflammasome activation and IL-1 beta production in macrophages.[249,250]

Although the pathogenic mechanism/pathway of autophagy in rheumatic heart disease (RHD) is unknown, several reports indicate the crucial role of autophagy in autoimmune diseases.[33] Beclin, LC3 and p62 are expressed differentially in peripheral blood mononuclear cells of patients with systemic lupus erythematosus (SLE).[251] Defects in autophagy result in increased production of proinflammatory cytokines and keratinocyte proliferation via excessive expression of p62 in psoriasis.[252] Although the pathogenic role of autophagy in rheumatoid arthritis is unclear, increased autophagy was found in RA patients[253], and formation of p62-positive polyubiquitinated protein aggregates promote apoptosis in RA synovial fibroblast under severe stress.[254] Deletion of Atg16L1 results in increased IL-1 beta production in macrophages in inflammatory bowel disease.[241]

Prominent inflammation of aortic valves in RHD patients has been reported to be associated with Beclin and LC3 expression. p62 directly interacts with LC3; however, p62 dysregulation in RHD valves has not been investigated. We therefore sought to investigate the expression and association of Beclin -1, LC3, p62, BAX, Bcl-2 and Caspase-3 in aortic valve pathology of RHD, which was compared to explanted valves from patients with degenerative AS, who served as positive controls, and explanted valves from cadavers without known CVD, who served as negative controls.

7.1 Methods

Patients and sample collection

Heart valve tissues were collected from patients undergoing cardiothoracic surgery at the GSH, Cape Town. Prior to valve explantation, suitable patients were approached for consent, as per patient information list and consent form submitted to the University of Cape Town HREC (see Appendix A). Tissue samples were immediately transferred into 10% formalin solution once excised by the surgeons to enable proper fixation of the valves.

For this preliminary study, 2 patients, each with confirmed RHD and degenerative AS, matched for age and sex with 2 cadaveric controls were enrolled from August of 2017 to May of 2019. Cadaveric participants were excluded if they showed evidence of previous cardiac surgery or had a history of CVD or new diagnosis of CVD at autopsy; LV hypertrophy (>15 mm measured 2 cm below the valve); heart weight outside the normal range (i.e., men: 212 – 373 g, women: 164 – 317 g); coronary artery (CA) atherosclerosis occluding >50% luminal surface area in right CA, left mainstem CA, left anterior descending CA, or circumflex artery; macroscopic previous myocardial infarction with area of fibrosis; subjective thickening, calcification or fusion of valve cusps or chordae tendinae; current or previous pericarditis (adhesions); and, had history or observation of sepsis infection at autopsy.

Primary antibodies

Anti-LC3B (rabbit polyclonal, clone DU4C) and p62/SQSTM1 (mouse monoclonal, clone D5L7G) antibodies were purchased from Cell Signalling Technology (Danvers, Massachusetts, USA), Beclin 1(BECN1), (mouse monoclonal, clone G-11), BAX (mouse monoclonal, clone 2D2), Bcl2 (mouse monoclonal, clone C2), and caspae-3 (mouse monoclonal, clone E-8) antibodies were obtained from Santa Cruz (Dallas, Texas, USA), whereas Envision horseradish peroxidase (HRP) system labelled polymer anti-mouse, Envision HRP system labelled polymer anti-rabbit, and liquid diaminobenzidine (DAB) + substrate chromogen system were obtained from Dako (California, USA).

Tissue processing

Valve tissue samples used for this research study were processed overnight in an automated Leica tissue processing machine, Leica TP 1020 (Leica microsystems, Nussloch Germany). This procedure entailed the tissues passing through solutions of graded alcohol, xylene, and wax to fix properly. The following morning the tissues were embedded in paraffin wax to complete the tissue processing. This process took approximately 22 hours (See table 7.1). After successful processing of tissues, they were embedded using the Leica EG1140H embedder (Leica microsystems, Nussloch Germany) and Leica EG1140C chiller plate (Leica microsystems, Nussloch Germany) was used to cool and harden the wax tissue blocks.

Table 7.1. Tissue Processing Schedule (Leica Tissue Processor)

Reagent	Time
10% Formalin	Optional delayed start
70% Ethanol	2 hours
96% Ethanol	2 hours
96% Ethanol	2 hours

100% Ethanol	2 hours
100% Ethanol	2 hours
100% Ethanol	2 hours
100% Ethanol	2 hours
Xylene	2 hours
Xylene	2 hours
Paraffin wax (55-56°C)	2 hours
Paraffin wax (55-56°C)	2 hours

Immunohistochemical examination

The paraffin sections were placed on silanised microscope slides and underwent a standardised laboratory immunohistochemical staining procedure. Three-micron (3µ) tissue sections embedded in paraffin wax were cut, trasferred onto Histobond slides (Marienfeld-Germany) and heat fixed on a hotplate for 10-15 minutes. Sections were dewaxed through xylene, cleared in ethanol, and rehydrated in water. Endogenous peroxidase activity was blocked by treating the slides with a 3% hydrogen peroxide (H_2O_2) solution for 10 minutes. Slides were washed thoroughly in water. Antigen retrieval was performed by pressure-cooking slides in 10mM Tris base, 1mM EDTA (TEDTA) solution, pH9 or 0.01M citric acid solution, pH 6 (refer to table 2) for 1 minute 30 seconds at full pressure. This was followed by washing in tap water. Thereafter, slides were rinsed with phosphate buffered saline (PBS), pH 7.6 (Oxoid, Backingstoke, Hampshire, UK). Non-specific binding was blocked by treating slides with a 5% goat serum solution (DAKO, Denmark). Serum was then drained off and sections were incubated with primary antibody (i.e., Beclin 1, p62, LC3, BAX, Bcl2 and caspase-3) at room temperature at specified times and dilutions (Refer to table 1). The slides were then washed well with PBS. This was followed by incubation with either the polyclonal DAKO Envision labelled polymer or the monoclonal variant, HRP (DAKO, USA) (refer to Table1 and 2) for 30

minutes at room temperature. Sections were washed well with PBS. Positivity was developed by applying the chromogenic substrate 3.3–diaminobenzidine (DAB), (DAKO, USA) for 5-10 minutes. Slides were washed in running tap water and counterstained with Mayer's haematoxylin for approximately 3 minutes. After washing in running tap water, sections were blued in ammoniated water. Finally, the slides were dehydrated through alcohol, cleared with xylene, and mounted with Entellan, (MERK, Germany). Specimens from the cadavers (with no history of CVD) collected for the analysis of the expression of Beclin, p62, LC3, BAX, Bcl2 and caspase-3 served as negative controls. Specimens of heart valves from patients with degenerative AS, stained according to the abovementioned protocol, were used as positive controls for the expression of the afore-listed markers. Photomicrographs of the examined tissues were subjected to computer-assisted image analysis, using a computer coupled to an optical Olympus VS120 microscope, equipped with an Olympus CCD camera (Olympus, Japan) and cell A software (Olympus Soft Imaging Solution GmbH, Germany).

This experiment was optimised for the expression of autophagy markers using diagnostic control tissues, obtained from the Anatomical Pathology department's archive. The following test tissues were used:

Beclin 1	Human smooth/skeletal muscle
SQSTM1/p62	Human colorectal carcinoma tissue
LC3 A/B	Human lung carcinoma/prostate tissue
BAX	Human spleen tissue
Bcl-2	Normal human colon tissue
Caspase-3 (E-8)	Human duodenum tissue

The same approach was used to detect the expressed antigen in the rheumatic valve tissues, by the means of antibodies. Samples preserved in 10% neutral buffered formalin were probed for

autophagy markers (Beclin-1, LC3, p62, BAX, Bcl-2 and caspase-3). A secondary step was performed using secondary IgG antibody (ABC kit, USA) and reactions developed with DAB. Histological and immunohistochemistry analysis and documentation were performed using Axioskop 2 Plus microscope (Zeiss, Germany) equipped with AxioCam HR colour camera and Axiovision Release 4.8.2 SP2 software.

Diagnostic controls for tissue stain optimisation

To optimize each immunohistochemistry (IHC) run, a combination of a diagnostic tissue was used with a negative reagent control in which the primary antibody was swapped out for PBS. (Table 7.2).

Table 7.2. Primary antibody information

Primary antibody	**Clonality**	**Supplier**	**Antigen retrieval**	**Dilution**	**Incubation time**	**Diagnostic control**
Beclin 1	G-11 Mono	Santa Cruz	TEDTA	1:50	Overnight	Skeletal muscle
SQSTM1/p62	D5L7G Mono	Cell Signalling	Citric acid	1:800	1 hour	Colorectal cancer
LC3A/B	D3U4C Poly	Cell Signalling	Citric acid	1:100	Overnight	Lung cancer
BAX	2D2 Mono	Santa Cruz	TEDTA	1:100	1 hour	Spleen
Bcl2	C2 Mono	Santa Cruz	TEDTA	1:50	1 hour	Normal colon
Caspase-3	E-8 Mono	Santa Cruz	TEDTA	1:200	1 hour	Duodenum

Table 7.3. Secondary antibody

Kits	Supplier
Envision HRP System Labelled Polymer Anti-mouse	Dako, CA, USA
Envision HRP System Labelled Polymer Anti-rabbit	Dako, CA, USA
Liquid DAB + Substrate chromogen system	Dako, CA, USA

Preparation of reagents

In 1000 ml of distilled water, haematoxylin, aluminium potassium sulphate, and sodium iodate were dissolved. Thereafter, both chloral hydrate and citric acid were added and dissolved. This solution was then boiled for 10 minutes, cooled, and finally filtered (see details in Appendix B).

Tissue immunohistological analysis

Staining was assessed by two experienced pathologists who were unaware of the patients' medical and clinicopathological histories. Detection of stroma and macrophages was performed by assessing the intensity, proportion and number of stroma and macrophages. Stromal and macrophage intensity was graded as 0,1,2,3 equivalent to, no staining, mild, moderate and strong respectively, whereas stromal and macrophage proportion was graded as 0, 1, 2, 3, 4, 5, as the percentage of the cells that are stained (i.e., 0 =No staining, 1= 1%, 2 = 2-10%, 3 = 10-32%, 4 = 33-66% and 5 = >66%). Number of macrophages were counted in 10 high per fields (HPF). The photographs were taken using the Olympus VS 120 slide microscope color camera (Tokyo, Japan) at 20 x-magnification of objective lens of Olympus slide microscope with a total magnification of 200 x.

7.2 Results

Immunohistochemistry (IHC) staining was optimised with diagnostic tissue samples obtained from the Division of Anatomical Pathology, Department of Pathology, University of Cape Town. For optimisation, IHC staining of formalin fixed paraffin embedded (FFPE) tissue shows a cytoplasmic expression of Beclin in the monocytes of the skeletal tissue, LC3 in the epithelial cells of the lungs, BAX in the cells of the white and red pulp of spleen, Bcl-2 in lymphoid cells of the colon, caspase-3 in the glandular cells of the duodenum; CD68 in the lymphocytes of the tonsil; and nuclear expression of p62 in colorectal adenocarcinoma cells. All the markers were expressed in the cytoplasm, except p62 which was seen in the nucleus (Figure 7.1).

Stromal and macrophage intensity and proportion were similar in RHD and degenerative AS groups compared to control, as they all show a strong intensity and proportion. However, RHD shows a reduced number of positively- stained macrophages compared to degenerative AS and compared control, respectively perhaps due to the advancement of the disease without much evidence of inflammatory process in the valves (Figure 7.2).

The ongoing inflammatory process shown by H&E stain, by the presence of inflammatory cells (Figure 7.3 (e&h)), was also observed in the strong stromal and macrophage expression of Beclin (Figure 7.3 (f&h)), LC3 A&B (Figure 7.3 (g&j)), and p62 (Figure 7.3 (h&k)), in both RHD and degenerative AS tissue samples.

CD68 staining shows a high expression of macrophages in the RHD and degenerative AS groups compared to control (Figure 7.4). There was a moderate staining of BAX, BCL-2 and caspase-3 observed in the RHD and degenerative AS cases compared to control (Figure 7.5).

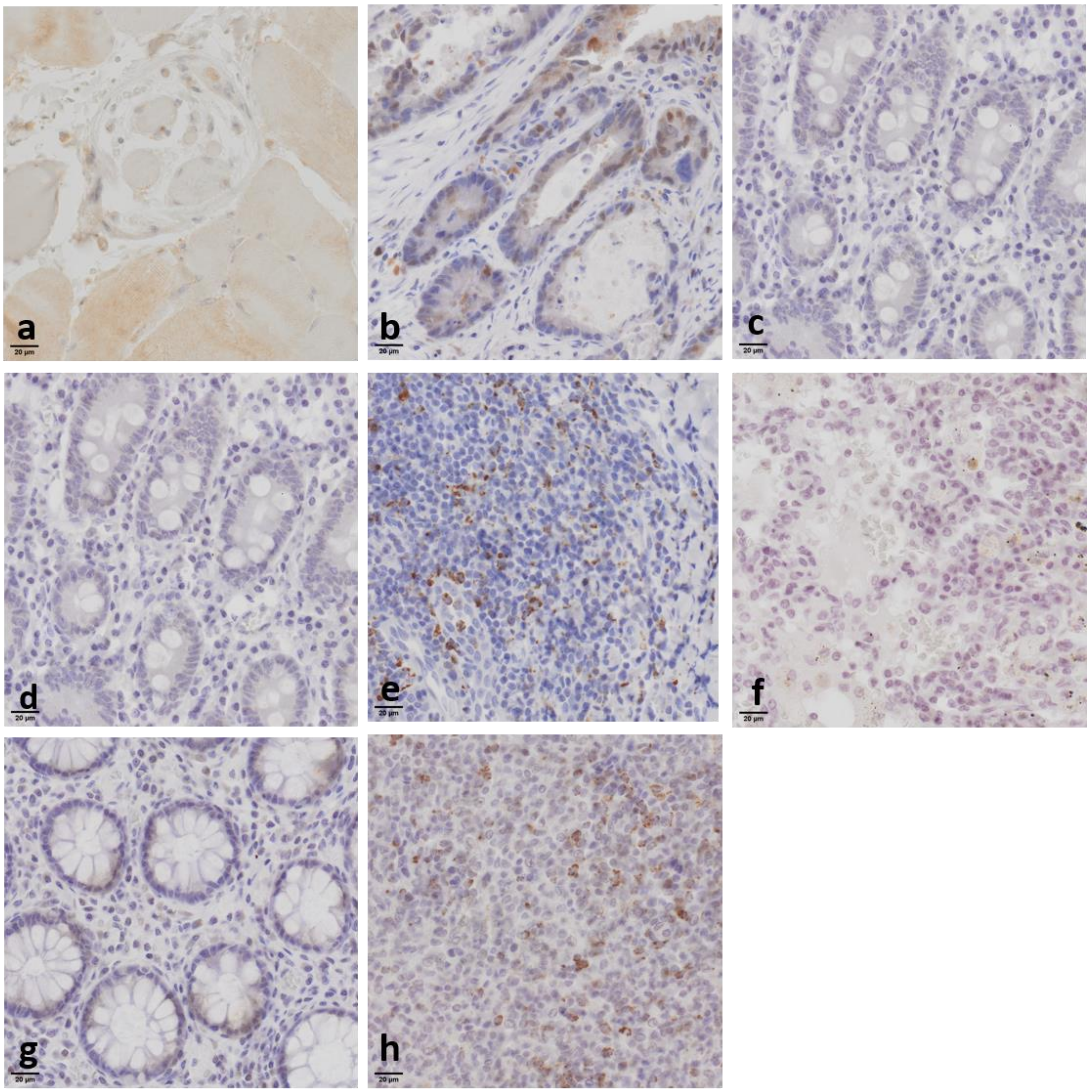

Figure 7.1. Diagnostic tissues optimisation for autophagy marker stains
IHC staining shows a) cytoplasmic staining of monocytes in the skeletal muscle (Beclin); b) nuclear staining of the colorectal adenocarcinoma cells (p62); c) cytoplasmic staining of glandular cells in the duodenum (Caspase-3); cytoplasmic lymphocytic staining in d) Spleen (CD68); e) and Tonsil (CD68); f) cytoplasmic staining of the epithelial cells lungs (LC3); g) cytoplasmic staining of the lymphoid cells of normal human colon (BCl2); h) white and red pulp Spleen (BAX). (Scale bar: 20 μm)

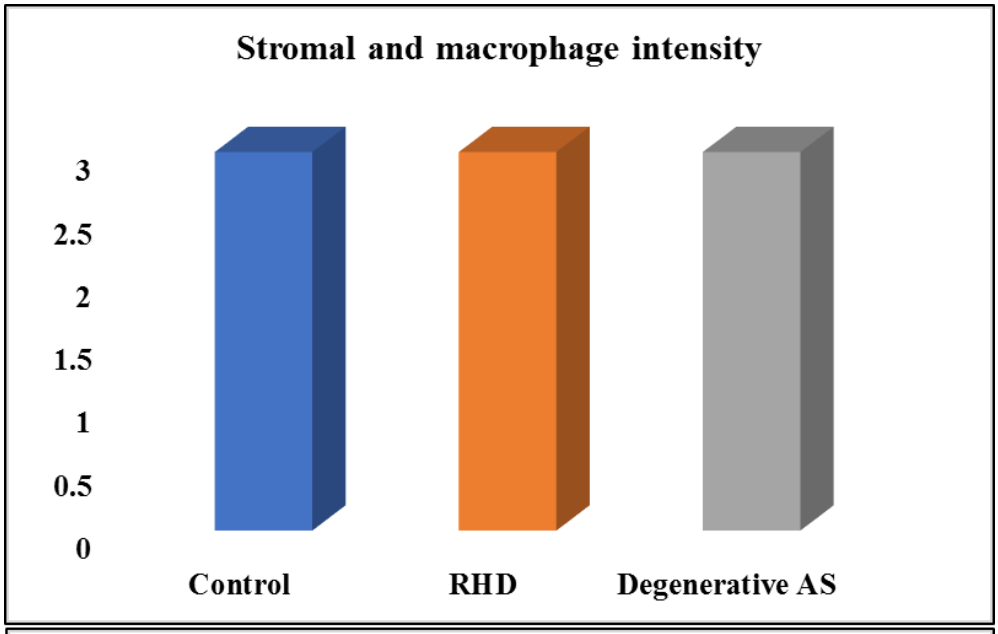
Stromal and macrophage intensity
3
2.5
2
1.5
1
0.5
0
Control
RHD
Degenerative AS

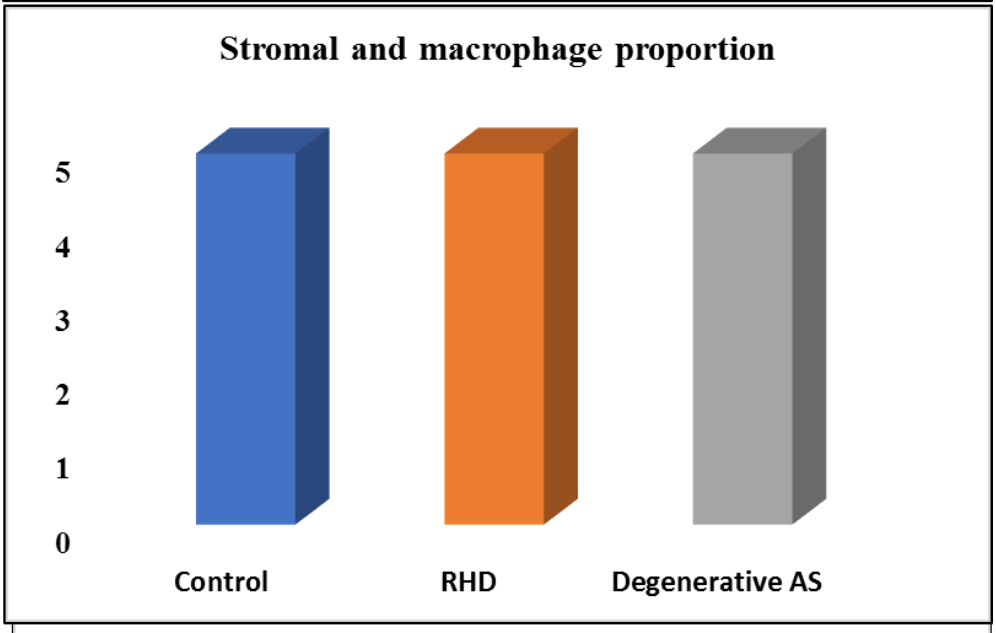
Stromal and macrophage proportion
5
4
3
2
1
0
Control
RHD
Degenerative AS

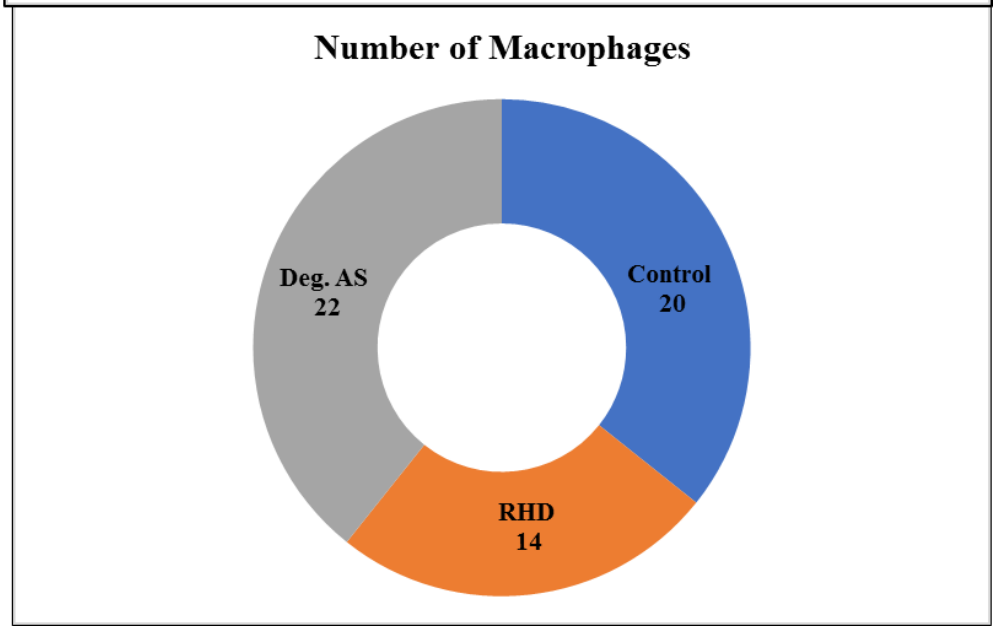
Number of Macrophages
Deg. AS
22
Control
20
RHD
14

Figure 7.2. Stromal and macrophage intensity and proportion.
Bar charts illustrate the stromal and macrophage intensity and proportion in RHD, degenerative AS and cadaveric heart valves. Doughnut shows the number of stained macrophages in RHD (n=14), degenerative AS (n=22) and cadaveric heart valves (n=20). RHD, rheumatic heart disease; degenerative AS, cardiovascular valve disease.

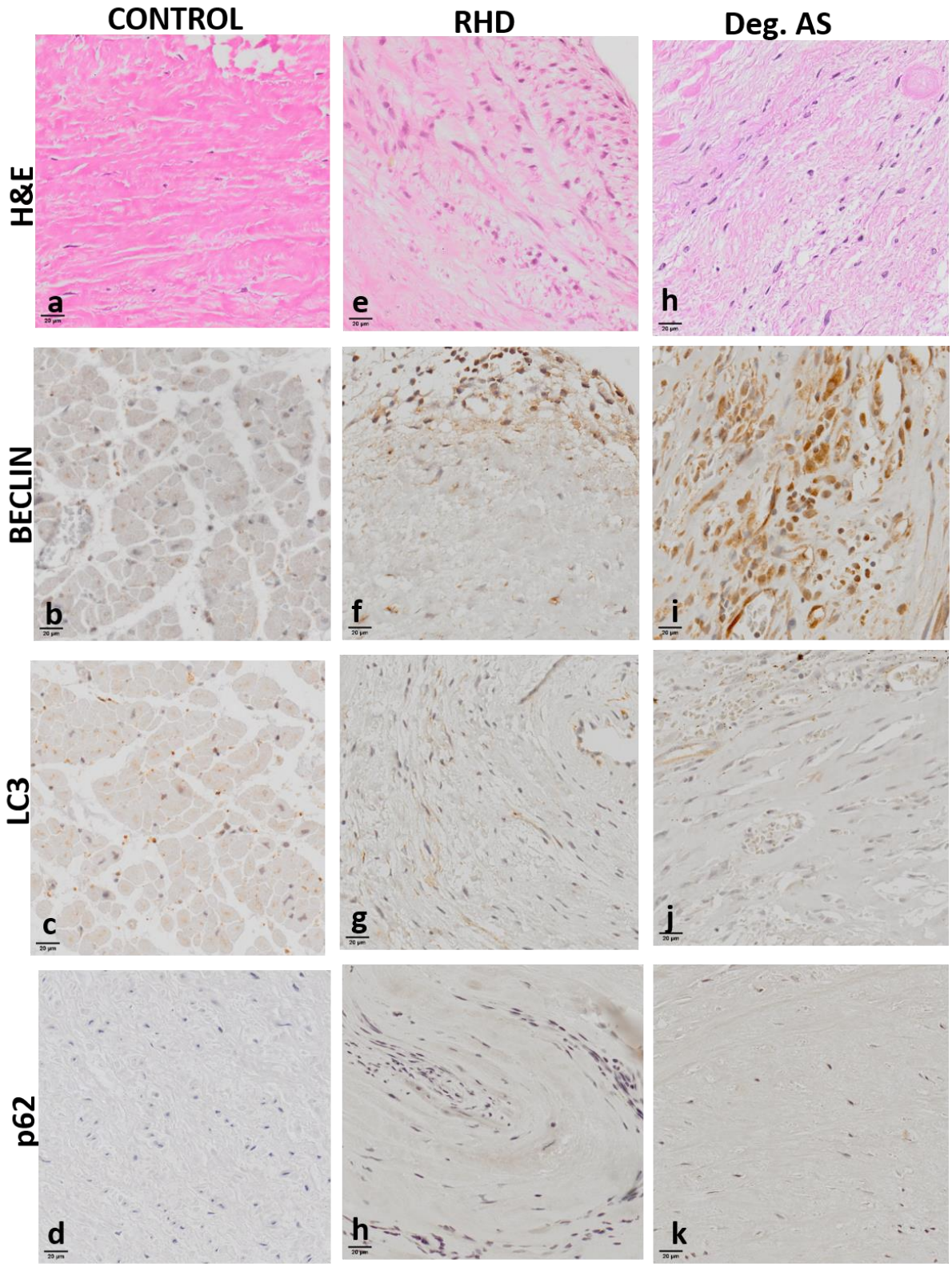

Figure 7.3. Expression of Beclin, LC3A&B and p62 in heart valves of patients with RHD and degenerative AS and, cadaveric valves.

IHC result shows control (a-d), RHD (e-h) and degenerative AS (i-l). Ongoing inflammatory process is shown in H&E stain by the presence of inflammatory cells (Figure 7.3 (e&h). Strong

stromal and macrophage staining for Beclin (f&h), LC3 (g&j), and p62 (h&k), in both RHD and degenerative AS tissue samples. RHD, rheumatic heart disease. (Scale bar: 20 μm).

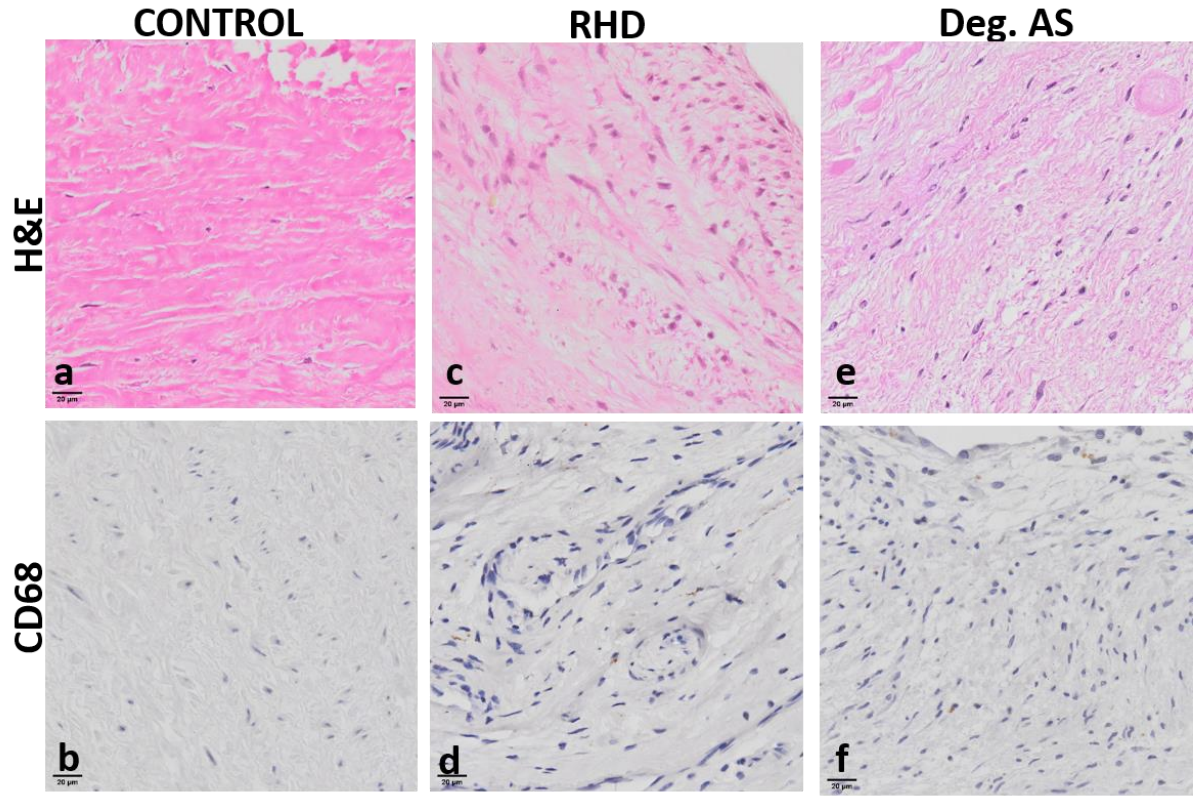

Figure 7.4. Detection of CD68 in heart valves in patients with RHD and degenerative AS and, cadaveric valves.
H&E and IHC staining show control (a-b) and, lymphocyte infiltration and macrophage staining in RHD (c-d) and degenerative AS (e-f). RHD, rheumatic heart disease. (Scale bar: 20 μm)

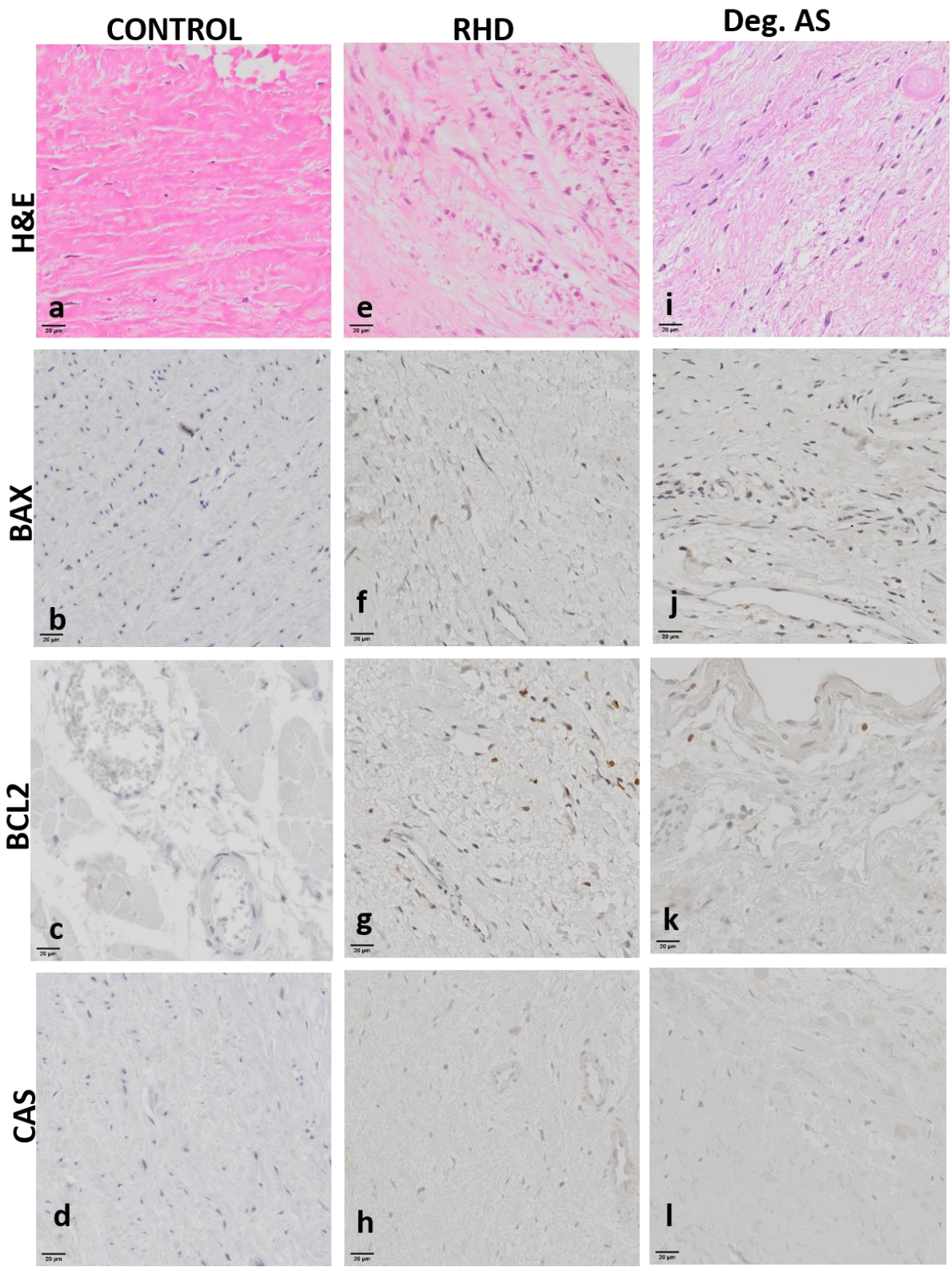

Figure 7.5. Detection of BAX, Bcl-2 and Caspase-3 in heart valves in RHD and degenerative AS and, cadaveric valves.
Control (a-d), RHD (e-h) and degenerative AS (i-l). RHD, rheumatic heart disease. (Scale bar: 20 μm)

7.3 Discussion

Autophagy is a lysosomal-mediated cellular process that degrades and reuses cytoplasmic cargo, specifically the senescent organelles and misfolded proteins, which play important roles in cellular homeostasis.[255]

Over the years, there have been increasing research regarding the crucial role of autophagy as a key factor in the pathogenesis of cardiovascular diseases.[242,256] However, few studies report the role of autophagy in the pathogenesis of RHD. Therefore, the present study is highly significant in RHD and may influence clinical practice.

In this study, H&E staining revealed the presence of inflammatory cells in the RHD and, degenerative AS cohorts compared to control cases. Further, we found some evidence of collagen deposition in our RHD cohort, as depicted by the H&E staining. We also observed a strong staining of Beclin, LC3, p62, BAX, Bcl-2 and caspase-3; and CD68 in RHD and degenerative AS cohorts compared to control cases. There is also a slight difference in the number of macrophages in RHD cohorts compared to degenerative AS and control cases. We observed a lower number of macrophages in the RHD cohorts versus degenerative AS and control cases respectively (14 versus 22 and 20 respectively). These findings taken altogether may imply an ongoing inflammatory process in the two cohorts. However, our RHD cohort are in the advanced stage, hence minimal evidence of inflammatory process was observed in the valves, therefore downregulation of autophagy.

Activation of autophagy pathway functions to prevent excessive inflammation, thereby inhibiting further damaging insults in cells and tissues.[257–259] Aberrant activated autophagy was reported to induce SLE, therefore contributing to the murine pathogenesis of SLE via increased production of proinflammatory cytokines TNF-alpha and IL-6.[260] Previous studies have

demonstrated the immense role of synovial fibroblast in RA, being an autoimmune disease. Production of fibroblast-like synoviocytes (FLS) and citrullinated peptides via increased autophagy in RA has been reported.[237,261,262] Degenerative aortic stenosis is age-related where the regulatory proteins and genes might be undergoing degradation, hence disturbed autophagy.[263] Briefly, during ageing, the aortic valve progressively degenerate, thereby causing a 0.1 cm^2 mean annular reduction of the aortic valve area, which could cause mechanical stress and further cellular damage, hence initiating autophagy. Autophagy is increasingly detectable in elderly patients, as demonstrated in a patient with aortic valve stenosis.[264] Imbalanced endoplasmic reticulum (ER) function and mitochondrial stress, contribute to impaired autophagy, apoptosis, and mitochondrial dysfunction.[265] Our cohort are in the advance RHD stage. Therefore, the role of ageing cannot be overemphasised in this study.

Quantification of Beclin-1 and LC3 gene expression reliably measure autophagosomes formation. Increased expressions of autophagy–related genes (Atgs) promote RA pathogenesis and decreased autophagy reduces disease severity. In the same study, Beclin-1 expression revealed a 3.41-fold increase in patients with early RA despite under treatment.[266] Similarly, reduced apoptosis correlates well with increased autophagy in synovial tissue of RA patients.[267] Beclin-1 and LC3 were overexpressed in the synovial lining layers of RA, which was correlated with decreased levels of miR-30a.[268] In SLE, significant upregulation of Beclin-1, LC3 and p62 expression was found in the peripheral blood mononuclear cells (PBMCs) of patients with SLE.[251] Contrastingly, Beclin-1 was reported to be downregulated in SLE patients.[269] LC3 expression was elevated in B and T lymphocytes in human SLE.[270] p62 was significantly expressed in psoriatic skin lesions compared to atopic dermatitis or control.[252]. In this study, we found a strong expression of Beclin-1, LC3 and p62 which may indicate that activated formation of autophagosomes was involved in the pathogenesis of RHD.

Autophagy prevents cells from undergoing apoptosis,[271] playing an important role in the pathogenesis of several human diseases including cardiomyopathies, bacterial and viral infections which relates to normal balance in the physiological state of tissue structures and functions.[32,272,273] Bcl-2, an inner mitochondrial membrane protein interferes with apoptosis.[274,275]. Bcl-2 plays a key role in vascular homeostasis, and when overexpressed, it protects the cell integrity, hence discontinuing apoptosis. Overexpression of Bcl-2 offered protection against cell death in sepsis.[276] In this study, Bcl-2, BAX and caspase-3 were investigated and found to be weakly expressed, suggesting some evidence of autophagy and progressive apoptosis. There is dearth of literature reporting the role and immunoexpression of Beclin, LC3, p62, BAX, Bcl-2, and caspase-3 in RHD. Nevertheless, a study in 2017 that reported an increased expression of inflammatory genes involved in the NFKB pathway and Th1 cytokine genes (IFNA and IL12B), only briefly addressed autophagy. RHD is an inflammation–driven process which involves an interplay of autophagy markers.[23,256,277–279] The crucial role of autophagy have been widely reported in some autoimmune diseases including SLE, MS, and RA.[251,269,270,280] However, scientific information on the function of autophagy markers in the pathogenesis of RHD is limited. Therefore, since RHD belongs to the myriads of autoimmune diseases, our findings would increase the knowledge base and provide answers to these existing knowledge gaps.

7.4 Conclusion

We used IHC to investigate autophagy in rheumatic and degenerative AS valves in this study. The results of this study probably suggest an ongoing inflammation in the pathogenesis of RHD and degenerative AS due to the presence a moderate to strong staining of the markers (Beclin 1, LC3, p62, BAX, Bcl-2 and caspase-3) investigated. However, further study is required to

ascertain the effect of autophagy in the rate of progression of the disease, and to generate a good statistical power. This might require a prospective comparison of excised valves from a range of between “slow” and “rapid” progressors of rheumatic heart disease.

7.5 Limitations of the study

This study is limited by the small sample size, especially for the cadaveric samples. The acquisition of normal valve tissue from patients with no history of heart disease at postmortem poses to be problematic. Hence the reason for a preliminary study. The presence of calcification, a common characteristic in rheumatic valves also disrupts the normal anatomical morphology of the organelles. Thus, leading to the poor quality of some tissue specimens. Visualisation of the immunopositively- and immunonegatively - stained macrophages was also difficult. Lastly, there was a significant tissue loss due to the non-adherence of the valves on the slides. This could be attributed to the high composition of collagen in valve tissues. To counteract this problem, we picked up the tissues on histobond slides and allowed them to dry on the slides for a lengthy period before commencing staining. Before this solution, several types of slides were tested including self-prepared isocyanide slides, but all was in vain. Altogether, a full study is recommended to statistically justify the detection and expression of the observed autophagy markers involved in the inflammatory process involved in the progression of rheumatic heart disease.

7.6 Acknowledgements

We appreciate the patients who voluntarily partook in this research. In addition, we thank staff at the Department of Anatomical Pathology including Dr. Riyaadh Roberts and Dr. Komala Pillay. Prof. Ntusi gratefully acknowledges support from the South African Medical Research Council, National Research Foundation and the Lily and Ernst Haussmann Trust. This research

was supported by the National Research Foundation by grants to Professors Skatulla and Ntusi (Grant Nos. 104839 and 105858).

8 Limitations

This study had some limitations. Firstly, we excluded patients with an eGFR<30 due to the risk of nephrogenic systemic fibrosis introducing selection bias. Secondly, image quality was impacted due to the lengthy CMR imaging protocol and patients with NYHA Class III symptoms also had trouble with breath-holding. Thirdly, some patients experienced anxiety when placed into the scanner, although they reported no history of claustrophobia. Fourthly, the functional distribution and pathophysiological tissue characterisation of the valve lesions reported is a combination of different degrees of severity, which could influence the distribution. Unfortunately, the sample size is insufficient for further grouping divisions and comparisons which could have influenced the statistical value of the results. Lastly, patients with prosthetic valves were excluded from the study.

The cellular study was limited by the small sample size, especially for the cadaveric samples. The presence of calcification, a common characteristic in rheumatic valves also disrupts the normal anatomical morphology of the organelles. Visualisation of the immunopositively- and immunonegatively stained macrophages was also challenging. Lastly, there was a significant tissue loss due to the non-adherence of the valve on the slide. However, we recut the slides and left for 7-14 days before staining.

8.1 Future work

Altogether, further research is required to correlate findings, especially late gadolinium enhancement and valvular lesions, and to statistically justify the detection and expression of the observed autophagy markers involved in the inflammatory process involved in the

progression of rheumatic heart disease. Further, due to a paucity of literature on CMR and autophagy markers in rheumatic valves, it was challenging to draw comparisons from the existing studies with small sample sizes. Moreover, the pathogenesis of RHD could be investigated holistically. The combination of novel clinical techniques based on proteomics, genomics and metabolomics could be necessary to reveal RHD mechanisms from cell to organ level, stratifying phenotypes and identifying biomarkers.

Chapter 9
Conclusion

9 Conclusion

We employed a multiparametric CMR approach to study the phenotypes of myocardial inflammation, and fibrosis in patients with chronic RHD. We confirmed myocardial fibrosis on LGE imaging in all patients, with no distinct pattern of enhancement and therefore cannot report a specific phenotype of LGE in RHD. We also demonstrated diffuse myocardial fibrosis and the presence of ongoing inflammation on parametric mapping i.e. elevated native T1 and ECV. Furthermore, we found statistically significant differences in LV functional parameters between patients and controls. LVEF was reduced in patients and as expected, the valves most affected were the mitral and aortic valves. Strain parameters were abnormal in RHD. Furthermore, native T1 was elevated in patients which correlates well with the findings of LGE in all patients. Isolated and mixed patterns of valve lesions are commonly seen in RHD, being a disease of the valve and myocardium. Most of RHD patients have severe form of MS, MR, and AS. High frequency of MMAVD with elevated native T1 was observed, indicating a phenotypic myocardial fibrosis. Using CMR tissue characteristic parameters, valvular lesions could be stratified in RHD and therefore, CMR can adequately complement echocardiography in valvular disease diagnosis.

We used IHC to investigate autophagy in rheumatic and degenerative AS valves in this study. The results of this study probably suggest an ongoing inflammation in the pathogenesis of RHD

and degenerative AS due to the presence a moderate to strong staining of the markers (Beclin 1, LC3, p62, BAX, Bcl-2 and caspase-3) investigated. However, further study is required to ascertain the effect of autophagy in the rate of progression of the disease, and to generate a good statistical power. This might require a prospective comparison of excised valves from a range of between “slow” and “rapid” progressors of rheumatic heart disease.

References

1. Zühlke, L. J., Engel, M. E., Watkins, D. & Mayosi, B. M. Incidence, prevalence and outcome of rheumatic heart disease in South Africa: A systematic review of contemporary studies. *Int. J. Cardiol.* **199**, 375–383 (2015).
2. Watkins, D. A., Sebitloane, M., Engel, M. E. & Mayosi, B. M. The burden of antenatal heart disease in South Africa : a systematic review. *BMC Cardiovasc. Disord.* **12**, 1471–2261 (2012).
3. Carapetis, J. R., Zühlke, L., Taubert, K. & Narula, J. Continued Challenge of Rheumatic Heart Disease. *Glob. Heart* **8**, 185–186 (2013).
4. Sliwa, K. *et al.* Incidence and characteristics of newly diagnosed rheumatic heart disease in urban African adults: insights from the heart of Soweto study. *Eur. Heart J.* **31**, 719–727 (2010).
5. Nulu, S., Bukhman, G. & Kwan, G. F. Rheumatic heart disease: the unfinished global agenda. *Cardiol. Clin.* **35**, 165–180 (2017).
6. Rothenbühler, M. *et al.* Active surveillance for rheumatic heart disease in endemic regions : a systematic review and meta-analysis of prevalence among children and adolescents. *Lancet Glob. Heal.* **2**, e717–e726
7. Longo-Mbenza, B. *et al.* Survey of rheumatic heart disease in school children of Kinshasa town. *Int. J. Cardiol.* **63**, 287–294 (1998).
8. Paar, J. A. *et al.* Prevalence of Rheumatic Heart Disease in Children and Young Adults in Nicaragua. *AJC* **105**, 1809–1814 (2010).

9. Noubiap, J. J. *et al.* Prevalence and progression of rheumatic heart disease: a global systematic review and meta-analysis of population-based echocardiographic studies. *Sci. Rep.* **9**, 1–14 (2019).

10. Sika-Paotonu, D., Beaton, A., Raghu, A., Steer, A. & Carapetis, J. Acute rheumatic fever and rheumatic heart disease. *Nat. Rev. Dis. Prim.* **2**, 15085 (2016).

11. Prasad, A., Kumar, S., Kr Singh, B. & Kumari, N. Mortality Due to Rheumatic Heart Disease in Developing World: A Preventable Problem. *J. Clin. Exp. Cardiolog.* **08**, 8–11 (2017).

12. Mendis, S., Puska, P. & Norrving, B. (eds). *Global Atlas on Cardiovascular Disease Prevention and Control.* (2011).

13. Carapetis, J. R., Steer, A. C., Mulholland, E. K. & Weber, M. The global burden of group A streptococcal diseases. *Lancet Infect. Dis.* **5**, 685–694 (2005).

14. Marijon, E., Mirabel, M., Celermajer, D. S. & Jouven, X. Rheumatic heart disease. *Lancet* **379**, 953–964 (2012).

15. Zühlke, L., Mirabel, M. & Marijon, E. Congenital heart disease and rheumatic heart disease in Africa : recent advances and current priorities. 1554–1561 (2013). doi:10.1136/heartjnl-2013-303896

16. Bryant, P. A., Robins-Browne, R., Carapetis, J. R. & Curtis, N. Some of the people, some of the time susceptibility to acute rheumatic fever. *Circulation* **119**, 742–753 (2009).

17. Zuhlke, L. J. *et al.* Group A Streptococcus, Acute Rheumatic Fever and Rheumatic Heart Disease: Epidemiology and Clinical Considerations. *Curr. Treat. Options Cardiovasc. Med.* **19**, (2017).

18. Ntusi, N. A. Cardiovascular magnetic resonance imaging in rheumatic heart disease. *Cardiovasc. J. Afr.* **29**, 135–136 (2018).

19. Abdolmaleki, F. & Kovanen, P. T. Resolvins : Emerging Players in Autoimmune and Inflammatory Diseases. *Clin. Rev. Allergy Immunol.* **2020**, 82–91 (2020).

20. Agrotis, A. *et al.* Redundancy of human ATG4 protease isoforms in autophagy and LC3 / GABARAP processing revealed in cells processing revealed in cells. *Autophagy* **15**, 976–997 (2019).

21. Mizushima, N. & Komatsu, M. Autophagy: renovation of cells and tissues. *Cell* **147**, 728–741 (2011).

22. Das, G., Shravage, B. V & Baehrecke, E. H. Regulation and Function of Autophagy during Cell Survival and Cell Death. *Cold Spring Harb Perspect Biol* **2012**, 1–14 (2012).

23. Condello, M., Pellegrini, E., Caraglia, M. & Meschini, S. Targeting Autophagy to Overcome Human Diseases. *Int. J. Mol. Sci.* **20**, 725 (2019).

24. Rubinsztein, D. C., Shpilka, T. & Elazar, Z. Mechanisms of Autophagosome Biogenesis Minireview. *Curr. Biol.* **22**, R29–R34 (2012).

25. Zaffagnini, G. & Martens, S. Mechanisms of Selective Autophagy. *J. Mol. Biol.* **428**, 1714–1724 (2016).

26. Wirth, M. *et al.* Molecular determinants regulating selective binding of autophagy adapters and receptors to ATG8 proteins. *Nat. Commun.* **10**, 2055 (2019).

27. Johansen, T. & Lamark, T. Selective Autophagy: ATG8 Family Proteins, LIR Motifs and Cargo Receptors. *J. Mol. Biol.* **432**, 80–103 (2020).

28. Johansen, T. & Lamark, T. Selective autophagy mediated by autophagic adapter proteins. *Autophagy* **7**, 279–296 (2011).

29. Itakura, E. & Mizushima, N. p62 Targeting to the autophagosome formation site requires self-oligomerization but not LC3 binding. *J. Cell Biol.* **192**, 17–27 (2011).

30. Schläfli, A. M., Berezowska, S., Adams, O., Langer, R. & Tschan, M. P. Reliable LC3

and p62 autophagy marker detection in formalin fixed paraffin embedded human tissue by immunohistochemistry. *Eur. J. Histochem.* **59**, 137–144 (2015).

31. Schläfli, A. M. *et al.* Prognostic value of the autophagy markers LC3 and p62/SQSTM1 in early-stage non-small cell lung cancer. *Oncotarget* **7**, 39544–39555 (2016).

32. Kang, R., Zeh, H. J., Lotze, M. T. & Tang, D. The Beclin 1 network regulates autophagy and apoptosis. *Cell Death Differ.* **18**, 571–580 (2011).

33. Lavandero, S., Chiong, M., Rothermel, B. A. & Hill, J. A. Autophagy in cardiovascular biology. *J. Clin. Invest.* **125**, 55–64 (2015).

34. Yin, H. *et al.* The therapeutic and pathogenic role of autophagy in autoimmune diseases. *Front. Immunol.* **9**, 1512 (2018).

35. Gros, F. & Muller, S. Pharmacological regulators of autophagy and their link with modulators of lupus. *Br. J. Pharmacol.* **2014**, 4337–4359 (2014).

36. Mendis, S., Puska, P. & Norrving, B. (eds). Global Atlas on Cardiovascular Disease Prevention and Control. (2011).

37. Makrexeni, Z. M. & Pepeta, L. Clinical presentation and outcomes of patients with acute rheumatic fever and rheumatic heart disease seen at a tertiary hospital setting in Port Elizabeth, South Africa. *Cardiovasc. J. Afr.* **28**, 1–7 (2017).

38. Aguilar, F. *et al.* Imaging modalities in valvular heart disease. *Curr. Cardiol. Rep.* **10**, 98–103 (2008).

39. Naoum, C., Blanke, P., Cavalcante, J. L. & Leipsic, J. Cardiac Computed Tomography and Magnetic Resonance Imaging in the Evaluation of Mitral and Tricuspid Valve Disease. *Circ. Cardiovasc. Imaging* **10**, (2017).

40. Chambers, J. B. *et al.* Appropriateness criteria for the use of cardiovascular imaging in heart valve disease in adults: a European Association of Cardiovascular Imaging report

of literature review and current practice. *Eur. Hear. J. - Cardiovasc. Imaging* **18**, 489–498 (2017).

41. Youngstein, T. *et al.* FDG Uptake by Prosthetic Arterial Grafts in Large Vessel Vasculitis Is Not Specific for Active Disease. *JACC Cardiovasc. Imaging* **10**, 1042–1052 (2017).

42. Nagesh, C. M. *et al.* The role of 18F fluorodeoxyglucose positron emission tomography (18F-FDG-PET) in children with rheumatic carditis and chronic rheumatic heart disease. *Nucl. Med. Rev.* **18**, 25–28 (2015).

43. Kirvan, C. A., Galvin, J. E., Hilt, S., Kosanke, S. & Cunningham, M. W. Identification of streptococcal m-protein cardiopathogenic epitopes in experimental autoimmune valvulitis. *J. Cardiovasc. Transl. Res.* **7**, 172–181 (2014).

44. Mcguinness, M., Sibanda, N. & Welsh, M. Modeling Acute Rheumatic Fever. *GMPS* **22**, 187–208 (2015).

45. Carapetis, J. R. *et al.* Acute rheumatic fever and rheumatic heart disease. *Nat. Rev. Dis. Prim.* **2**, 15084 (2016).

46. Dougherty, S., Khorsandi, M. & Herbst, P. Rheumatic heart disease screening : Current concepts and challenges. *Ann Pediatr Card* **10**, 39–50 (2017).

47. Currie, B. J. Critical issues in prevention and control of rheumatic fever and rheumatic heart disease. *Int. Congr. Ser.* **1289**, 281–284 (2006).

48. Ellis, N. M. J. *et al.* Priming the Immune System for Heart Disease : A Perspective on Group A Streptococci. *J. Infect. Dis.* **202**, 1059–1067 (2010).

49. Cunningham, M. W. Pathogenesis of Group A Streptococcal Infections. *Clin. Microbiol. Rev.* **13**, 470–511 (2000).

50. Cunningham, M. W. *Post-Streptococcal Autoimmune Sequelae : Rheumatic Fever and Beyond*. (Streptococccus Pyogenes, 2016).

51. Martin, W. J. *et al.* Post-infectious group A streptococcal autoimmune syndromes and the heart. *Autoimmun. Rev.* **14**, 710–725 (2015).

52. Galvin, J. E. *et al.* Cytotoxic mAb from rheumatic carditis recognizes heart valves and laminin Find the latest version : Cytotoxic mAb from rheumatic carditis recognizes heart valves and laminin. **106**, 217–224 (2000).

53. Fae, K. T cell molecular mimicry and rheumatic heart disease. *Int. Congr. Ser.* **1289**, 293–295 (2006).

54. Tandon, R. *et al.* Revisiting the pathogenesis of rheumatic fever and carditis. *Nat. Rev. Cardiol.* **10**, 171–177 (2013).

55. Williamson, D. A. *et al.* M-Protein Analysis of Streptococcus pyogenes Isolates Associated with Acute Rheumatic Fever in New Zealand. **53**, 3618–3620 (2015).

56. Henningham, A., Barnett, T. C., Maamary, P. G. & Walker, M. J. Pathogenesis of group A streptococcal infections. *Discov. Med.* **13**, 329–342 (2012).

57. Romani, L., Steer, A. C., Whitfeld, M. J. & Kaldor, J. M. Prevalence of scabies and impetigo worldwide : a systematic review. *Lancet Infect. Dis.* **15**, 960–967 (2015).

58. Kumar, R. K. *et al.* Contemporary diagnosis and management of rheumatic heart disease: implications for closing the gap: a scientific statement from the American heart association. *Circulation* **142**, e337–e357 (2020).

59. Refat, M., Rashad, E. S., Gazar, F. A. El, Soubky, M. K. El & Eissa, A. M. A CLINICOEPIDEMIOLOGIC STUDY OF HEART DISEASE IN SCHOOLCHILDREN OF MENOUFIA , EGYPT. *Ann. Saudi Med.* **14**, 225–229 (1994).

60. Beaton, A. *et al.* Echocardiography Screening for Rheumatic Heart Disease in Ugandan Schoolchildren. *Circulation* **2012**, 3127–3132 (2012).

61. Sims, N. A. Does anti-sclerostin therapy promote inflammation in rheumatoid

arthritis ? *Nat. Rev. Endocrinol.* **12**, 314+ (2016).

62. Yadeta, D. *et al.* Prevalence of rheumatic heart disease among school children in Ethiopia : A multisite echocardiography-based screening. *Int. J. Cardiol.* **221**, 260–263 (2016).

63. Gleason, B. *et al.* Prevalence of Latent Rheumatic Heart Disease Among HIV-Infected Children in Kampala , Uganda. *J Acquir Immune Defic Syndr.* **71**, 196–199 (2016).

64. Gapu, P. *et al.* Rheumatic fever and rheumatic heart disease among children presenting to two referral hospitals in Harare , Zimbabwe. *S Afr Med J* **105**, 384–388 (2015).

65. Van Zyl, M. L., Van Staden, D. A. & Potgieter, M. D. Beta-hemolytic streptococci as a cause of sore throat in the Pretoria area. *South African Med. journal= Suid-Afrikaanse Tydskr. vir Geneeskd.* **59**, 783–784 (1981).

66. Engel, M. E. & Mayosi, B. M. Clinical and epidemiological aspects of streptococcus pyogenes pharyngitis and carriage in Africa: streptococcus pyogenes in Africa. *SA Hear.* **10**, 434–439 (2013).

67. Soma-Pillay, P., Macdonald, A. P., Mathivha, T. M., Bakker, J. L. & Mackintosh, M. O. Cardiac disease in pregnancy: A 4-year audit at Pretoria Academic Hospital. *South African Med. J.* **98**, 553–556 (2008).

68. Sliwa, K. *et al.* Spectrum of cardiac disease in maternity in a low-resource cohort in South Africa. *Heart* **2014**, 1967–1974 (2014).

69. Zühlke, L., Watkins, D. & Engel, M. E. Incidence , prevalence and outcomes of rheumatic heart disease in South Africa : a systematic review protocol. *BMJ Open* **2014**, 1–6 (2014).

70. Lawrence, J. G. *et al.* Epidemiology and Prevention Acute Rheumatic Fever and Rheumatic Heart Disease. *Circulation* **2013**, 492–501 (2013).

71. Parnaby, M. G. & Carapetis, J. R. Rheumatic fever in Indigenous Australian children.

J. Paediatr. Child Health **46**, 527–533 (2010).

72. Nana, M. L. A., Anderson, J. L., Carlquist, J. F. & Nanas, J. N. HLA-DR typing and lymphocyte subset evaluation in rheumatic heart disease: a search for immune response factors. *Am. Heart J.* **112**, 992–997 (1986).

73. Saether, S. G., Otto, H., Haugen, B. O., Banteyrga, L. & Skjaerpe, T. High Prevalence of Subclinical Rheumatic Heart Disease in Pregnant Women in a Developing Country: An Echocardiographic Study. *Echocardiography* **28**, 1049–1053 (2011).

74. Yacoub, M. H. & Cohn, L. H. From Structure to Function : Part II. *Circulation* **2004**, 1064–1072 (2004).

75. Murray, C. J. L. *et al.* Disability-adjusted life years (DALYs) for 291 diseases and injuries in 21 regions, 1990–2010: a systematic analysis for the Global Burden of Disease Study 2010. *Lancet* **380**, 2197–2223 (2012).

76. Bonny, A. *et al.* Rationale and design of the Pan-African Sudden Cardiac Death survey : the Pan-African SCD study. *Cardiovasc. J. Afr.* **25**, 176–181 (2014).

77. Krishnamurthi, R. V *et al.* The global burden of hemorrhagic stroke: a summary of findings from the GBD 2010 study. *Glob. Heart* **9**, 101–106 (2014).

78. Yew, H. Sen & Murdoch, D. R. Global Trends in Infective Endocarditis Epidemiology. *Curr Infect Dis Rep* **2012**, 367–372 (2012).

79. Gewitz, M. H. *et al.* Revision of the Jones criteria for the diagnosis of acute rheumatic fever in the era of Doppler echocardiography a scientific statement from the American heart association. *Circulation* **131**, 1806–1818 (2015).

80. Remenyi, B., Elguindy, A., Smith, S. C., Yacoub, M. & Holmes, D. R. Valvular aspects of rheumatic heart disease. *Lancet* **387**, 1335–1346 (2016).

81. Mutnuru, P. C., Singh, S., D' Souza, J. & Perubhotla, L. M. Cardiac mr imaging in the evaluation of rheumatic valvular heart diseases. *J. Clin. Diagnostic Res.* **10**, AC06–

AC09 (2016).

82. Guo, Q. *et al.* Early Detection of Silent Myocardial Impairment in Drug-Naive Patients With New-Onset Systemic Lupus Erythematosus: A Three-Center Prospective Study. *Arthritis Rheumatol.* **70**, 2014–2024 (2018).

83. De Oliveira Martins, C. *et al.* Rheumatic heart disease and myxomatous degeneration: Differences and similarities of valve damage resulting from autoimmune reactions and matrix disorganization. *PLoS One* **12**, 1–12 (2017).

84. Hall, P. *et al.* LEFT ATRIAL ENLARGEMENT IN CHILDREN SCREENED FOR RHEUMATIC HEART DISEASE IN. *J. Am. Coll. Cardiol.* **73**, 2027 (2019).

85. Lane, A. S., Clancy, D. J., Seppelt, I. M., Orde, S. R. & Hospital, N. Massive Left Atrium from Severe Mitral Stenosis due to Rheumatic Heart Disease: Clinical Images Not Usually Seen in Modern Radiology and Ultrasound. *J. Clin. Case Reports Images* **1**, 1–6 (2019).

86. Özkartal, T. *et al.* Asymptomatic post-rheumatic giant left atrium. *World J Cardiol* **8**, 375–379 (2016).

87. Anandan, P. K., Shukkarbhai, P. J. & Cholenahally, M. N. Giant left and right Atrium in rheumatic mitral stenosis and tricuspid regurgitation. *J. Cardiovasc. Echogr.* **25**, 113 (2015).

88. Unger, P., Clavel, M., Lindman, B. R. & Mathieu, P. Pathophysiology and management of multivalvular disease. *Nat. Publ. Gr.* (2016). doi:10.1038/nrcardio.2016.57

89. Topal, A. E., Eren, M. N. & Celik, Y. Left ventricle and left atrium remodeling after mitral valve replacement in case of mixed mitral valve disease of rheumatic origin. *J. Card. Surg.* **25**, 367–372 (2010).

90. Motiwala, S. R. & Delling, F. N. Assessment of Mitral Valve Disease: A Review of

Imaging Modalities. *Curr. Treat. Options Cardiovasc. Med.* **17**, (2015).

91. Steinmetz, M. & C Preus, H. Non-Invasive Imaging for Congenital Heart Disease – Recent Progress in Cardiac MRI. *J. Clin. Exp. Cardiolog.* **01**, (2012).

92. Saxena, A., Zühlke, L. & Wilson, N. Echocardiographic screening for rheumatic heart disease: Issues for the cardiology community. *Glob. Heart* **8**, 197–202 (2013).

93. Jouan, J. Mitral valve repair over five decades. *Ann. Cardiothorac. Surg.* **4**, 322–34 (2015).

94. Leśniak-Sobelga, A. *et al.* Relationship between mitral leaflets angles, left ventricular geometry and mitral deformation indices in patients with ischemic mitral regurgitation: Imaging by echocardiography and cardiac magnetic resonance. *Int. J. Cardiovasc. Imaging* **28**, 59–67 (2012).

95. Lancellotti, P. *et al.* The use of echocardiography in acute cardiovascular care: recommendations of the European Association of Cardiovascular Imaging and the Acute Cardiovascular Care Association. *Eur. Heart J. Cardiovasc. Imaging* **16**, 119–146 (2015).

96. Zoghbi, W. A. *et al.* Recommendations for Noninvasive Evaluation of Native Valvular Regurgitation: A Report from the American Society of Echocardiography Developed in Collaboration with the Society for Cardiovascular Magnetic Resonance. *J. Am. Soc. Echocardiogr.* **30**, 303–371 (2017).

97. Nishimura, R. A. *et al.* 2014 AHA/ACC guideline for the management of patients with valvular heart disease: A report of the American college of cardiology/American heart association task force on practice guidelines. *J. Am. Coll. Cardiol.* **63**, 1–234 (2014).

98. Dudzinski, D. M. & Hung, J. Echocardiographic assessment of ischemic mitral regurgitation. *Cardiovasc. Ultrasound* **12**, 46 (2014).

99. Beniwal, R., Bhaya, M., Panwar, R. B., Panwar, S. & Singh, A. Diagnostic criteria in

rheumatic heart disease. *Glob. Heart* **10**, 81–82 (2015).

100. Szyszka, A. *et al.* Echocardiography in adults. *J Ultrason 2019* **19**, 54–61 (2019).

101. Reméanyi, B. *et al.* World Heart Federation criteria for echocardiographic diagnosis of rheumatic heart disease-an evidence-based guideline. *Nat. Rev. Cardiol.* **9**, 297–309 (2012).

102. Taylor, A. J., Salerno, M., Dharmakumar, R. & Jerosch-Herold, M. T1 Mapping Basic Techniques and Clinical Applications. *JACC Cardiovasc. Imaging* **9**, 67–81 (2016).

103. Haaf, P. *et al.* Cardiac T1 Mapping and Extracellular Volume (ECV) in clinical practice: a comprehensive review. *J. Cardiovasc. Magn. Reson.* **18**, 89 (2017).

104. Gräni, C. *et al.* Comparison of myocardial fibrosis quantification methods by cardiovascular magnetic resonance imaging for risk stratification of patients with suspected myocarditis. *J. Cardiovasc. Magn. Reson.* **0**, 1–11 (2019).

105. Kim, K.-H., Park, C. H., Park, H. S., Kim, Y.-R. & Choi, E.-Y. Amyloidosis-induced tricuspid stenosis mimicking rheumatic heart disease. *European heart journal* 1167 (2014).

106. Kim, P. K. *et al.* Myocardial T1 and T2 mapping: Techniques and clinical applications. *Korean J. Radiol.* **18**, 113–131 (2017).

107. Kellman, P. & Hansen, M. S. T1-mapping in the heart: accuracy and precision. *J. Cardiovasc. Magn. Reson.* **16**, 2 (2014).

108. Dabir, D. *et al.* Reference values for healthy human myocardium using a T1 mapping methodology: results from the International T1 Multicenter cardiovascular magnetic resonance study. *J. Cardiovasc. Magn. Reson.* **16**, 69 (2014).

109. Piechnik, S. K. *et al.* Normal variation of magnetic resonance T1 relaxation times in the human population at 1 . 5 T using ShMOLLI. *J. Cardiovasc. Magn. Reson.* **15**, 1–11 (2013).

110. Dass, S. *et al.* Myocardial Tissue Characterization Using Magnetic Resonance Noncontrast T1 Mapping in Hypertrophic and Dilated Cardiomyopathy. *Circ Cardiovasc Imaging.* **2012**, 726–733 (2012).

111. Ugander, M. *et al.* Extracellular volume imaging by magnetic resonance imaging provides insights into overt and sub-clinical myocardial pathology. *Eur. Heart J.* **im**, 1268–1278 (2012).

112. Messroghli, D. R. *et al.* Clinical recommendations for cardiovascular magnetic resonance mapping of T1 , T2 , T2 * and extracellular volume : A consensus statement by the Society for Cardiovascular Magnetic Resonance (SCMR) endorsed by the European Association for Cardiovascular. *J. Cardiovasc. Magn. Reson.* **2017**, 1–24 (2017).

113. Ferreira, V. M., Piechnik, S. K., Robson, M. D., Neubauer, S. & Karamitsos, T. D. Myocardial Tissue Characterization by Magnetic Resonance Imaging. *J. Thorac. Imaging* **29**, 147–154 (2014).

114. Hinojar, R. *et al.* Native T1 in discrimination of acute and convalescent stages in patients with clinical diagnosis of myocarditis: A proposed diagnostic algorithm using CMR. *JACC Cardiovasc. Imaging* **8**, 37–46 (2015).

115. Mapping, M. T. *et al.* Identification and Assessment of Anderson-Fabry Disease by Cardiovascular Magnetic Resonance Noncontrast. 16–18 (2013). doi:10.1161/CIRCIMAGING.112.000070

116. Sado, D. M. *et al.* Noncontrast Myocardial T 1 Mapping Using Cardiovascular Magnetic Resonance for Iron Overload. **1511**, 1505–1511 (2015).

117. Moon, J. C., Treibel, T. A. & Schelbert, E. B. T1 mapping for diffuse myocardial fibrosis: a key biomarker in cardiac disease? *Journal of the American College of Cardiology* **62**, 1288–1289 (2013).

118. Barison, A., Grigoratos, C., Todiere, G. & Aquaro, G. D. Myocardial interstitial remodelling in non-ischaemic dilated cardiomyopathy: insights from cardiovascular magnetic resonance. *Heart Fail. Rev.* **20**, 731–749 (2015).

119. Schelbert, E. B. & Messroghli, D. R. State of the Art: Clinical Applications of Cardiac T1 Mapping. *Radiology* **278**, 658–676 (2016).

120. Haaf, P. *et al.* Cardiac T1 Mapping and Extracellular Volume (ECV) in clinical practice : a comprehensive review. *J. Cardiovasc. Magn. Reson.* 1–12 (2016). doi:10.1186/s12968-016-0308-4

121. Kellman, P., Arai, A. E. & Xue, H. T1 and extracellular volume mapping in the heart: estimation of error maps and the influence of noise on precision. *J. Cardiovasc. Magn. Reson.* **15**, 56 (2013).

122. Ntusi, N. A. B. *et al.* Diffuse myocardial fibrosis and inflammation in rheumatoid arthritis: Insights from CMR T1 Mapping. *JACC Cardiovasc. Imaging* **8**, 526–536 (2015).

123. Ntusi, N. A. *et al.* Subclinical myocardial inflammation and diffuse fibrosis are common in systemic sclerosis - A clinical study using myocardial T1-mapping and extracellular volume quantification. *J. Cardiovasc. Magn. Reson.* **16**, 1–12 (2014).

124. Seung-Pyo Lee, Whal Lee, Joo Myung Lee, Eun-Ah Park, Hyung-Kwan Kim, Yong-Jin Kim, D.-W. S. Assessment of Diffuse Myocardial Fibrosis by Using MR Imaging in Asymptomatic. *Radiology* **274**, 359–369 (2015).

125. Gulsin, G. S., Singh, A. & McCann, G. P. Cardiovascular magnetic resonance in the evaluation of heart valve disease. *BMC Med. Imaging* **17**, 1–14 (2017).

126. Pennell, D. J. Cardiovascular magnetic resonance. *Circulation* **121**, 692–705 (2010).

127. Durand, M. & Miranda. Cardiovascular magnetic resonance imaging in valvular heart disease. *South African J. Radiol.* **20**, 8 pages (2016).

128. Tarkiainen, M. *et al.* Cardiovascular magnetic resonance of mitral valve length in hypertrophic cardiomyopathy. *J. Cardiovasc. Magn. Reson.* **18**, 1–10 (2016).

129. Kon, M. W. S., Myerson, S. G., Moat, N. E. & Pennell, D. J. Quantification of regurgitant fraction in mitral regurgitation by cardiovascular magnetic resonance: comparison of techniques. *J. Heart Valve Dis.* **13**, 600—607 (2004).

130. Uretsky, S. *et al.* Discordance between echocardiography and MRI in the assessment of mitral regurgitation severity: A prospective multicenter trial. *J. Am. Coll. Cardiol.* **65**, 1078–1088 (2015).

131. Sachdev, V. *et al.* Are Echocardiography and CMR Really Discordant in Mitral Regurgitation? *JACC Cardiovasc. Imaging* **10**, 823–824 (2017).

132. Mehta, N. K. *et al.* Utility of cardiac magnetic resonance for evaluation of mitral regurgitation prior to mitral valve surgery. *J. Thorac. Dis.* **9**, S246–S256 (2017).

133. Saremi, F., Hassani, C., Millan-Nunez, V. & Sánchez-Quintana, D. Imaging Evaluation of Tricuspid Valve: Analysis of Morphology and Function With CT and MRI. *AJR. Am. J. Roentgenol.* **204**, W531-42 (2015).

134. Motiwala, S. R. & Delling, F. N. Assessment of Mitral Valve Disease: A Review of Imaging Modalities. *Curr Treat Options Cardio Med* **17**, 1–16 (2015).

135. Krieger, E. V., Lee, J., Branch, K. R. & Hamilton-Craig, C. Quantitation of mitral regurgitation with cardiac magnetic resonance imaging: A systematic review. *Heart* **102**, 1864–1870 (2016).

136. Sommer, G., Bremerich, J. & Lund, G. Magnetic resonance imaging in valvular heart disease: Clinical application and current role for patient management. *J. Magn. Reson. Imaging* **35**, 1241–1252 (2012).

137. Srivatsa, S. S. *et al.* Liquefaction necrosis of mitral annular calcification (LNMAC): Review of pathology, prevalence, imaging and management: Proposed diagnostic

imaging criteria with detailed multi-modality and MRI image characterization. *Int. J. Cardiovasc. Imaging* **28**, 1161–1171 (2012).

138. Wu, V., Chyou, J. Y., Chung, S., Bhagavatula, S. & Axel, L. Evaluation of diastolic function by three-dimensional volume tracking of the mitral annulus with cardiovascular magnetic resonance : comparison with tissue Doppler imaging. *J. Cardiovasc. Magn. Reson.* **16**, 1–14 (2014).

139. Leng, S. *et al.* Imaging 4D morphology and dynamics of mitral annulus in humans using cardiac cine MR feature tracking. *Sci. Rep.* **8**, 1–13 (2018).

140. Taylor, R. J. *et al.* Myocardial strain measurement with feature-tracking cardiovascular magnetic resonance : normal values. *Eur. Hear. J. – Cardiovasc. Imaging* **16**, 871–881 (2018).

141. Myerson, S. G. *et al.* Aortic regurgitation quantification using cardiovascular magnetic resonance: Association with clinical outcome. *Circulation* **126**, 1452–1460 (2012).

142. Myerson, S. G. Heart valve disease: investigation by cardiovascular magnetic resonance. *J. Cardiovasc. Magn. Reson.* **14**, 7 (2012).

143. Armstrong, A. C. *et al.* LV Mass Assessed by Echocardiography and CMR, Cardiovascular Outcomes, and Medical Practice. *JACC Cardiovasc. Imaging* **5**, 837 LP – 848 (2012).

144. Kutty, S. *et al.* Qualitative Echocardiographic Assessment of Aortic Valve Regurgitation with Quantitative Cardiac Magnetic Resonance: A Comparative Study. *Pediatr. Cardiol.* **30**, 971–977 (2009).

145. Choo, W. S. & Steeds, R. P. Cardiac imaging in valvular heart disease. *Br. J. Radiol.* **84 Spec No**, S245-57 (2011).

146. Rong Bing; João L. Cavalcante; Russell J. Everett, Marie-Annick Clavel, David E. Newby, M. R. D. Imaging and Impact of Myocardial Fibrosis in Aortic Stenosis.

JACC. Cardiovasc. Imaging **12**, 283–296 (2019).

147. Hashkes, P. J. *et al.* Naproxen as an alternative to aspirin for the treatment of arthritis of rheumatic fever: a randomized trial. *J. Pediatr.* **143**, 399–401 (2003).

148. Nishimura, R. A. *et al.* 2014 AHA/ACC guideline for the management of patients with valvular heart disease: A report of the American college of cardiology/American heart association task force on practice guidelines. *J. Am. Coll. Cardiol.* **63**, (2014).

149. Derya, E.-Y., Ukke, K., Taner, Y. & Izzet, A. Y. Applying manual pressure before benzathine penicillin injection for rheumatic fever prophylaxis reduces pain in children. *Pain Manag. Nurs.* **16**, 328–335 (2015).

150. Association, W. M. World Medical Association Declaration of Helsinki: Ethical Principles for Medical Research Involving Human Subjects. *JAMA* **310**, 2191–2194 (2013).

151. Zuhlke, L. *et al.* Characteristics, complications, and gaps in evidence-based interventions in rheumatic heart disease: The Global Rheumatic Heart Disease Registry (the REMEDY study). *Eur. Heart J.* **36**, 1115–1122 (2015).

152. White, S. K. *et al.* T1 mapping for myocardial extracellular volume measurement by CMR: bolus only versus primed infusion technique. *JACC. Cardiovasc. Imaging* **6**, 955–962 (2013).

153. Doltra, A., Amundsen, B. H., Gebker, R., Fleck, E. & Kelle, S. Emerging Concepts for Myocardial Late Gadolinium Enhancement MRI. *Curr. Cardiol. Rev.* **9**, 185–190 (2013).

154. Hajsadeghi, S., Hassanzadeh, M., Hajahmadi, M. & Kadivar, M. Concurrent diagnosis of infective endocarditis and acute rheumatic fever: A case report. *J. Cardiol. Cases* 10–13 (2018). doi:10.1016/j.jccase.2017.12.011

155. Pattanayak, P. & Bleumke, D. A. Tissue Characterization of the Myocardium. *Radiol.*

Clin. **53**, 413–423 (2018).

156. Jellis, C. L. & Kwon, D. H. Myocardial T1 mapping : modalities and clinical applications. *Cardiovasc Diagn Ther* **4**, 126–137 (2014).

157. Ays, C. The evaluation of non‐ischemic dilated cardiomyopathy with T1 mapping and ECV methods using 3T cardiac MRI. *Radiol med* **122**, 106–112 (2017).

158. Scully, P. R., Bastarrika, G., Moon, J. C. & Treibel, T. A. Myocardial Extracellular Volume Quantification by Cardiovascular Magnetic Resonance and Computed Tomography. *Curr. Cardiol. Rep.* **20**, 14–24 (2018).

159. Pattanayak, P. & Bleumke, D. A. Tissue characterization of the myocardium: state of the art characterization by magnetic resonance and computed tomography imaging. *Radiol. Clin. North Am.* **53**, 413–23 (2015).

160. Harrigan, C. J. *et al.* Hypertrophic Cardiomyopathy : Quantifi cation of Late Gadolinium Enhancement with Contrast-enhanced Cardiovascular MR Imaging 1 Methods : Results : *Radiology* **258**, 128–133 (2011).

161. Mavrogeni, S. *et al.* Cardiac magnetic resonance imaging in myocardial inflammation in autoimmune rheumatic diseases: An appraisal of the diagnostic strengths and limitations of the Lake Louise criteria. *Int. J. Cardiol.* **252**, 216–219 (2018).

162. Mavrogeni, S. I. *et al.* Cardiac Tissue Characterization and Imaging in Autoimmune Rheumatic Diseases. *JACC. Cardiovasc. Imaging* **10**, 1387–1396 (2017).

163. Cereda, A. F., Pedrotti, P., De Capitani, L., Giannattasio, C. & Roghi, A. Comprehensive evaluation of cardiac involvement in eosinophilic granulomatosis with polyangiitis (EGPA) with cardiac magnetic resonance. *Eur. J. Intern. Med.* **39**, 51–56 (2017).

164. Bami, K., Haddad, T., Dick, A., Dennie, C. & Dwivedi, G. Noninvasive imaging in acute myocarditis. *Curr Opin Cardiol* **31**, 217–223 (2016).

165. Ripley, D. P., Musa, T. A., Dobson, L. E., Plein, S. & Greenwood, J. P. Cardiovascular magnetic resonance imaging: what the general cardiologist should know. *Heart* **102**, 1589–1603 (2016).

166. Tozatto, M. *et al.* Mini Review Rheumatic heart disease in the modern era : recent developments and current challenges. *J. Brazilian Soc. Trop. Med.* **52**, 1–9 (2019).

167. Suthahar, N., Meijers, W. C., Silljé, H. H. W. & de Boer, R. A. From Inflammation to Fibrosis—Molecular and Cellular Mechanisms of Myocardial Tissue Remodelling and Perspectives on Differential Treatment Opportunities. *Curr. Heart Fail. Rep.* **14**, 235–250 (2017).

168. Guilherme, L. & Kalil, J. Rheumatic Heart Disease: Molecules Involved in Valve Tissue Inflammation Leading to the Autoimmune Process and Anti-S. pyogenes Vaccine. *Front. Immunol.* **4**, 352 (2013).

169. Mrsic, Z., Mousavi, N., Hulten, E. & Bittencourt, M. S. The Prognostic Value of Late Gadolinium Enhancement in Nonischemic Heart Disease. *Magn Reson Imaging Clin N Am* **27**, 545–561 (2019).

170. Fent, G. J., Greenwood, J. P., Plein, S. & Buch, M. H. The role of non-invasive cardiovascular imaging in the assessment of cardiovascular risk in rheumatoid arthritis: where we are and where we need to be. *Ann. Rheum. Dis.* **76**, 1169–1175 (2017).

171. Sree, K. *et al.* Long term prognostic importance of late gadolinium enhancement in fi rst-presentation non-ischaemic dilated cardiomyopathy. *Int. J. Cardiol.* **280**, 124–129 (2019).

172. Meel, R. *et al.* Cardiovascular Topics Assessment of myocardial fibrosis by late gadolinium enhancement imaging and biomarkers of collagen metabolism in chronic rheumatic mitral regurgitation. *Cardiovasc. J. Afr.* **29**, 1–5 (2018).

173. Shriki, J., Talkin, B., Thomas, I. C., Farvid, A. & Colletti, P. M. Delayed gadolinium

enhancement in the atrial wall: a novel finding in 3 patients with rheumatic heart disease. *Tex. Heart Inst. J.* **38**, 56–60 (2011).

174. Harris;, C. B. C. C. C. Rheumatic heart disease. *Ann. Cardiothorac. Surg.* **4**, 492 (2015).

175. Shen, X. *et al.* Cardiovascular magnetic resonance – derived myocardial strain in asymptomatic heart transplanted patients and its correlation with late gadolinium enhancement. *Eur Radiol* **2020**, 4337–4346 (2020).

176. Johnson, C., Johnson, C., Kuyt, K., Oxborough, D. & Stout, M. Practical tips and tricks in measuring strain , strain rate and twist for the left and right ventricles. *Br. Soc. Echocardiogr.* **6**, 87–98 (2019).

177. Scatteia, A. & Bucciarelli-Ducci, A. B. & C. Strain imaging using cardiac magnetic resonance. *Hear. Fail Rev* **2017**, 465–476 (2017).

178. Swoboda, P. P. *et al.* Relationship between cardiac deformation parameters measured by cardiovascular magnetic resonance and aerobic fitness in endurance athletes. *J. Cardiovasc. Magn. Reson.* 1–8 (2016). doi:10.1186/s12968-016-0266-x

179. Buss, S. J. *et al.* Assessment of myocardial deformation with cardiac magnetic resonance strain imaging improves risk stratification in patients with dilated cardiomyopathy. *Eur. Hear. J. – Cardiovasc. Imaging* **2015**, 307–315 (2015).

180. Wu, L. *et al.* Feature tracking compared with tissue tagging measurements of segmental strain by cardiovascular magnetic resonance. *J. Cardiovasc. Magn. Reson.* **16**, 1–11 (2014).

181. Pedrizzetti, G., Claus, P., Kilner, P. J. & Nagel, E. Principles of cardiovascular magnetic resonance feature tracking and echocardiographic speckle tracking for informed clinical use. *J. Cardiovasc. Magn. Reson.* 1–12 (2016). doi:10.1186/s12968-016-0269-7

182. Muser, D. *et al.* Clinical applications of feature-tracking cardiac magnetic resonance imaging. *World J Cardiol* **10**, 210–221 (2018).

183. Cao, J. J. *et al.* A comparison of both DENSE and feature tracking techniques with tagging for the cardiovascular magnetic resonance assessment of myocardial strain. *J. Cardiovasc. Magn. Reson.* **20**, 1–9 (2018).

184. Lim, C., Blaszczyk, E., Riazy, L., Wiesemann, S. & Schüler, J. Quantification of myocardial strain assessed by cardiovascular magnetic resonance feature tracking in healthy subjects — influence of segmentation and analysis software. *Eur. Radiol.* **31**, 3962–3972 (2020).

185. Moody, W. E. *et al.* Comparison of Magnetic Resonance Feature Tracking for Systolic and Diastolic Strain and Strain Rate Calculation With Spatial Modulation of Magnetization Imaging Analysis. *J. Magn. Reson. Imaging* **1012**, 1000–1012 (2015).

186. Rommel, K.-P., Lücke, C. & Lurz, P. Diagnostic and Prognostic Value of CMR T 1 - Mapping in Patients With Heart Failure and Preserved Ejection Fraction. *Rev. Española Cardiol. (English Ed.* **70**, 848–855 (2017).

187. Lurz, J. A. *et al.* CMR – Derived Extracellular Volume Fraction as a Marker for Myocardial Fibrosis. *JACC Cardiovasc. Imaging* **11**, 38–45 (2018).

188. Puntmann, V. O. *et al.* Native myocardial T1 mapping by cardiovascular magnetic resonance imaging in subclinical cardiomyopathy in patients with systemic lupus erythematosus. *Circ Cardiovasc Imaging.* **2013**, 295–301 (2013).

189. Barison, A. *et al.* Earlymyocardial and skeletal muscle interstitial remodelling in systemic sclerosis: Insights from extracellular volume quantification using cardiovascular magnetic resonance. *Eur. Hear. J. – Cardiovasc. Imaging* **2015**, 74–80 (2015).

190. Banerjee, T. *et al.* Clinical Significance of Markers of Collagen Metabolism in

Rheumatic Mitral Valve Disease. *PLoS One* **9**, 1–12 (2014).

191. Shah, A. M. *et al.* Prognostic Importance of Impaired Systolic Function in Heart Failure With Preserved Ejection Fraction and the Impact of Spironolactone. *Circulation* **132**, 402–414 (2015).

192. Park, J. J., Park, J.-B., Park, J.-H. & Cho, G.-Y. Global Longitudinal Strain to Predict Mortality in Patients With Acute Heart Failure. *J. Am. Coll. Cardiol.* **71**, 1947–1957 (2018).

193. Cheng, S. *et al.* Distinct Aspects of Left Ventricular Mechanical Function Are Differentially Associated With Cardiovascular Outcomes and All-Cause Mortality in the Community. *J. Am. Heart Assoc.* **4**, e002071 (2015).

194. Choi, E.-Y. *et al.* Prognostic value of myocardial circumferential strain for incident heart failure and cardiovascular events in asymptomatic individuals: the Multi-Ethnic Study of Atherosclerosis. *Eur. Heart J.* **34**, 2354–2361 (2013).

195. Nair, G., Lakshman, S. G. S., Vellani, H., Govindan, C. & Thomas, B. Strain patterns in primary mitral regurgitation due to rheumatic heart disease and mitral valve prolapse. *Indian Heart J.* **73**, 85–90 (2021).

196. Podlesnikar, T., Delgado, V. & Bax, J. J. Cardiovascular magnetic resonance imaging to assess myocardial fibrosis in valvular heart disease. *Int. J. Cardiovasc. Imaging* **34**, 97–112 (2018).

197. Rami Kafa, Kenya Kusunose, Andrew L. Goodman, Lars G. Svensson, Joseph F. Sabik, Brian P. Griffin, M. Y. D. Association of Abnormal Postoperative Left Ventricular Global Longitudinal Strain With Outcomes in Severe Aortic Stenosis Following Aortic Valve Replacement Owing to improved survival , aortic valve replacement is a class. *Am. Med. Assoc.* **1**, 2015–2017 (2022).

198. Cardiovasc, J. *et al.* The association of reduced left ventricular strains with increased

extracellular volume and their collective impact on clinical outcomes. *J. Cardiovasc. Magn. Reson.* 1–10 (2021). doi:10.1186/s12968-021-00776-7

199. Unger, P., Clavel, M.-A., Lindman, B. R., Mathieu, P. & Pibarot, P. Pathophysiology and management of multivalvular disease. *Nat. Rev. Cardiol.* **13**, 429–440 (2016).

200. Maganti, K., Rigolin, V. H., Sarano, M. E. & Bonow, R. O. Valvular heart disease: diagnosis and management. *Mayo Clin. Proc.* **85**, 483–500 (2010).

201. Baessler, B. & Emrich, T. The role of cardiovascular magnetic resonance imaging in rheumatic heart disease. *Clin. Exp. Rheumatol.* **36 Suppl 1**, 171–176 (2018).

202. Cannaò, P. M. *et al.* Novel cardiac magnetic resonance biomarkers: Native T1 and extracellular volume myocardial mapping. *Eur. Hear. Journal, Suppl.* **18**, E64–E71 (2016).

203. Pradella, S. *et al.* Cardiac magnetic resonance in patients with mitral valve prolapse : Focus on late gadolinium enhancement and T1 mapping. *Eur. Radiol.* **2019**, 1546–1554 (2019).

204. Lee, H. *et al.* Noncontrast Myocardial T1 Mapping by Cardiac Magnetic Resonance Predicts Outcome in Patients With Aortic Stenosis. **11**, (2018).

205. Karamitsos, T. D. *et al.* Noncontrast T1 mapping for the diagnosis of cardiac amyloidosis. *JACC Cardiovasc. Imaging* **6**, 488–497 (2013).

206. Baggiano, A. *et al.* Noncontrast Magnetic Resonance for the Diagnosis of Cardiac Amyloidosis. *JACC. Cardiovasc. Imaging* **13**, 69–80 (2020).

207. Antunes, M. J. The Global Burden of Rheumatic Heart Disease : Population-Related Differences (It is Not All the Same !). *Brazilian J. Cardiovasc. Surg.* **35**, 958–963 (2020).

208. Mocumbi, A. O., Madeira, G. C., Manafe, N., Beaton, A. & Children, C. Rheumatic heart disease and endomyocardial fi brosis : Distinguishing the etiology of mitral

regurgitation in low-resourced areas. *SAHeart* **14**, 36–41 (2017).

209. Carapetis, J. R., McDonald, M. & Wilson, N. J. Acute rheumatic fever. *Lancet* **366**, 155–168 (2005).

210. Tracey R Hoke, M. D. S. The worldwide epidemiology of acute rheumatic fever and rheumatic heart disease. *Clin. Epidemiol.* **1**, 67–84 (2011).

211. Roberts, K., Colquhoun, S., Steer, A., Reményi, B. & Carapetis, J. Screening for rheumatic heart disease: current approaches and controversies. *Nat. Rev. Cardiol.* **10**, 49 (2012).

212. Peters, F., Karthikeyan, G., Abrams, J., Muhwava, L. & Zühlke, L. Rheumatic heart disease : current status of diagnosis and therapy. *Cardiovasc. Diagn. Ther.* **10**, 305–315 (2020).

213. Doherty, J. U., Kort, S., Mehran, R., Schoenhagen, P. & Soman, P. ACC/AATS/AHA/ASE/ASNC/HRS/SCAI/SCCT/SCMR/STS 2017 appropriate use criteria for multimodality imaging in valvular heart disease: a report of the American college of cardiology appropriate use criteria task force, American association for thoracic surgery, . *J. Am. Coll. Cardiol.* **70**, 1647–1672 (2017).

214. Aremu, O. O. *et al.* Cardiovascular imaging modalities in the diagnosis and management of rheumatic heart disease. *Int. J. Cardiol.* **325**, 176–185 (2020).

215. Gomes, N. F. A. *et al.* Original Article Histopathological Characterization of Mitral Valvular Lesions from Patients with Rheumatic Heart Disease. *Arq Bras Cardiol* **116**, 404–412 (2020).

216. Shafi, M. J. & Nasrin, S. Incidence & Pattern of Valvular Heart Disease in Patients attended in Echo Lab at a tertiary care Hospital : A single Centre Study. **0**, (2020).

217. Aremu, O., Samuels, P., Jermy, S. & Ntusi, N. PHENOTYPES OF MYOCARDIAL INFLAMMATION AND FIBROSIS IN CHRONIC RHEUMATIC HEART

DISEASE ASSESSED WITH CARDIOVASCULAR MAGNETIC RESONANCE. **2**, 31

218. Bennett, C. J., Maleszewski, J. J. & Philip, A. CT and MR Imaging of the Aortic Valve : *Radiographics* **2012**, 1399–1420 (2012).

219. Passos, L. S. A., Nunes, M. C. P. & Aikawa, E. Rheumatic Heart Valve Disease Pathophysiology and Underlying Mechanisms. *Front. Cardiovasc. Med.* **7**, 1–10 (2021).

220. Vasconcelos, M. *et al.* Incidence and predictors of stroke in patients with rheumatic heart disease. *Heart* **107**, 748 LP – 754 (2021).

221. Sani, M. U., Karaye, K. M. & Borodo, M. M. Prevalence and pattern of rheumatic heart disease in the Nigerian savannah: an echocardiographic study. *Cardiovasc. J. Afr.* **18**, 295–9 (2007).

222. Laudari, S. & Subramanyam, G. A study of spectrum of rheumatic heart disease in a tertiary care hospital in Central Nepal. *IJC Hear. Vasc.* **15**, 26–30 (2021).

223. Mulugeta, T., Kumela, K. & Chelkeba, L. Clinical , Echocardiographic Characteristics and Management Practices in Patients with Rheumatic Valvular Heart Disease. *Open Access Rheumatol. Res. Rev. 202012* **2020**, 233–239 (2020).

224. Boudoulas, K. D., Borer, J. S. & Boudoulas, H. Etiology of valvular heart disease in the 21st century. *Cardiology* **126**, 139–52 (2013).

225. Yutzey, K. E. *et al.* Calcific aortic valve disease: a consensus summary from the Alliance of Investigators on Calcific Aortic Valve Disease. *Arterioscler. Thromb. Vasc. Biol.* **34**, 2387–2393 (2014).

226. Mukhopadhyay, S. *et al.* ScienceDirect Circulating level of regulatory T cells in rheumatic heart disease : An observational study. *Indian Heart J.* **68**, 342–348 (2016).

227. Butt, H. I., Shahbaz, A., Nawaz, H. & Butt, K. Comparative Clinical Characteristics of

Rheumatic Heart Disease Patients Undergoing Surgical Valve Replacement. *Cureuxs* **11**, 1–13 (2019).

228. Aurakzai, H. A. *et al.* Echocardiographic profile of rheumatic heart disease at a tertiary cardiac centre. *J. Ayub Med. Coll. Abbottabad* **21**, 122–126 (2009).

229. Lee, D. C. *et al.* Diffuse cardiac fibrosis quantification in early systemic sclerosis by magnetic resonance imaging and correlation with skin fibrosis. *J. Scleroderma Relat. Disord.* **3**, 159–169 (2018).

230. Lee, H. *et al.* Noncontrast Myocardial T1 Mapping by Cardiac Magnetic Resonance Predicts Outcome in Patients With Aortic Stenosis. *JACC. Cardiovasc. Imaging* **11**, 974–83 (2018).

231. Sparrow, P. *et al.* Myocardial T1 mapping for detection of left ventricular myocardial fibrosis in chronic aortic regurgitation: pilot study. *AJR. Am. J. Roentgenol.* **187**, W630-5 (2006).

232. de Meester de Ravenstein, C. *et al.* Histological Validation of measurement of diffuse interstitial myocardial fibrosis by myocardial extravascular volume fraction from Modified Look-Locker imaging (MOLLI) T1 mapping at 3 T. *J. Cardiovasc. Magn. Reson. Off. J. Soc. Cardiovasc. Magn. Reson.* **17**, 48 (2015).

233. Esson, G. *et al.* Myocardial Fibrosis and Cardiac Decompensation in Aortic Stenosis. *J Am Coll Cardiol Img.* **10**, 1320–1333 (2017).

234. Shibutani, S. T., Saitoh, T., Nowag, H., Münz, C. & Yoshimori, T. Autophagy and autophagy-related proteins in the immune system. *Nat. Immunol.* **16**, 1014–1024 (2015).

235. Dice, J. F. Chaperone-mediated autophagy. *Autophagy* **3**, 295–299 (2007).

236. Li, L., Tan, J., Miao, Y., Lei, P. & Zhang, Q. ROS and Autophagy: Interactions and Molecular Regulatory Mechanisms. *Cell. Mol. Neurobiol.* **35**, 615–621 (2015).

237. Vomero, M. *et al.* Reduction of autophagy and increase in apoptosis correlates with a favorable clinical outcome in patients with rheumatoid arthritis treated with anti-TNF drugs. *Arthritis Res. Ther.* **21**, 1–11 (2019).

238. Clarke, A. J. & Simon, A. K. Autophagy in the renewal , differentiation and homeostasis of immune cells. *Nat. Rev. Immunol.* **19**, (2019).

239. Yu, X., Long, Y. C. & Shen, H. Differential regulatory functions of three classes of phosphatidylinositol and phosphoinositide 3-kinases in autophagy. 1711–1728 (2015).

240. Klionsky, D. J. *et al.* Guidelines for the use and interpretation of assays for monitoring autophagy (3rd edition). *Autophagy* **12**, 1–222 (2016).

241. Saitoh, T. *et al.* Loss of the autophagy protein Atg16L1 enhances endotoxin-induced IL-1 b production. *Nature* **456**, 264–268 (2008).

242. Kaludercic, N. *et al.* Comprehensive autophagy evaluation in cardiac disease models. *Cardiovasc. Res.* **116**, 483–504 (2020).

243. Fujita, N. & Takashi Itoh, Hiroko Omori, Mitsunori Fukuda, Takeshi Noda, and T. Y. The Atg16L Complex Specifies the Site of LC3 Lipidation for Membrane The Atg16L Complex Specifies the Site of LC3 Lipidation for Membrane Biogenesis in Autophagy. *Mol. Biol. Cell* **19**, 2092–100 (2008).

244. Gong, L., Devenish, R. J. & Prescott, M. Autophagy as a Macrophage Response to Bacterial Infection. *Life* **64**, 740–747 (2012).

245. Liu, W. J. *et al.* P62 Links the Autophagy Pathway and the Ubiqutin-Proteasome System Upon Ubiquitinated Protein Degradation. *Cell. Mol. Biol. Lett.* **21**, 1–14 (2016).

246. Yang, Z., Goronzy, J. J. & Weyand, C. M. Autophagy in autoimmune disease. *J. Mol. Med.* **93**, 707–717 (2015).

247. Trocoli, A. & Djavaheri-Mergny, M. The complex interplay between autophagy and

NF-κB signaling pathways in cancer cells. *Am. J. Cancer Res.* **1**, 629 (2011).

248. Xiao, F. *et al.* Sex-dependent aortic valve pathology in patients with rheumatic heart disease. *PLoS One* **12**, 1–18 (2017).

249. Paul, S., Kashyap, A. K., Jia, W., He, Y.-W. & Schaefer, B. C. Selective autophagy of the adaptor protein Bcl10 modulates T cell receptor activation of NF-κB. *Immunity* **36**, 947–958 (2012).

250. Zhong, Z., Sanchez-Lopez, E. & Karin, M. Autophagy, NLRP3 inflammasome and auto-inflammatory/immune diseases. *Clin Exp Rheumatol* **34**, 12–16 (2016).

251. Wu, Z. *et al.* Expression of autophagy related genes mTOR , Becline-1 , LC3 and p62 in the peripheral blood mononuclear cells of systemic lupus erythematosus. *Am J Clin Exp Immunol* **6**, 1–8 (2017).

252. Lee, H. *et al.* Autophagy Negatively Regulates Keratinocyte Inflammatory Responses via Scaffolding Protein p62/SQSTM1. *J. Immunol.* **186**, 1248–1258 (2011).

253. Zhu, L. *et al.* The Autophagy Level Is Increased in the Synovial Tissues of Patients with Active Rheumatoid Arthritis and Is Correlated with Disease Severity. *Mediators Inflamm.* **2017**, 9 pages (2017).

254. Kato, M., Ospelt, C., Gay, R. E., Gay, S. & Klein, K. Dual Role of Autophagy in Stress-Induced Cell Death in Rheumatoid Arthritis Synovial Fibroblasts. *ARTHRITIS Rheumatol.* **66**, 40–48 (2014).

255. Luo, S. *et al.* Cargo Recognition and Function of Selective Autophagy Receptors in Plants. *Int. J. Mol. Sci.* **22**, 1–17 (2021).

256. Klionsky, D. J. *et al.* Autophagy in major human diseases. *EMBO J.* **40**, 1–64 (2021).

257. Deretic, V., Saitoh, T. & Akira, S. Autophagy in infection , inflammation and immunity. *Nat. Rev. Immunol.* **13**, 722–737 (2013).

258. Martins, D. *et al.* Autophagy and Inflammasome Interplay. *DNA Cell Biol.* **34**, 274–

281 (2015).

259. Chiu, B., Jantuan, E., Shen, F., Chiu, B. & Sergi, C. Autophagy-Inflammasome Interplay in Heart Failure : A Systematic Review on Basics , Pathways , and Therapeutic Perspectives. **47**, (2017).

260. Li, B., Yue, Y., Dong, C., Shi, Y. & Xiong, S. Blockade of macrophage autophagy ameliorates activated lymphocytes-derived DNA induced murine lupus possibly via inhibition of proinflammatory cytokine production. *Clin. Exp. Rheumatol.* **32**, 705–714 (2014).

261. Sorice, M. *et al.* Original article Autophagy generates citrullinated peptides in human synoviocytes : a possible trigger for anti-citrullinated peptide antibodies. *Rheumatology* **55**, 1374–1385 (2016).

262. Vomero, M. *et al.* Autophagy and Rheumatoid Arthritis : Current Knowledges and Future Perspectives. *Front. Immunol.* **9**, 1–10 (2018).

263. Roth, G. A. Global, Regional, and National Burden of Calcific Aortic Valve and Degenerative Mitral Valve Diseases, 1990–2017. *Circulation* **2020**, 1670–1680 (2020).

264. Mistiaen, W. P. *et al.* Autophagy as Mechanism for Cell Death in Degenerative Aortic Valve Disease ND ES SC. **8627**, 3–6 (2006).

265. Li, J., Zhang, D. & Brundel, B. J. J. M. Imbalance of ER and Mitochondria Interactions : Prelude to Cardiac Ageing and Disease ? *Cells* **1617**, 1–15 (2019).

266. Kardideh B, Sadeghalvad M, Samimi Z, Mohammadi-Motlagh HR, T. M. Evaluation of Beclin-1 and Atg5 genes expression levels in peripheral blood cells of patients with rheumatoid arthritis TT - بررسی میزان بیان ژن های Beclin-1 و Atg5 در سلول های خون محیطی بیماران مبتلا به آرتریت روماتوئید. *FEYZ* **23**, 135–142 (2019).

267. Xu, K., Xu, P. & Zhang, J. Y. Y. Reduced apoptosis correlates with enhanced

autophagy in synovial tissues of rheumatoid arthritis. *Inflamm. Res.* **2013**, 229–237 (2013).

268. Wei, H. & Lu, S. Reduced apoptosis correlates with enhanced autophagy in synovial tissues of rheumatoid arthritis Reduced apoptosis correlates with enhanced autophagy in synovial tissues of rheumatoid arthritis. (2012). doi:10.1007/s00011-012-0572-1

269. Luo, X. *et al.* Decreased expression of BECN1 mRNA is associated with lupus nephritis . *Biomed. Res.* **28**, 2952–2956 (2017).

270. Kamel, A. M., Badary, M. S., Mohamed, W. A., Ahmed, G. H. & El-feky, M. A. Evaluation of autophagy-related genes in Egyptian systemic lupus erythematosus patients. *Int. J. Rheum. Dis.* **5**, 1226–1232 (2020).

271. Hill, C. & Wang, Y. ScienceDirect Autophagy in pulmonary fibrosis : friend or foe ? *Genes Dis.* (2021). doi:10.1016/j.gendis.2021.09.008

272. Islam, M. A., Sooro, M. A. & Zhang, P. Autophagic regulation of p62 is critical for cancer therapy. *Int. J. Mol. Sci.* **19**, (2018).

273. He, Y., Hara, H. & Arbor, A. Mechanism and regulation of NLRP3 inflammasome activation. *Trends Biochem Sci.* **41**, 1012–1021 (2017).

274. Burton, T. R. & Gibson, S. B. The role of Bcl-2 family member BNIP3 in cell death and disease : NIPping at the heels of cell death. *Cell Death Differ.* **16**, 515–523 (2011).

275. Ko, J., He, F. & Diego, S. Amphipathic Tail-anchoring Peptide and Bcl-2 Homology Domain-3 (BH3) Peptides from Bcl-2 Family Proteins Induce Apoptosis through Different Mechanisms. *J. Biol. Chem.* **286**, 9038–9048 (2010).

276. Cheng, Z. *et al.* The Critical Roles and Mechanisms of Immune Cell Death in Sepsis. *Front. Immunol.* **11**, 1–10 (2020).

277. Levine, B. & Mizushima, N. Autophagy in immunity and inflammation. *Nature* **469**, 323–335 (2011).

278. Linton, P. J., Gurney, M., Sengstock, D., Mentzer, R. M. & Gottlieb, R. A. This old heart: Cardiac aging and autophagy. *J. Mol. Cell. Cardiol.* **83**, 44–54 (2015).

279. Bah, A. & Vergne, I. Macrophage Autophagy and Bacterial Infections. *Front. Immunol.* **8**, 1–9 (2017).

280. Choi, Y. J. & Yoo, W. Pathogenic Role of Autophagy in Rheumatic Diseases. *J Rheum Dis* **23**, 202-211 (2016).

APPENDIX

1. Human Research Council (HREC) approval and renewal documents for the RHD study.
2. Participant's information list (PIL) and informed consent for participation in RHD study.
3. Pressure cooking technique for antigen retrieval.

UNIVERSITY OF CAPE TOWN
Faculty of Health Sciences
Human Research Ethics Committee

Room E53-46 Old Main Building
Groote Schuur Hospital
Observatory 7925
Telephone [021] 406 6626
Email: shuretta.thomas@uct.ac.za
Website: www.health.uct.ac.za/fhs/research/humanethics/forms

01 August 2017

HREC REF: 554/2017

Prof Ntobeko Ntusi
Medicine
J-Floor, OMB

Dear Prof Ntusi

PROJECT TITLE: CHARACTERISATION OF PHENOTYPES OF INFLAMMATION, FIBROSIS AND REMODELING IN CHRONIC RHEUMATIC HEART DISEASE USING MULTIPARAMETRIC CARDIOVASCULAR MAGNETIC RESONANCE-(PhD-candidate-A Olukayode)

Thank you for submitting your study to the Faculty of Health Sciences Human Research Ethics Committee.

It is a pleasure to inform you that the HREC has **formally approved** the above-mentioned study.

- Please add the word Human in the Informed consent form where the HREC is named.

Approval is granted for one year until the 30 August 2018.

Please submit a progress form, using the standardised Annual Report Form if the study continues beyond the approval period. Please submit a Standard Closure form if the study is completed within the approval period.
(Forms can be found on our website: www.health.uct.ac.za/fhs/research/humanethics/forms)

Please quote the HREC REF in all your correspondence.

Please note that the ongoing ethical conduct of the study remains the responsibility of the principal investigator.

Please note that for all studies approved by the HREC, the principal investigator **must** obtain appropriate institutional approval before the research may occur.

The HREC acknowledge that the student, Aramu Olukayode will also be involved in this study.

Yours sincerely

Signed by candidate

PROFESSOR M BLOCKMAN
CHAIRPERSON, FHS HUMAN RESEARCH ETHICS COMMITTEE
Federal Wide Assurance Number: FWA00001637.

Institutional Review Board (IRB) number: IRB00001938
This serves to confirm that the University of Cape Town Human Research Ethics Committee complies to the Ethics Standards for Clinical Research with a new drug in patients, based on the Medical Research Council (MRC-SA), Food and Drug Administration (FDA-USA), International Convention on Harmonisation Good Clinical Practice (ICH GCP), South African Good Clinical Practice Guidelines (DoH 2006), based on the Association of the British Pharmaceutical Industry Guidelines (ABPI),and Declaration of Helsinki (2013) guidelines.
The Human Research Ethics Committee granting this approval is in compliance with the ICH Harmonised Tripartite Guidelines E6: Note for Guidance on Good Clinical Practice (CPMP/ICH/135/95) and FDA Code Federal Regulation Part 50, 56 and 312.

HREC 554/2017

UNIVERSITY OF CAPE TOWN

FACULTY OF HEALTH SCIENCES
Human Research Ethics Committee

FHS016: Annual Progress Report / Renewal

HREC office use only (FWA00001637, IRB00001938) This serves as notification of annual approval, including any documentation described below.			
☑ Approved	Annual progress report	Approved until/next renewal date	30.08.2020
☐ Not approved	See attached comments		
Signature Chairperson of the HREC	Signed by candidate	Date Signed	4/9/2019

Comments to PI from the HREC

Principal Investigator to complete the following:

1. Protocol information

Date (when submitting this form)	27/08/2019		
HREC REF Number	554/2017	Current Ethics Approval was granted until	Aug 30, 2019
Protocol title	Characterization of phenotypes of inflammation, fibrosis and ventricular remodeling in chronic rheumatic heart disease using multiparametric cardiovascular magnetic resonance.		
Protocol number (if applicable)			
Are there any sub-studies linked to this study?	☐ Yes No x		
If yes, could you please provide the HREC Ref's for all sub-studies? **Note:** A separate FHS016 must be submitted for each sub study.			
Principal Investigator	Prof. N. Ntusi		

UNIVERSITY OF CAPE TOWN
IYUNIVESITHI YASEKAPA • UNIVERSITEIT VAN KAAPSTAD

FACULTY OF HEALTH SCIENCES
Human Research Ethics Committee

Form FHS006: Protocol Amendment

HREC office use only (FWA00001637; IRB00001938)		
☑ Approved	☑ Type of review: Expedited	☐ Full committee
This serves as notification that all changes and documentation described below are approved.		
Signature Chairperson of the HREC	Signed by candidate	Date 7/10/2019

Note: All major amendments must include a local **PI Synopsis** justifying the changes for the amendment.
Please note that incomplete amendment submissions will not be reviewed.

Comments from the HREC to the Principal Investigator:
Subject to approval from the Head of anatomical pathology, noting that there will be in future an approved registry for these diagnostic samples
Note: The approval of this protocol amendment does not grant annual approval. Please complete the FHS016 / FHS017 form for annual approval at least one month before study expiration.

Principal Investigator to complete the following:

1. Protocol information

Date (when submitting this form)	04/10/2019
HREC REF Number	554/2017
Protocol title	Characterization of phenotypes of inflammation, fibrosis and ventricular remodeling in chronic rheumatic heart disease using multiparametric cardiovascular magnetic resonance and autophagy markers.
Protocol number (if applicable)	
Principal Investigator	Prof. N. Ntusi
Department / Office Internal Mail Address	Department of Medicine, Faculty of Health Sciences, University of Cape Town Room J 46.53 | Old Main Building | Groote Schuur Hospital Main Road | Observatory | 7925 | South Africa.

1.1 Is this a major or a minor amendment? (see FHS006hlp) Major (tick box) Minor (tick box)	☐ Major	x	Minor
1.2 Does this protocol receive US Federal funding?	☐ Yes	x	No

UNIVERSITY OF CAPE TOWN

FACULTY OF HEALTH SCIENCES
Human Research Ethics Committee

Form FHS006: Protocol Amendment

HREC office use only (FWA00001637; IRB00001938)		
☐ Approved	☐ Type of review: Expedited	☐ Full committee
This serves as notification that all changes and documentation described below are approved.		
Signature Chairperson of the HREC	Signed by candidate	Date 4/9/2019

Note: All major amendments must include a local **PI Synopsis** justifying the changes for the amendment. Please note that incomplete amendment submissions will not be reviewed.

Comments from the HREC to the Principal Investigator:
Thank you for the updated informed consent document
Note: The approval of this protocol amendment does not grant annual approval. Please complete the FHS016 / FHS017 form for annual approval at least one month before study expiration.

Principal Investigator to complete the following:

1. Protocol information

Date (when submitting this form)	30/08/2019
HREC REF Number	554/2017
Protocol title	Characterization of phenotypes of inflammation, fibrosis and ventricular remodeling in chronic rheumatic heart disease using multiparametric cardiovascular magnetic resonance and autophagy markers.
Protocol number (if applicable)	
Principal Investigator	Prof. N. Ntusi
Department / Office Internal Mail Address	Department of Medicine, Faculty of Health Sciences, University of Cape Town Room J 46.53 | Old Main Building | Groote Schuur Hospital Main Road | Observatory | 7925 | South Africa.

1.1 Is this a major or a minor amendment? (see FHS005hlp) Major (tick box) Minor (tick box)	☐ Major	[x] Minor
1.2 Does this protocol receive US Federal funding?	☐ Yes	[x] No
1.3 If the amendment is a major amendment and receives US Federal Funding, does the amendment require full committee approval? Note: Any protocol amendments for **Full Committee** review MUST be submitted on the monthly HREC submission dates. (Please email an electronic copy to hrec-enquiries@uct.ac.za)	☐ Yes	[x] No

Department / Office Internal Mail Address	Department of Medicine, Faculty of Health Sciences, University of Cape Town Room J 46.53 | Old Main Building | Groote Schuur Hospital Main Road | Observatory | 7925 | South Africa.

1.1 Does this protocol receive US Federal funding?	☐ Yes	[x] No
1.2 If the study receives US Federal Funding, does the annual report require full committee approval? **Note:** Any annual approvals for **Full Committee** review MUST be submitted on the monthly HREC submission dates. (Please send electronic copy for full committee review to hrec-enquiries@uct.ac.za)	☐ Yes	No [x]
If yes in 1.2 please complete section 1.3 below for invoicing purposes		
1.3 Annual Approval for **full committee** review	- R 3420 (inclusive of vat)	
For invoicing purposes, please provide:		
Sponsor's name		
Contact person		
Address		
Telephone number		
Email Address		

2. List of documentation for approval

1. Detailed protocol
2. Annual Progress Report/Renewal document (FHS 016)
3. Protocol Amendment (FHS 006)

3. Protocol status (tick ✓)

☐	Open to enrolment
☐	Closed to enrolment (tick ✓)
[x]	Research-related activities are ongoing
☐	Research-related activities are complete, long-term follow-up only
☐	Research-related activities are complete, data analysis only
☐	Main study is complete but sub-study research-related activities are ongoing
☐	Study is closed → Please submit a Study Closure Form (FHS010)

(Note: Please complete the Closure form (FHS010) if the study is completed within the approval period)

4. Enrolment

Number of participants enrolled to date	114
Number of participants enrolled, since last HREC Progress report (continuing review)	15
Additional number of participants still required	86

5. Refusals

Total number of refusals (participants invited to join the study, but refused to take part)	7

6. Cumulative summary of participants

Total number of participants who provided consent	114
Number of participants determined to be ineligible (i.e. after screening)	20
Number of participants currently active on the study	82
Number of participants completed study (without events leading to withdrawal)	82
Number of participants withdrawn at participants' request (i.e. changed their mind)	7
Number of participants withdrawn by PI due to toxicity or adverse events	0
Number of participants withdrawn by PI for other reasons (e.g. pregnancy, poor compliance)	1
Number of participants lost to follow-up. Please comment below on reasons for loss of follow-up.	1
DIED post-surgery	
Number of participants no longer taking part for reasons not listed above. Please provide reasons below:	
1	

7. Progress of study

Please provide a brief summary of the research to date including the overall progress and the progress since the last annual report as well as any relevant comments/issues you would like to report to the HREC:
The research project was progressing well. The below listed progresses have been documented: 1. Three-quarter of the enrolled patients' data have been completely post-processed. 2. Completed data curation on spreadsheet. 3. Completed preliminary data analysis using SPSS analysis tool. 4. Presented preliminary results at the weekly departmental journal club and seminar forum. 5.

8. Protocol violations and exceptions (tick ✓ all that apply)

x	No prior violations or exceptions have occurred since the original approval

(Note: Please complete the Closure form (FHS010) if the study is completed within the approval period)

☐	Prior violations or exceptions have been reported since the last review and have already been acknowledged or approved
☐	Unreported minor violations that have occurred since the last review, as well as significant deviations not yet reported, are attached for review

9. Amendments (tick ✓ all that apply)

☐	No prior amendments have been made since the original approval
☐	Prior amendments have been reported since the last review and have already been approved
x	New protocol changes/ amendments are requested as part of this continuing review (See note below)

Note: If new protocol changes are being requested in this review, please complete an amendment form (FHS006).
Specific changes in the amended protocol and consent/assent forms must be **bolded**, *italicised* or tracked and all changes must include a rationale.

10. Adverse events

10.1 Please provide below or attach a narrative summary of serious adverse events and/ or unanticipated problems since the last progress report. Please indicate changes made to the protocol and informed consent document(s) as a result (if not already reported to the HREC). Please comment on whether causality to any study procedure or intervention could be established.
No reported adverse event and/or unanticipated problems documented. Also, no casualty to the study procedure or intervention was established.

10.2 Have participants received appropriate treatment/ follow-up/ referral when indicated (e.g. in the case of abnormal or incidental clinical findings, distress or anxiety)?		
☐ Yes	☐ No	x Not applicable
If yes, please describe:		

11. Summary of Monitoring and Audit Activities (tick ✓)

11.1 Was this study monitored or audited by an external agency (e.g. SAHPRA, FDA)?		
☐ Yes	☐ No	x Not applicable

11.2 Did a Data and Safety Monitoring Board publish a report?		
☐ Yes	☐ No	x Not applicable

11.3 If yes, please identify the agency and attach a summary of the findings.					
Agency Name		Report attached	☐ Yes	☐ No	x Not applicable
		DSMB report attached	☐ Yes	☐ No	x Not applicable

11.4 Has there been any agency, institutional or other inquiry into non-compliance in this study, or any finding of non-compliance concerning a member of the research team?	
☐ Yes	[x] No
If yes, please explain:	

12. Level of risk (tick ✓)

12.1 In light of your experience of this research, please indicate whether the level of risk to participants has:	
☐	Increased
☐	Decreased
[x]	Shown no change
If there has been a change, please explain:	

12.2 Please provide a narrative summary of recent relevant literature that may have a bearing on the level of risk.

13. Statement of conflict of interest

Has there been any change in the conflict of interest status of this protocol since the original approval? (tick ✓)	
☐ Yes	[x] No
If yes, please explain and if necessary attach a revised conflict of interest statement (Section #7 in the New Protocol Application Form FHS013):	

14. Signature

My signature certifies that the above is complete and correct.			
Signature of PI	Signed by candidate	Date	02 September 2019

(Note: Please complete the Closure form (FHS010) if the study is completed within the approval period)

UNIVERSITY OF CAPE TOWN

FACULTY OF HEALTH SCIENCES
Human Research Ethics Committee

Form FHS006: Protocol Amendment

HREC office use only (FWA00001637; IRB00001938)		
☑ Approved	☐ Type of review: Expedited	☐ Full committee
This serves as notification that all changes and documentation described below are approved.		
Signature Chairperson of the HREC: Signed by candidate	Date: 4/9/2019	

Note: All major amendments must include a local **PI Synopsis** justifying the changes for the amendment. Please note that incomplete amendment submissions will not be reviewed.

Comments from the HREC to the Principal Investigator:
Thank you for the updated informed consent document
Note: The approval of this protocol amendment does not grant annual approval. Please complete the FHS016 / FHS017 form for annual approval at least one month before study expiration.

Principal Investigator to complete the following:

1. Protocol Information

Date (when submitting this form)	30/08/2019
HREC REF Number	554/2017
Protocol title	Characterization of phenotypes of inflammation, fibrosis and ventricular remodeling in chronic rheumatic heart disease using multiparametric cardiovascular magnetic resonance and autophagy markers.
Protocol number (if applicable)	
Principal Investigator	Prof. N. Ntusi
Department / Office Internal Mail Address	Department of Medicine, Faculty of Health Sciences, University of Cape Town Room J 46.53 | Old Main Building | Groote Schuur Hospital Main Road | Observatory | 7925 | South Africa.

1.1 Is this a major or a minor amendment? (see FHS005hlp) Major (tick box) Minor (tick box)	☐ Major	☒ Minor
1.2 Does this protocol receive US Federal funding?	☐ Yes	☒ No
1.3 If the amendment is a major amendment and receives US Federal Funding, does the amendment require full committee approval? Note: Any protocol amendments for **Full Committee** review MUST be submitted on the monthly HREC submission dates. (Please email an electronic copy to hrec-enquiries@uct.ac.za)	☐ Yes	☒ No

UNIVERSITY OF CAPE TOWN

FACULTY OF HEALTH SCIENCES
Human Research Ethics Committee

Form FHS006: Protocol Amendment

HREC office use only (FWA00001637; IRB00001938)		
☑ Approved	☑ Type of review: Expedited	☐ Full committee
This serves as notification that all changes and documentation described below are approved.		
Signature Chairperson of the HREC	Signed by candidate	Date 4/10/2019

Note: All major amendments must include a local **PI Synopsis** justifying the changes for the amendment. Please note that incomplete amendment submissions will not be reviewed.

Comments from the HREC to the Principal Investigator:
Subject to approval from the Head of anatomical Pathology and noting that Mark will obtain further approval regarding for these diseased samples
Note: The approval of this protocol amendment does not grant annual approval. Please complete the FHS016 / FHS017 form for annual approval at least one month before study expiration.

Principal Investigator to complete the following:

1. Protocol information

Date (when submitting this form)	04/10/2019
HREC REF Number	554/2017
Protocol title	Characterization of phenotypes of inflammation, fibrosis and ventricular remodeling in chronic rheumatic heart disease using multiparametric cardiovascular magnetic resonance and autophagy markers.
Protocol number (if applicable)	
Principal Investigator	Prof. N. Ntusi
Department / Office Internal Mail Address	Department of Medicine, Faculty of Health Sciences, University of Cape Town Room J 46.53 | Old Main Building | Groote Schuur Hospital Main Road | Observatory | 7925 | South Africa.

1.1 Is this a major or a minor amendment? (see FHS006hlp) Major (tick box) Minor (tick box)	☐ Major	☒ Minor
1.2 Does this protocol receive US Federal funding?	☐ Yes	☒ No

2. List of Proposed Amendments with Revised Version Numbers and Dates

Please itemise on the page below, all amendments with revised version numbers and dates, which need approval.
This page will be detached, signed and returned to the PI as notification of approval. Please add extra pages if necessary.

We want to request for diagnostic control tissues from the Anatomical pathology laboratory archive for optimization of the experiment.
According to the immunohistochemistry technique that we shall be using, the following control diagnostic tissues are important in order to be able to determine and quantify the expressed autophagy markers. Hence, we are requesting for the following control tissues:

BECN1	Human smooth/skeletal muscle
SQSTM1/p62	Human Colon carcinoma
LC3 A/B	Human Lung carcinoma/prostate tissue
Bax	Human spleen
Bcl-2	Normal human colon
Caspase 3 (E-8)	Human duodenum tissue

3. Protocol status (tick ✓)

☐	Open to enrolment
☐	No participants have been enrolled
☐	Closed to enrolment (tick ✓)
x	Research-related activities are ongoing
☐	Research-related activities are complete, long-term follow-up only
☐	Research-related activities are complete, data analysis only

4. Proposed changes will affect: (tick ✓ all the categories that apply)

	Protocol
x	Study objectives, design (including investigator's brochure, clinical activities, study length)
☐	Study instruments, questionnaires, interview schedules
☐	Sample size
☐	Recruitment methods
☐	Eligibility criteria (inclusion and exclusion criteria)
☐	Drug/device (composition, amount, schedule, route of administration, combination with other drugs/devices, safety information)
☐	Data collection/ analysis

6. Ethics Review Levy – cost including vat

Cost for Major Amendments - R3 691.20 (Protocols funded by UCT (e.g. departmental funding / student research) and by certain grant funding organizations (e.g. MRC, NRF, CANSA,) are exempt from charges)	
For invoicing purposes, please provide:	
Sponsor's name	
Contact person	
Address	
Telephone number	
Email Address	

7. Signature

My signature certifies that I will maintain the anonymity and/ or confidentiality of information collected in this research. If at any time I want to share or re-use the information for purposes other than those disclosed in the original approval, I will seek further approval from the HREC.			
Signature of PI	Signed by candidate	Date	07 Oct 2019

UNIVERSITY OF CAPE TOWN

FACULTY OF HEALTH SCIENCES
Human Research Ethics Committee

HUMAN RESEARCH ETHICS COMMITTEE
HEALTH SCIENCES FACULTY
UNIVERSITY OF CAPE TOWN

FHS016: Annual Progress Report / Renewal

HREC office use only (FWA00001637; IRB00001938) This serves as notification of annual approval, including any documentation described below.			
☑ Approved	Annual progress report	Approved until/next renewal date	30.11.22
☐ Not approved	See attached comments		
Signature Chairperson of the HREC/ Designee	Signed by candidate	Date Signed	11/11/2021

Note: Please email this form and supporting documents (if applicable) in a combined pdf-file to hrec-enquiries@uct.ac.za.
Please clarify your plan for research-related activities during COVID-19 lockdown.
Please use the latest form found on our website:
http://www.health.uct.ac.za/fhs/research/humanethics/forms

Comments to PI from the HREC

Principal Investigator to complete the following:

1. Protocol information

Date (when submitting this form)	28 October 2021		
HREC REF Number	554/2017	Current Ethics Approval was granted until	30 August 2021
Protocol title	Characterisation of phenotypes of inflammation, fibrosis and ventricular remodeling in chronic rheumatic heart disease using multiparametric cardiovascular magnetic resonance and autophagy markers		
Protocol number (if applicable)			
Are there any sub-studies linked to this study?	☐ Yes	x No	
If yes, could you please provide the HREC Reference number for all sub-studies? **Note:** A separate FHS016 must be submitted for each sub-study.			

(Note: Please complete the Closure form (FHS010) if the study is completed within the approval period)

Principal Investigator	Prof N Ntusi
Department / Office Internal Mail Address	Department of Medicine Ntobeko.ntusi@uct.ac.za

1.1 Does this protocol receive US Federal funding?	☐ Yes	✓ No
1.2 If the study receives US Federal Funding, does the annual report require full committee approval? **Note:** Any annual approvals for **Full Committee** review MUST be submitted on the monthly HREC submission dates. (Please send electronic copy for full committee review to hrec-submission@uct.ac.za)	☐ Yes	✓**No**

If yes in 1.2 please complete section 1.3 below for invoicing purposes

1.3 Ethics Renewal Fee

Please **(tick ✓)**appropriate box for billing purposes:

Submission Type	***Description***	***New fee (Vat Incl.)***	***tick ✓***
Research funded solely from UCT departmental/ divisional/group budget	Annual evaluation of research progress report for re-certification	**R0,00**	☐
Non-sponsored student research for degree purposes at UCT/Other Universities & Colleges	Annual evaluation of research progress report for re-certification	**R0,00**	☐
Annual re-certification / Progress report (FHS016 Form)	Clinical Trial & International Grant Funded Research - Annual evaluation of research progress report for re-certification for Full Committee Approval	**R7000,00**	☐
Annual re-certification / Progress report (FHS016 Form)	Clinical Trial & International Grant Funded Research - Annual evaluation of research progress report for re-certification for Expedited review	**R3 710.00**	☐
Annual re-certification / Progress report (FHS016 Form)	National grant funded research - Annual evaluation of research progress report for re-certification for Full Committee Approval	**R6000.00**	☐
Annual re-certification / Progress report (FHS016 Form)	National Grant funded research for Annual evaluation of research progress report for re-certification for Expedited review	**R1 500,00**	☐

NB: Protocols funded by UCT (e.g. departmental funding / student research) and by certain grant funding organizations (e.g. MRC, NRF, CANSA,) are exempt from these charges.

Please provide details for Invoicing, either complete section 1 or 2 :

1. Invoice billing – Directly to Sponsor

Sponsor's name	

(Note: Please complete the Closure form (FHS010) if the study is completed within the approval period)

Billing Address of Sponsor:	
Vat Number:	
Contact person	
Telephone number	
Email Address	
2. **Internal Journal Billing:**	
Fund Number:	
Cost Centre Number:	
Account Holder Name:	
Division of Account Holder:	

2. List of documentation for approval

None

3. Protocol status (tick ✓)

☐	Open Enrolment
☐	Closed to enrolment (tick ✓)
☐	Research-related activities are ongoing
✓	Research-related activities are complete, long-term follow-up only
☐	Research-related activities are complete, data analysis only
☐	Main study is complete but sub-study research-related activities are ongoing
☐	Study is closed → Please submit a Study Closure Form (FHS010)

4. Enrolment

Number of participants enrolled to date	114
Number of participants enrolled, since last HREC Progress report (continuing review)	15
Additional number of participants still required	86

(Note: Please complete the Closure form (FHS010) if the study is completed within the approval period)

5. Refusals

Total number of refusals (participants invited to join the study, but refused to take part)	7

6. Cumulative summary of participants

Total number of participants who provided consent	114
Number of participants determined to be ineligible (i.e. after screening)	20
Number of participants currently active on the study	82
Number of participants completed study (without events leading to withdrawal)	82
Number of participants withdrawn at participants' request (i.e. changed their mind)	7
Number of participants withdrawn by PI due to toxicity or adverse events	0
Number of participants withdrawn by PI for other reasons (e.g. pregnancy, poor compliance)	1
Number of participants lost to follow-up. Please comment below on reasons for loss of follow-up.	1
Number of participants no longer taking part for reasons not listed above. Please provide reasons below:	

7. Progress of study

Please provide a brief summary of the research to date including the overall progress and the progress since the last annual report as well as any relevant comments/issues you would like to report to the HREC:

8. Protocol violations and exceptions (tick ✓ all that apply)

✓	No prior violations or exceptions have occurred since the original approval
☐	Prior violations or exceptions have been reported since the last review and have already been acknowledged or approved
☐	Unreported minor violations that have occurred since the last review, as well as significant deviations not yet reported, are attached for review

(Note: Please complete the Closure form (FHS010) if the study is completed within the approval period)

9. Amendments (tick ✓ all that apply)

☐	No Prior amendments have been made since the original approval
✓	Prior amendments have been reported since the last review and have already been approved
☐	New protocol changes/ amendments are requested as part of this continuing review (See note below)

Note: If new protocol changes are being requested in this review, please complete an amendment form (FHS006).
Specific changes in the amended protocol and consent/assent forms must be **bolded**, *italicised* or tracked and all changes must include a rationale.

10. Adverse events

10.1 Please provide below or attach a narrative summary of serious adverse events and/ or unanticipated problems since the last progress report. Please indicate changes made to the protocol and informed consent document(s) as a result (if not already reported to the HREC). Please comment on whether causality to any study procedure or intervention could be established.

10.2 Have participants received appropriate treatment/ follow-up/ referral when indicated (e.g. in the case of abnormal or incidental clinical findings, distress or anxiety)?		
☐ Yes	☐ No	✓ Not applicable
If yes, please describe:		

11. Summary of Monitoring and Audit Activities (tick ✓)

11.1 Was this study monitored or audited by an external agency (e.g. SAHPRA, FDA)?		
☐ Yes	☐ No	✓ Not applicable

11.2 Did a Data and Safety Monitoring Board publish a report?		
☐ Yes	☐ No	✓ Not applicable

11.3 If yes, please identify the agency and attach a summary of the findings.					
Agency Name		Report attached	☐ Yes	☐ No	☐ Not applicable
		DSMB report attached	☐ Yes	☐ No	☐ Not applicable

(Note: Please complete the Closure form (FHS010) if the study is completed within the approval period)

11.4 Has there been any agency, institutional or other inquiry into non-compliance in this study, or any finding of non-compliance concerning a member of the research team?	
☐ Yes	✓ No
If yes, please explain:	

12. Level of risk (tick ✓)

12.1 In light of your experience of this research, please indicate whether the level of risk to participants has:	
☐	Increased
☐	Decreased
✓	Shown no change
If there has been a change, please explain:	

12.2 Please provide a narrative summary of recent relevant literature that may have a bearing on the level of risk.

13. Insurance

Please confirm that valid no fault insurance is still in place? **(tick ✓)**			
☐ Yes		✓No	
If yes, please complete the following:			
Insurer's name:			
Policy no.		*Coverage Period:	
For UCT sponsored studies please liaise the Insurance office via fhs.sponsorship@uct.ac.za regarding the required documentation and information required obtain a renewed UCT No-fault Insurance Certificate.			

14. Statement of conflict of interest

Has there been any change in the conflict of interest status of this protocol since the original approval? (tick ✓)	
☐ Yes	✓ No

If yes, please explain and if necessary, attach a revised conflict of interest statement (Section #7 in the New Protocol Application Form FHS013):

15. Signature

My signature certifies that the above is complete and correct.			
Signature of PI	Signed by candidate	Date	28 October 2021

(Note: Please complete the Closure form (FHS010) if the study is completed within the approval period)

PARTICIPANT INFORMATION SHEET

Characterisation of phenotypes of inflammation, fibrosis and remodelling in chronic rheumatic heart disease using multiparametric cardiovascular magnetic resonance and autophagy biomarkers

You are invited to take part in a research study. Before you decide, it is important for you to understand why the research is being done and what it will involve. Please take time to read the following information carefully and discuss it with friends, relatives and your doctor, if you wish. This leaflet will tell you the purpose of the study, what will happen to you when you take part and gives you detailed information about the conduct of the study.

Ask us if there is anything that is not clear or if you would like more information. Thank you for taking time to read this.

What is the purpose of the study?

Patients with rheumatic heart disease (RHD) have inflammation of the heart valves which causes the valves to leak, narrow and/or thickened, and may result in disease of the heart muscle which may lead to dilatation of the heart chambers and scarring or fibrosis. The inflammation of the heart valves may also be seen as inflammation in the muscle of the heart, where the disease results in episodic flare of the inflammatory process. We would like to assess the frequency of heart valve disease and inflammation and scarring in the heart muscle in patients with RHD, as assessed by MRI. In the future, we will also be interested to assess the relationship of myocardial inflammation and scarring on MRI with cardiovascular outcomes.

If you take part in this study, you will be seen at a visit, where you will be examined, have a resting electrocardiogram (ECG). If you have not had a recent ultrasound scan of the heart, you will be offered one. We will then examine the structure and function of your heart with an MRI scan. You will not be asked to take any additional long-term pill or alter your regular medication in any way.

Why have I been invited?

You have been invited because you have previously been diagnosed with RHD which may later require a valve replacement. This study will help to understand your improvement after operation of the damaged valve(s).

Do I have to take part?

It is up to you to decide whether or not to take part. If you decide to take part, you are free to withdraw consent at any time without giving a reason. Your decision will not affect the standard of care you receive. If you decide that you no longer wish to continue with the study, we would still retain any data already obtained from you up to the point of your withdrawal.

What would happen to me if I take part?

You would attend a visit that will last about 2 hours. At this visit, we will ask some general questions about your health and regular medication. Next, we will do a brief examination that includes measurement of your pulse, blood pressure, weight and height. An ECG trace of your heart's electrical impulse will be done. After that, we may perform an ultrasound scan of your heart. We will then scan your heart non-invasively using cardiac MRI. If your ultrasound or MRI scan suggests abnormalities, we will advise your doctors to refer you to a cardiologist for review.

Below, all the above-mentioned tests are discussed in a little bit more detail:

a. Clinical assessment

The assessment will start by asking you a set of questions about your health and previous medical conditions, using a structured questionnaire. The physical exam will include measurement of your pulse, blood pressure, weight and height, as well as an examination of the cardiovascular system.

b. The heart MRI scan (approximately 60 minutes)

The MRI scan of your heart will be the most important part of this study. MRI scans are painless but involve the use of a strong magnetic field, so if you have any of the following, you would not be suitable for a scan, and would not be able to take part in this study:

• A permanent pacemaker	• shrapnel injuries
• metal clips in blood vessels of the brain	• other metal or electronic implants affected by magnetic field
• an injury to the eye involving fragments of metal	• Neurostimulators
• insulin pump	• cochlear implant

The MRI scanner is shaped like a polo mint, the hole inside measuring about 70 cm wide, with a table that slides in and out. You will be asked to change into a hospital gown and to lie still on your back on the table, while your heart is scanned. You will also be asked to breathe in and out and hold your breath for several seconds for some of the scans. Pictures of the heart are created using a magnetic field, radio waves and computers. When images are being taken, the MRI scanner makes a loud noise, and you will be provided with earphones to protect your ears. It is important that you lie still for the duration of the scan.

To evaluate fully the blood circulation and your heart muscle for inflammation and scarring and tissue characteristics we shall inject some contrast dye, called gadolinium, through a drip in your arm.

c. The ECG (5 minutes)

We will take an electrocardiogram (ECG) of your heart. An ECG is a tool that uses surface electrodes on certain points on your chest and arms to monitor the electrical properties of your heart.

d. The ultrasound of the heart (15-20 minutes)

An echocardiogram or ultrasound of your heart is a safe and painless procedure to study heart structure and function. You will be asked to lie on a couch on your left side, and a probe will be placed on your chest. Lubricating jelly is used so the probe makes good contact with the skin. Ultrasound waves then create images of your heart on the scanner monitor. It normally takes 15-20 minutes to acquire these images.

What about travel expenses?

We will reimburse travel expenses to and from the hospital. Lunch will be provided or reimbursed.

What will I have to do, if I agree to take part in this study?

1. Attend a visit at Groote Schuur Hospital for the assessment, blood tests and for the scans.

2. Some 20ml of blood will be taken from you by a nurse while you are in the hospital ward waiting your operation. Remains of the heart valves removed during your valve change operation will be taken. They will be used to study changes in molecules due to RHD.

3.You will have repeat visit to Groote Schuur Hospital for another scan 6 months after operation. During your repeat visit, some blood will also be collected for study, alongside with CMR scan to check any improvement in the studied molecules and heart functions respectively.

4. Consent to taking part in this study by signing a form.

5.We will ask that you do not have anything to eat the 4-6 hours before the visit.

6.Undergo the procedures as described above.

Are there any other possible risks from taking part?

The scanning is done using an MRI scanner which is also used routinely in clinical practice to acquire images of various body parts. MRI scans are safe, non-invasive and do not involve any ionising radiation (X-rays). Some people find the space limitation in the scanner uncomfortable, but you will be given a chance to see the scanner to make sure that you are comfortable in it before the study starts. The scan is noisy and we provide headphones to protect your ears. The whole time that you are in the scanner you will be given a buzzer which you will be able to use at any time if you wish to stop the study. As the scanner consists of a powerful magnet, it may attract certain metallic objects. You must not have a scan if you have had metallic objects or medical devices (e.g. pacemaker) inserted into your body during an operation. While MRI is safe in pregnancy, because this is a research study, as a precaution we advise you to tell us if there is any chance you might be pregnant. The doctor or radiographer will go through a list of possible risks with you before you go into the scanner.

In the unlikely event of us seeing any structural abnormalities on your MRI scan, a member of our research team will discuss the implications with you and, with your permission, your doctor may be notified. However, it is important to note that we do not carry out scans for diagnostic purposes, and therefore these scans are not a substitute for a clinical appointment. Rather, our scans are intended for research purposes only. Some people find having a drip in their arm uncomfortable and there can be bruising at the site of needle entry. Our staff is trained in drip insertion and we will make sure you are as comfortable as possible.

Gadolinium, the dye used for the MRI scans, has been in clinical use for over 20 years. As the dye is being injected, some people report a sensation of warmth at the injection site. It is unusual to feel pain, and in this case, we would stop the injection immediately. Rarely, some people feel slightly nauseous or have a metallic taste following the injection, but vomiting is exceedingly rare. Occasionally, people have developed a rash; however, severe allergic reactions are very rarely. Again, this dye is injected through a drip in the arm. There is no pain associated with the injection at the site. There is a small risk of an allergic reaction to the dye.

ECG and ultrasound are safe, non-invasive tests, with no known serious risks/harm. Rarely, individuals having either test may develop an allergic reaction to placement of electrodes that results in a mild rash. This rash disappears in a few days without any treatment.

It is important to note that in a large-volume MRI centre like Groote Schuur Hospital, where our experienced staff has been doing MRI scans for many years, the risk of harm from the MRI and other tests is exceedingly small.

What will happen to the samples?

We will collect and store blood, heart valves, heart muscle biopsies and health information of participants. We will prepare your blood samples and tissues right away and store them for analysis at a future date. When this project is complete, we would like to store your blood and heart tissues and information. We will store it together with other samples that people have given. The materials will be stored in University of Cape Town protected by material transfer agreements approved by University of Cape Town Human Research Ethics Committee. Samples might be stored for some time by the investigators. No samples will be sent out of University of Cape Town or South Africa before a material transfer agreement has been permitted. The samples will not be sold, but investigators may develop products based on studying your samples. If this happens, you will not be able to share in any profits.

We would like to use your leftover blood samples and tissues for future research on heart diseases. If we use your blood samples for future heart disease research, we will label them with a code instead of your name. No information obtained from this research will point back to you.

Do you agree to let us store your samples for future research on heart diseases? Below you will find the question clearly asking for your permission to store and use the specimens for future work on heart diseases.

You may still take part in this study if you don't allow samples to be used in the future. This type of research is being done to answer research questions, not to provide you with care. You and your doctor will not be given the results of these tests.

What are the possible benefits?

There is no direct benefit for you as an individual taking part in this study. We hope that by studying people with your condition using cardiac MRI, we may be able to improve understanding of this condition and help to inform screening/treatment of future patients.

What happens when the research study stops?

The end of the study will not affect the care you receive from your doctors. The end of the study will mark the official end of your participation in this project. Copies of any publications connected to this study will be available on request from Dr Ntusi.

Will my taking part in the study be kept confidential?

Yes. We will follow ethical and legal practice and all information about you will be handled in confidence. If you take part in the study, some of the data collected from the study would be looked at by authorised persons from the University of Cape Town, to check that the study is being carried out correctly. All investigators have a duty of confidentiality to you as a research participant, and nothing that could reveal your identity would be disclosed outside the research site. The data collected from the study will be recorded anonymously and you would not be identifiable from this.

What if relevant new information becomes available?

Sometimes, we (the study investigators) get new information about the procedures being studied. If this happens, one of us will tell you and discuss whether you should continue in the study. If there is sufficient evidence to suggest you may be harmed from participating in this study, the study could be stopped.

Unexpected findings on your scan

In the unlikely event of us seeing any structural abnormalities on your MRI scan, a designated clinical specialist will discuss the implications with you and may arrange for further investigations as necessary. However, it is important to note that we do not carry out scans for diagnostic purposes, and therefore these scans are not a substitute for a clinical appointment. Rather, our scans are intended for research purposes only. So if we find anything unusual, it would be appropriate for us to contact your GP/specialist so that they can arrange on-going clinical care for you. But we would only do this after we and the specialist had discussed your options and gained your permission.

What will happen if I don't want to carry on with the study?

You are free to withdraw from the study at any time. Anonymised data will be kept till the point you choose to end your participation in the study. Data collected till the point of your withdrawal will be included in the analysis.

What will happen to the results of the research study?

We anticipate that the results will be published in a scientific journal for the benefit of the wider medical community. However, individual patients will not be identified in any publication and your personal and clinical details will remain strictly confidential. Any scientific publications arising from the study will be available on request to all participants. You would have no legal right to a share of any profits that may arise from the research.

Will your test results be shared with you?

We will show you the images we acquire from the ultrasound and MRI scans when we finish performing the scans. The results of the other tests will only be available on publication of the results. If however, results of any of any of the tests are grossly abnormal, we will contact you to discuss these with you before suggesting a course of action and contacting your doctor/specialist.

Who is organising and funding the research?

The study is organised and conducted by researchers from the University of Cape Town and Groote Schuur Hospital. The studies are funded, in part, by a grant from the National Research Foundation of South Africa.

Who has reviewed the study?

The University of Cape Town Human Research Ethics Committee has reviewed and approved the study.

Insurance and financial arrangements

Study doctors are covered by insurance. UCT has a no fault insurance policy for trial related injuries which states:

"UCT undertakes that in the event of you suffering any significant deterioration in health or well-being, or from any unexpected sensitivity or toxicity that is caused by your participation in the study it will provide immediate medical care. UCT has appropriate insurance cover to provide prompt payment of compensation for any trial-related injury according to the guidelines outlined by the Association of the British Pharmaceutical Industry, ABPI 1991. Broadly-speaking, the ABPI guidelines recommend that the insured company (UCT), without legal commitment, should compensate you without you having to prove that UCT is at fault. An injury is considered trial-related if, and to the extent that, it is caused by study activities. You must notify the study doctor immediately of any side effects and/or injuries during the trial, whether they are research-related or other related complications.

UCT reserves the right not to provide compensation if, and to the extent that, your injury came about because you chose not to follow the instructions that you were given while you were taking part in the study. Your right in law to claim compensation for injury where you prove negligence is not affected. Copies of these guidelines are available on request"

Further information and contact details

Should you wish to know more about any aspects of this study, please contact Dr Ntusi at 021 4066200.

Should you have any concerns regarding your rights or welfare as a research participant, please contact the Faculty of Health Sciences Research Ethics Committee at 021 406 6626.

CONSENT FORM

Study Full Title	Characterisation of phenotypes of inflammation, fibrosis and remodelling in chronic rheumatic heart disease using multiparametric cardiovascular magnetic resonance and autophagy biomarkers
Patient ID	
Principal investigator	**Prof. Ntobeko Ntusi**
Researcher	**Mr Olukayode Aremu**

	I agree	I disagree
I confirm that I have read and understand the information sheet for the above study. I have had the opportunity to consider the information, ask questions and have had these answered satisfactorily.	☐	☐
I understand that my participation is voluntary and that I am free to withdraw at any time without giving any reason, without my medical care or legal rights being affected.	☐	☐
I understand that relevant sections of my medical notes and data collected during the study may be looked at by authorized individuals from the University of Cape Town, where it is relevant to my taking part in this research.	☐	☐
I understand that my doctor will, with my permission, be informed of the results of medical tests performed as part of the research, which are important for my health care.	☐	☐
I also understand that I may be invited to return for a second MRI scan, which is optional.	☐	☐
I agree to being contacted in the future to ask if I am interested in future related studies.	☐	☐

There could be some leftovers of some of the tissues collected from you at the end of this study. Do you agree to let us store your samples for future heart diseases research?		

CERTIFICATE OF CONSENT

I have read the information letter, or it has been read to me. I have had the opportunity to ask questions about it and any questions I have asked have been answered to my satisfaction. I consent voluntarily to be a participant in this study

Print Name of Participant _____

Signature of Participant _____

Date _____

Day/ Month/ Year

If illiterate

I have witnessed the accurate reading of the consent form to the potential participant, and the individual has had the opportunity to ask questions. I confirm that the individual has given consent freely.

Print name of witness _____ Thumb print of witness _____

Signature of witness _____

Date _____

Day/ Month / Year

Statement by the researcher/person taking consent

I have accurately read out the information sheet to the potential participant, and to the best of my ability made sure that the participant understands the study that is going to be done. I confirm that the participant was given an opportunity to ask questions about the study. All questions asked by the participant have been answered correctly and to the best of my ability. I confirm that the individual has not been coerced into giving consent and the consent has been given freely and voluntarily.

A copy of the Informed consent has been provided to the participant.

Print Name of Researcher/ person taking the consent _____

Signature of Researcher/ person taking the consent _____

Date_____

Day/ Month / Year

NB: PLEASE KEEP THIS FORM ON A SAFE AND SECURE PLACE

APPENDIX

A. PRESSURE COOKING TECHNIQUE FOR ANTIGEN RETRIEVAL

1. Two litres of antigen retrieval buffer (TEDTA/Citric acid) was placed into a pressure cooker (Russell Hobbs, 6 L).

2. The pressure cooker was placed on the hotplate, with the lid in place, but not locked into position or tightened.

3. The temperature dial of the hotplate was turned on to the highest setting.

4. Once the solution in the pressure cooker began to boil, the steel rack of slides was placed inside.

5. To enable safe closure of the lid, it was initially correctly aligned to the pot and tightened into position by turning it clockwise.

6. To lock the lid securely, the grey button was pushed down into position.

7. Timing of the process was only initiated when the pressure built up and a hissing sound and steam emanated from the release valve.

8. After the designated time was reached the hotplate was switched off, the pressure cooker carefully removed and placed in a sink with cold water running over it to allow it to cool down.

9. Once the pressure cooker had cooled down sufficiently, the lid was opened and the rack of slides removed.

B. PREPARATION OF REAGENTS

1. 1 mM EDTA (TEDTA) solution, pH9

2.42g of Tris Base (Sigma Aldrich) + 0.74g of EDTA (Sigma Aldrich) was dissolved in 2 litres of distilled water. This solution was pH to 9.

2. 0.01 M Citric acid solution, pH6

4.2 g of Citric acid (Merck) was dissolved in 2 litres of distilled water. This solution was pH to 6.

3. 1 % Bovine Serum Albumin (BSA)

1 g of BSA (Roche) was dissolved in 100 ml of PBS.

4. Mayers Haematoxylin

    1 g Haematoxylin (Merck)

    50 g Aluminium Potassium Sulphate (Merck)

    0.2 g Sodium iodate (Merck)

    1 g Citric acid (Merck)

    50 g Chloral hydrate (Merck)

    1000ml Distilled water

University of Cape Town

Department of Medicine
RHD Ntusi Group

Standard Operating Procedure

Title	Governance and Storage of Samples for Future Use		
No.	01		
Version	01		
P. Is	**Name**	**Department**	**Email**
	Prof. Ntobeko Ntusi	Medicine	ntobeko.ntusi@uct.ac.za
	Prof. Richard Naidoo	Pathology	richard.naidoo@uct.ac.za
	A/Prof. Sebastian Skatulla	Civil Engineering	sebastian.skatulla@uct.ac.za
Researchers	**Name**	**Department**	**Email**
	Dr. Evelyn Lumngwena	Medicine,	EN.Lumngwena@uct.ac.za
	Aremu Olukayode	Medicine	solomonpeace23@gmail.com
	Daniel Mutithu	Medicine	mttdan008@myuct.ac.za

Introduction

This document describes how the samples collected during this study will be stored and how their future use will be controlled.

In this document samples means human blood, valve tissues, heart ventricle and atrium biopsies collected from patients who have consented to the study.

Samples collection

Blood samples

Blood samples will be collected from patients after they have been explained about the study and have signed the consent forms. The samples will be treated as per the procedures and safety conditions as stated by the collaborating laboratories biosafety policies.

While collecting the sample tubes will be marked with the patient's information sticker that shows the GSH number, DOB and names of the patient. This is for tracking purposes where the medical history of the patient will be needed during interpretation of the study results.

The samples will be transported to the collaborating laboratories safely following laid out human blood shipping policies. The distance between the wards to the laboratories is short thus samples will mostly be shipped by hand.

In the laboratory the blood samples will be processed as per the approved protocols for isolation of serum, plasma and PBMCs. They will be stored in aliquots of approximately 500µl - 1000µl in cryovials.

From this time on, the serum, plasma and PBMCs here after "processed samples" will be given a unique identification code that does not bear the name of the patient and is hard to associate it with the patient

directly. This is done to ensure the privacy rights of the patient are preserved during the current and subsequent studies.

The samples will be stored in carefully marked boxes that are marked with the name of the study and the names of the researcher. The processed samples will be stored in -80 °C freezers located in secure laboratories at Hatter Institute for Cardiovascular Research in Africa.

Heart valves, ventricle and atrium samples

Heart tissues will be obtained from patients undergoing cardiothoracic surgery at the GSH cardiothoracic theater.

Only patients who have consented for the study will have their specimens collected for study purposes.

Patients will be explained that they have a right to withdraw from the study at any time of the process and that their samples will be used for current and future studies.

They will also be told their identity during the study will remain confidential and they have an option to have their names and medical information disassociated with the samples in case of future studies using the samples collected.

Immediately after acquiring the specimens they will be cut as per the approved protocols into different specimen vials that will be labeled with a unique identification code that cannot be directly associated with the consented participant.

Immediately the number of vials and the names for study will be recorded in hard copy sheet for secure storage. The samples logging sheet contains the name of patient, DOB, GSH file number and a check list if the patient consented for this study and samples can be used for current and subsequent studies.

The vials will be stored in a clearly marked tissues boxes in -80 °C freezers in a secure laboratory facility.

Samples storage and authorizations to access samples

The samples logging sheet (find attached) will be filled and stored in a locked cabinet. Further a similar information will be captured in an excel file that will be stored online for back up purposes.

Upon collection and storage, the materials become the property of the research group and thus their access will be strictly controlled and monitored.

1. The only individuals allowed to access the samples will be those that have been authorized by the PI and have had ethics approval from HREC of UCT to conduct study on the tissues.
2. The research group will provide an updated logging sheet for all the samples collected, those used and those still in possession of the research group and their exact location.
3. The collection and use of the materials will be always recorded in the corresponding researcher's laboratory journals. This will be used while accounting for the materials used and those still under storage.
4. Data and information of the samples stored will only be shared among the researchers and the collaborating laboratories.
5. The samples will not be shipped to other institutions or laboratories for whatever reasons and in the event of shipping University HREC sample shipping policies will be strictly adhered to.

Name of Patient			
Study No.			
Date			
GSH File No.			
Date of Birth		Sex:	
Height		Weight:	
Ethnic Group			
Pulse:	BP:		

Consent Signed			
History Obtained		ARF:	Other:
Echo (Confirmed)			
CMR		Date:	
Date of Surgery:			

Specimen Collected

1. Blood	**Date and Time:**			**Processed:**
		Serum	Plasma	
	Proteomics			
	Metabolomics			
	Antibody Array			
	MiRNA			
	Cytokines			
	Exosomes			
		PBMC		
		Cell count		
2. Right Atrium	**Date and Time:**			**Processed:**
	Proteomics			
	Metabolomics			
	Autophagy			
	Histology			
	IPMS			
3. Left Ventricle	**Date and time:**			**Processed:**
	Proteomics			
	Metabolomics			
	Autophagy			
	Histology			
	IPMS			
4. Valve Tissue:	**Date and Time:**			**Processed:**
		Mitral	Aortic	
	Proteomics			
	Metabolomics			
	Autophagy			
	Histology			
	MicroRNA			
	IPMS			

RHD – Proteomics/Molecular study – Sampling check list

Sample management log

Sample ID	Project code	Date picked	Amount	Researcher Name	Authorizing signature